

# DIPLOMARBEIT

Titel der Diplomarbeit

## **Expression, Regulation and Function of FGF18 in Melanoma**

Verfasserin

**Katharina Vejdovszky**

angestrebter akademischer Grad

**Magistra der Naturwissenschaften (Mag. rer. nat.)**

Wien, 2012

Studienkennzahl lt. Studienblatt

A 441

Studienrichtung lt. Studienblatt:

Diplomstudium Genetik - Mikrobiologie

Betreuer:

ao. Univ.-Prof. Dr. Josef Loidl

This Diploma Thesis was conducted at the

**Medical University of Vienna**

**Institute of Cancer Research**

**Department of Medicine I**

Practical Supervisor:

**Asst. Prof. Dr. Michael Grusch**

## **Zusammenfassung**

FGF18 ist einer von insgesamt 22 Fibroblasten Wachstumsfaktoren (FGFs). Deregulierung der zugehörigen RezeptorTyrosinkinasen (FGFR1-4) ist in diversen Krebsarten in der Tumorigenese involviert. FGF18 wird hauptsächlich von FGFR3 IIIc und FGFR4 gebunden. Seine Funktion ist vor allem in der Embryogenese und in der Entwicklung von Knochen- und Knorpelgewebe bekannt. Im Erwachsenenalter wird FGF18 in Haarfollikeln exprimiert und reguliert die Instandhaltung der Haut und das Haarwachstum. Melanome sind bösartige Tumore, die aus Melanocyten entstehen und die meisten Todesfälle durch Hautkrebs verursachen. Untersuchungen haben ergeben, dass FGF18 in hepatozellulären und kolorektalen Karzinomen erhöht exprimiert wird und die Expression mit fortschreitender Tumorentwicklung steigt. In kolorektalen Karzinomen wird FGF18 durch den Wnt-Signaltransduktionsweg aktiviert und stimuliert das Wachstum von Darmkrebszellen sowie die Blutgefäßbildung durch endotheliale Zellen. Jüngste Untersuchungen zeigten erhöhte Expressionsmengen an FGF18 in Melanom Zelllinien, was als Rationale zur genaueren Analyse über die Funktion von FGF18 in Melanom in dieser Diplomarbeit diene.

Eines der Ziele dieser Diplomarbeit war es die Expressionsanalyse auf weitere Zelllinien auszudehnen. Weiters wurde die Expression von FGF18 als Protein in Gewebeproben von Nävi und malignen Läsionen in einem „tissue microarray“ verglichen. Die zwei Melanom Zelllinien MJZJ, welche geringe endogene FGF18 Expression zeigt, und FTSL/a, die FGF18 mittelhoch exprimiert, wurden herangezogen, um mittels „knock-down“ und Überexpression genauere Funktion von FGF18, bezüglich Viabilität, Migration und Invasion in diesen Zellen zu analysieren. Da bereits bekannt ist, dass FGF18 Expression im kolorektalen Karzinom durch den Wnt-Signalweg aktiviert wird, wurde der Zusammenhang zwischen FGF18 Expression und der Wnt-Signaltransduktionsaktivität in Melanom Zelllinien überprüft. Um festzustellen inwiefern FGF18 die Neoangiogenese in Melanomen beeinflusst, wurden zweierlei Tests durchgeführt. Einerseits wurde festgestellt, ob in Melanom Zelllinien, wie es in Wachstumsfugen der Knochen der Fall ist, FGF18 die Expression von VEGF induziert

und dadurch die Neovascularisierung steuert. Andererseits wurden Lymph- und Blutendothelzellen auf ihre Expression von FGF18 und allen FGF-Rezeptoren getestet, um ihre potenzielle Signalverarbeitung von FGF18 zu überprüfen.

Die Expressionsanalyse zeigte hohe Werte von FGF18 in einem großen Teil der Melanom Zelllinien. Ebenso wurde im „tissue microarray“ eine signifikante Erhöhung von FGF18 in malignen Läsionen gefunden. Die Analyse etwaiger autokriner Effekte von FGF18 hat gezeigt, dass die Überexpression keine Auswirkung auf Viabilität, jedoch einen positiven Effekt auf Migration und Invasion in den endogen wenig exprimierenden MJZJ Zellen hat. FGF18 Überexpression in den für gewöhnlich moderat exprimierenden FTSL/a Zellen hatte keinerlei Auswirkung, jedoch zeigte der „knock-down“ einen steigernden Effekt auf Viabilität und die Formation von Zellklonen in 2D Zellkulturen und 3D Soft Agar Zellkulturen. Eine direkte Korrelation zwischen Wnt-Signalaktivität und FGF18 Expression in Melanom Zelllinien konnte nicht nachgewiesen werden, weshalb hier vermutlich andere Regulationsmechanismen zugrunde liegen. Ebenso scheint die VEGF-A Expression im Melanom nicht von FGF18 induziert zu werden. Jedoch ist eine Beteiligung von FGF18 and der Neoangiogenese nicht ausgeschlossen. In Lymph- und Blutendothelzellen wurde eine prinzipiell niedrige Expressionsrate an FGF18 gefunden, was autokrine Stimulation dieser Zellen ausschließen lässt. Andererseits exprimieren diese Zellen adäquate Mengen an FGFR4, was die Signalverarbeitung von FGF18, das aus den Melanomzellen stammt, generell möglich macht.

## Abstract

FGF18 is one of 22 fibroblast growth factors. Research findings show that associated receptor tyrosin kinases (FGFR1-4) are involved in tumorigenesis in a variety of cancer types. FGF18 predominantly binds FGFR3 IIIc and FGFR4 and plays a role in embryonic morphogenesis and in development of bone and cartilage. In adulthood it is expressed in hair follicles and regulates skin maintenance and hair growth. Melanoma is a malignancy derived from melanocytes and causes most skin cancer deaths. Previous publications reported upregulation of FGF18 in hepatocellular and colorectal carcinoma with increasing levels during tumour progression. FGF18 was regulated via the Wnt-pathway and stimulated growth of colon cancer cells and of colon-associated fibroblasts as well as tube formation of endothelial cells. Recent studies unravelled a generally high level of FGF18 in melanoma cell lines, which lead to investigation of the roles of FGF18 in melanoma.

First, a panel of melanoma cell models was analysed for FGF18 transcript expression. Furthermore a tissue array of 100 samples was evaluated for expression data on the protein level. Two melanoma cell lines, MJZJ with low endogenous FGF18 expression and FTSL/a with moderate endogenous expression were chosen for knock-down and overexpression, in order to analyse effects of FGF18 on growth and viability as well as migration and invasion. Since FGF18 was found to be controlled by the Wnt-pathway in colorectal cancer, the correlation between  $\beta$ -catenin activation and FGF18 expression was investigated. To unravel the contribution of FGF18 to neoangiogenesis in melanoma, two approaches were performed. Since FGF18 regulates expression of VEGF in the growth plate and thereby coordinates skeletal vascularisation, VEGF-A expression was analysed in melanoma cell lines and correlation to FGF18 expression was determined. Furthermore, immortalised lymph and blood endothelial cells were analysed for their expression of FGFRs and FGF18.

The FGF18 expression data of 28 cell lines showed high expression in a considerable fraction of melanoma cells. However, a correlation between type and origin of

melanoma and FGF18 expression was not found. Tissue array data revealed significant increase of FGF18 in malignant lesions compared to nevi. Analysis of autocrine effects suggest, that FGF18 overexpression has no impact on viability, but induces migration and invasion in a low expressing melanoma cell line. In FTSL/a, a cell line with higher endogenous FGF18 expression, overexpression did not show any effect. Interestingly, knock-down of FGF18 in these cells seems to increase their viability and clone formation in 2D clonogenic assay and 3D soft agar assay. Unlike in colorectal cancer, FGF18 expression is at least not directly regulated by Wnt-pathway. Neither does FGF18 induce VEGF-A expression, in contrast to what is described for the growth plate. Analysis of lymph and blood endothelial cells unravelled the possibility of paracrine angiogenic effects of FGF18. Expression data showed very low levels of FGF18, which precludes autocrine signalling in endothelial cells, but sufficient levels of FGFR4 to enable signal reception.

## Table of Contents

I.	Introduction.....	1
1.1	Cancer .....	1
1.2	RTKs and cancer .....	2
1.3	FGFs and FGFRs .....	2
1.3.1	Downstream signalling of FGFs.....	5
1.3.2	Regulation of FGF signalling .....	6
1.3.3	Physiological role of FGF signalling .....	7
1.3.4	Mechanisms of aberrant FGF signalling regulation in cancer .....	8
1.4	FGF18 .....	11
1.4.1	Structure, receptor binding and signalling pathways of FGF18 .....	11
1.4.2	Physiological role of FGF18.....	11
1.4.3	FGF18 in cancer.....	15
1.5	Melanoma .....	15
1.5.1	Melanocytes and the development of melanoma .....	16
1.5.2	Deregulated signalling pathways in melanoma.....	19
1.5.3	Senescence and how it is overcome in melanoma.....	22
1.5.4	Strategies of therapy .....	23
1.6	Aims .....	26
II.	Materials and Methods.....	31
2.1	Cell culture .....	32
2.2	Expression analysis on protein level - Tissue Micro Array.....	33
2.3	Expression analysis on RNA level .....	34
2.4	Determination of the impact of Wnt-pathway activity on FGF18 expression .....	37

2.5 Potential of autocrine signalling of FGF18 in melanoma .....	40
2.5.1 Establishment of FGF18 knock-down in FTSL/a.....	41
2.5.2 Inducing overexpression of FGF18 in FTSLA/a and MJZJ .....	45
Analysis of viability and growth .....	47
2.5.3 Viability test - MTT assay.....	47
2.5.4 Apoptosis test – caspase assay .....	47
2.5.5 Clonogenicity assay .....	48
2.5.6 Growth curve establishment .....	49
2.5.7 Cell cycle analysis .....	50
Analysis of migration and metastasis auxiliary skills .....	50
2.5.8 Scratch assay.....	50
2.5.9 Transmigration assay .....	51
2.5.10 Invasion Assay .....	51
2.5.11 Anchorage independent growth – soft agar assay .....	52
III. Results .....	53
3.1 FGF18 protein expression in melanoma tissue samples - Tissue Microarray .....	53
3.2 FGF18 gene expression in melanoma cell models .....	54
3.3 Contribution of FGF18 to neoangiogenesis in melanoma .....	56
3.4 Determination of the impact of endogenous Wnt-pathway activity on FGF18 expression in melanoma cells .....	59
3.5 Potential of autocrine signalling of FGF18 in melanoma .....	62
3.5.1 Evaluation of the lentiviral transfection efficacy.....	62
Analysis of viability and growth .....	63
3.5.3 Viability test – MTT assay .....	63
3.5.4 Apoptosis test – caspase assay .....	64



3.5.5 Clonogenicity assay .....	65
3.5.6 Growth curve establishment .....	67
3.5.7 Cell cycle analysis .....	69
Analysis of migration and metastasis auxiliary skills .....	69
3.5.8 Scratch assay.....	69
3.5.9 Transmigration assay .....	71
3.5.10 Invasion assay .....	73
3.5.11 Anchorage-independent growth – soft agar assay.....	74
IV. Discussion .....	77
V. List of Abbreviations .....	83
VI. List of Figures .....	87
VII. List of Tables .....	93
VIII. References .....	95
IX. Curriculum Vitae .....	108

## **I. Introduction**

### **1.1 Cancer**

The development of cancer is a process that can last for decades, in which a normal cell becomes highly malignant. The disruption of homeostatic regulation is generally regarded as the event that enables any kind of tumourigenesis in the first place. Homeostasis determines whether cells remain quiescent, proliferate, differentiate or undergo apoptosis.[1] By the accumulation of several genetic changes the cell acquires specific properties to evade this control mechanism and enable malignancy. Six so called classic hallmarks of cancer are described in the literature. One of them is the self-sufficiency of the cells in growth signals. In combination with insensitivity to anti-growth signals, the ability to evade apoptosis and limitless replicative potential, uncontrolled cancer cell proliferation is enabled. Another crucial feature of malignant cells is the capability to invade adjacent normal tissue and metastasise to distant organs. When the tumour has reached a certain size, the sustainment of angiogenesis is essential to provide the cells with nutrients and oxygen. [2-6] In the last couple of years, research revealed some additional hallmarks of cancer. Enhanced anabolic metabolism, cancer-related inflammation and genetic instability also seem to be universal features of malignancy.[4, 7]

Carcinogenesis is a highly complex process and the variety of mutations which finally lead to malignancy in each individual case is huge. Frequently, multiple genes are affected by mutations. In many cases chromosomal abnormalities promote malignancies and very often gene expression patterns are altered.[5] Generally, it is distinguished between so-called “driver mutations” and “passenger mutations”. The former, in principle lead to over-activation of growth promoting oncogenes and to inactivation of growth-inhibiting tumour suppressor genes and therefore lead to a growth-advantage. The “passenger mutations” have no contribution to cancer

progression and exacerbate the quest to identify the malignancy promoting mutations. [8-9] However, in many cases malignancy depends to a large part on aberrant expression of one single oncogene. This so-called “oncogene addiction” denotes the relevance of molecular targeted therapies.[10]

### **1.2 RTKs and cancer**

Receptor tyrosine kinases (RTK) are one family of growth factor receptors, which is commonly affected by mutations or expression alterations in human cancer. RTKs feature an extracellular ligand binding domain, a single-pass transmembrane domain and an intracellular tyrosine kinase domain. Ligand binding at the extracellular domain leads to homo- or heterodimerisation of two RTKs. Thereby intracellular kinase domains are activated and induce auto- and transphosphorylation. The phosphorylated tyrosines act as docking sites for adaptor proteins. An intracellular signalling cascade follows, which alters gene expression patterns. The signalling pathways activated by RTKs often regulate cellular processes like proliferation, differentiation, migration and survival. [11] As already mentioned, deregulation of RTKs is commonly found in human cancer and in most of the cases RTKs act as oncoproteins. Rarely, RTKs are found to be tumour suppressive. [12-13]

Not only RTKs but also their ligands potentially enhance progression of malignancies. Receptors and growth factors may be involved in epithelial-mesenchymal transition (EMT), a process by which an epithelial cancer cell acquires a mesenchymal phenotype in terms of migratory capacity, a requirement for invasion and metastasis. Furthermore RTKs and their ligands also play a role in cancer cell expansion and angiogenesis.[13-14]

### **1.3 FGFs and FGFRs**

One group of ligands and corresponding receptors of the RTK family, which are known to be potentially involved in tumour progression are fibroblast growth factors (FGFs)

## Introduction

and their receptors (FGFRs). There are 22 FGF genes in the human genome that code for peptide mediators which are related in structural motives and their functions. [15] FGF11, 12, 13 and 14 are referred to as FGF homologous factors (FHF). They are FGF-like peptides which are not secreted and neither bind to FGFRs nor activate FGF dependent signalling pathways. Nevertheless, they show high sequence identity with FGFs.[16]

Eighteen of the 22 genes encode genuine FGFs which are secreted. They are divided into two sub-families, the hormone-like and the canonical sub-family. The former consists of FGF19, 21 and 23 which act as endocrine factors in a FGFR-dependent manner. FGF 1-10 16-18, 20 and 22 belong to the canonical sub-family and produce autocrine and/or paracrine signals by receptor binding.[17] By means of structure homology and phylogeny, the canonical FGFs are subdivided into 5 groups. The FGF1 group consists of FGF1 and FGF2. In contrast to all the other canonical FGFs, the members of the FGF1 group are not actively secreted by cells but remain intracellular till the cell decays. Genes of the FGF4 group (FGF 4-6), FGF7 group (FGF3, 7, 10, 22) and FGF8 group (FGF8, 17, 18) encode a signal peptide which enables secretion by the endoplasmatic reticulum pathway. Members of the FGF9 group (FGF9, 16, 20) are also secreted although they do not contain such signal peptides.[15, 18-19]

Heparan sulphate proteoglycans (HSPG) play a considerable role in the efficacy of FGF-FGFR binding. They consist of a proteoglycan core that is bound to two or three linear polysaccharides. FGFs bind these negatively charged polysaccharides via electrostatic interactions.[19] In the extracellular matrix of connecting tissue, HSPGs prevent degradation, limit the diffusion and build micro environmental stores of FGFs. FGFs can be released from these stores either by proteolytic enzymes or FGF binding protein (FGF-BP). This protein is also secreted into the extracellular space and reduces the affinity of heparin to FGFs, which, thereby, become available for signalling. Additionally, membrane-bound HSPG acts as co-receptor and is involved in complex formation between FGF, FGFR and heparin sulphate.[11, 19-20]

## Introduction

The high affinity receptors for FGFs, the FGFRs, are a sub-family of RTKs, of which 4 genes are found in the human genome, *FGFR1*, *FGFR2*, *FGFR3* and *FGFR4*. The gross structure of FGFRs is very similar to most RTKs, and consists of an extracellular binding domain, a single-pass transmembrane domain and an cytoplasmatic kinase domain.[21] A schematic picture of FGFR structures can be seen in figure 1. The kinase domain is split by an insert, a feature that is shared by kinase domains of two other RTK families, VEGFRs (vascular endothelial growth factor receptors) and PDGFRs (platelet-derived growth factor receptors). Within the FGFR family the extracellular domains are also highly homologous and consist of three Ig-like (immunoglobulin-like) loops, I, II and III, and an acidic, serine rich region called the “acid box”. Ig-like loop I and the acid box act autoinhibitory, while Ig-like loops II and III enable FGF ligand binding.[22] FGFR1, 2 and 3 occur in two splicing variants in Ig-like loop III, referred to as IIIb and IIIc. Accordingly, there are 7 FGFRs (FGFR1 IIIb, FGFR1 IIIc, FGFR2 IIIb, FGFR2 IIIc, FGFR3 IIIb, FGFR3 IIIc and FGFR4), which differ in the spectrum of FGFs that they can bind.[23-24] Table 1 shows the most prominent FGF receptor isoforms and their binding ligands.

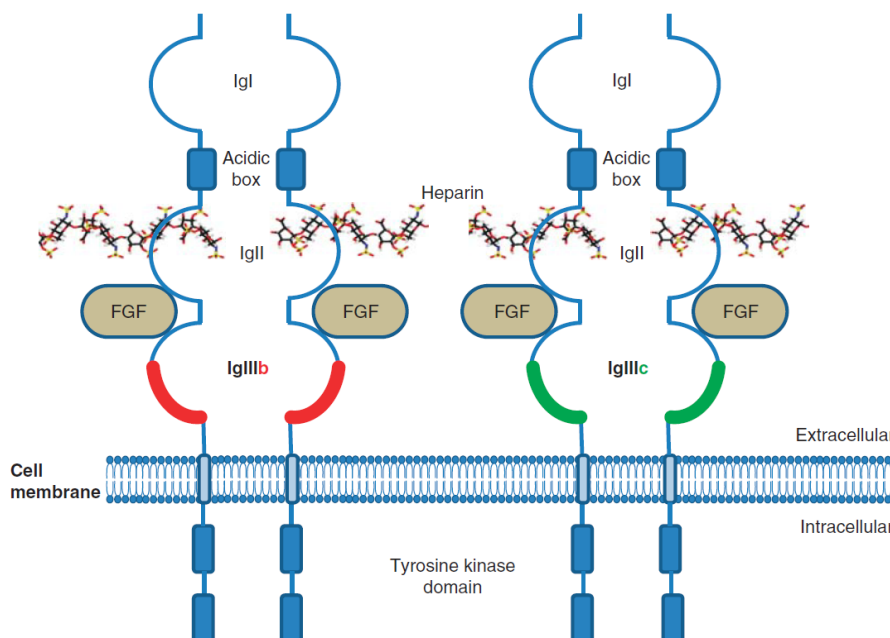


Figure 1: Structure of FGFRs, taken from Heinzle et al., 2011[25]

**Table 1: FGF receptor isoforms and their binding ligands [25]**

Receptor	Ligands
FGFR1-IIIb	FGF1, FGF2, FGF3, FGF10, FGF22
FGFR1-IIIc	FGF1, FGF2, FGF4, FGF5, FGF6, FGF8, FGF9, FGF16, FGF17, FGF18, FGF20, FGF21, FGF23
FGFR2-IIIb	FGF1, FGF3, FGF7, FGF10, FGF22
FGFR2-IIIc	FGF1, FGF2, FGF4, FGF5, FGF6, FGF8, FGF9, FGF16, FGF17, FGF18, FGF20, FGF21, FGF23
FGFR3-IIIb	FGF1, FGF9, FGF16
FGFR3-IIIc	FGF1, FGF2, FGF4, FGF5, FGF6, FGF8, FGF9, FGF16, FGF17, FGF18, FGF20, FGF21
FGFR4	FGF1, FGF2, FGF4, FGF5, FGF6, FGF8, FGF9, FGF16, FGF17, FGF18, FGF19, FGF20, FGF21, FGF23

### 1.3.1 Downstream signalling of FGFs

Activation of FGF/FGFR signalling is accomplished by extracellular ligand binding whereby the receptors are dimerised. This brings the cytoplasmic kinase domains in close proximity and enables transphosphorylation of tyrosine residues. Some of the phosphorylated tyrosine sites act as docking sites for downstream signalling molecules containing SH2 domains.[26-27] Downstream intracellular signalling pathways of FGFRs are shown in figure 2. PLC $\gamma$  (Phospholipase C $\gamma$ ) for example, binds a phosphotyrosine on the C-terminal tail of activated FGFR and hydrolyses PIP<sub>2</sub> (phosphatidylinositol 4, 5-triphosphate) and thereby produces DAG (diacylglycerol) and PI<sub>3</sub> (inositol 1, 4, 5-triphosphate). This triggers the release of calcium and PKC (protein kinase C) gets activated. PKC is known to activate the MAPK (mitogen-activated protein kinase) pathway.[27-28] Another adaptor protein, FRS2 (FGFR substrate 2) binds a phosphotyrosine at the juxtamembrane region of the receptor and gets phosphorylated. FRS2 potentially activates several downstream pathways. Growth-factor-receptor-bound protein 2 (GRB2) interacts with FRS2, followed by the recruitment of either SOS which activates the MAPK pathway, or GRB2 associated binding protein 1 (GAB1) whereby the PI3K/Akt (phosphatidylinositol-3 kinase/protein kinase B) pathway is regulated.[23] A number of other signalling molecules are known to be activated by FGFRs, like RSK2 (p90 ribosomal protein S6 kinase 2), STATs (signal transducers and activators of transcription) and the non-receptor tyrosine kinase Src[19, 29]

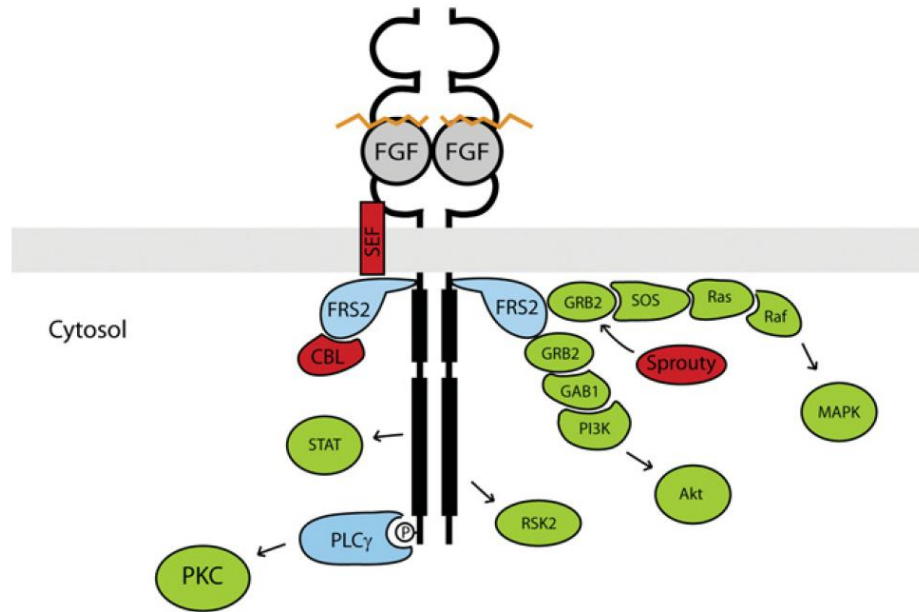


Figure 2: Downstream signalling of FGFs, taken from Wesche et al., 2011 [30]

### 1.3.2 Regulation of FGF signalling

The duration and intensity of FGF signalling is strictly controlled by auto-regulatory negative feedback-loops.[31] Sprouty proteins are the most important endogenous inhibitors of signalling which are induced by FGFs and thus create a self-limiting feedback loop. In all analysed organisms Sprouty was found to have an inhibiting function.[32-35] There seem to be several mechanisms by which Sprouty inhibits FGF signalling. One of them leads to binding of GRB2, by which downstream signalling is interrupted.[36] MKP3 (MAPK phosphatase 3) and Sef (similar expression of FGF) are two other FGF signal inhibiting factors. Both attenuate the MAPK pathway.[29, 37-39] MAP kinases, in general, cause a negative feedback-loop by phosphorylation of additional serine and threonine sites of FRS2 which inhibits the recruitment of GRB2.[40] On the other hand there exist some positive regulators as well. The transmembrane protein FLRT3 (fibronectin-leucine-rich transmembrane protein 3) advances MAPK signalling activated by FGFR.[41] FLRT1 and FLRT2 also positively regulate FGF signalling.[42]

## Introduction

The final termination of an FGF signal happens via internalisation of the receptors by endocytosis, followed by degradation in lysosomes. The establishment of FGFR ubiquitination, the signal for receptor degradation, is accomplished by the ubiquitin ligase Cbl. After binding activated FRS2 the receptor gets ubiquitinated. [43] Alternatively, endocytotic adaptor protein extended-synaptogamin binds FGFR, which leads to clathrin-mediated and ubiquitin-independent endocytosis via adaptin-2.[44] After endocytosis the ubiquitylated receptors are sorted by the ESCRT (endosomal sorting complex required for transport) machinery. Depending on their grade of ubiquitination, receptors are either transported to lysosomes where they undergo degradation, or they are recycled by endosomes and transported back to the membrane. [45-46] FGFR1 for example generally becomes heavily ubiquitinated and subsequently degraded in lysosomes. FGFR4 normally receives light ubiquitination and is therefore rather recycled to the membrane. This is consistent with the fact that FGFR4 shows prolonged signalling compared to FGFR1.[45, 47] SPRED2 (Sprouty related protein) is one factor which attenuates signalling by directing the FGFR to lysosomes and causing degradation.[48] Different ligand binding can influence the route of the receptor, as it was shown for FGFR2IIb (KGFR, keratinocyte growth factor receptor). FGF7 leads to degradation in lysosomes, while FGF10 prevents ubiquitination and causes recycling of the receptor and prolonged signalling.[49] The binding of N-CAM, a membrane bound cell adhesion molecule which can act as alternative ligand of FGFR1, leads to recycling and sustained signalling of FGFR1 which is important for cell migration.[50]

### **1.3.3 Physiological role of FGF signalling**

In many cell types, FGF signalling was found to be involved in proliferation by activating pro-survival, or anti-apoptotic pathways. In this context the MAPK pathway is known to induce proliferation while the PI3K/Akt pathway has an anti-apoptotic effect. By signalling cross-talk of MAPK and PI3K/Akt pathway migration can be stimulated via FGF signalling.[19] Several FGFs are found to play a crucial role as stimulating agents of cell growth and migration during embryonal development.[51-



52] A very important function of FGFs is their role in wound healing. After damaged tissue is removed by proteases FGFs are recruited. The upregulation of FGF-BP also mobilises FGFs to lesions.[53-54] In detail, FGF1, FGF2 and the epithelial specific FGF7 and FGF10 greatly support wound closure and re-epithelialisation by stimulating proliferation and cell migration of mesenchyme and epithelium.[55-56] The fact that epithelial cells predominantly express splicing variant IIIb of FGFRs and mesenchymal cells mainly harbour FGFR IIIc creates an epithelial-mesenchymal tissue cross-talk which was found to have important functions in embryonal development and wound healing.[53, 57-58] The FGF19 subfamily members, the hormone-like FGFs, predominantly circulate systemically and show a variety of metabolic control functions. To generate full activity, the binding of co-receptors like HSPG or klotho, a transmembrane protein, is necessary.[17, 59] This subfamily predominantly binds FGFR4 compared to most other FGFs. Studies with transgenic and knock-out mice suggest a function in energy metabolism of FGF15/19.[60-62] Furthermore, FGF21 was found to regulate lipid metabolism and FGF23 controls serum phosphatase levels and vitamin D synthesis.[63-64] By influencing other key signalling molecules like HGF (hepatocyte growth factor) and VEGF (vascular endothelial growth factor), FGFs potentially influence angiogenesis. [65]

### **1.3.4 Mechanisms of aberrant FGF signalling regulation in cancer**

As already mentioned, FGF signalling is involved in a variety of key processes within the whole body and therefore needs to be regulated tightly. Aberrations in FGF signalling are very often connected to human disease including the development of malignancies whereat constitutive activation is implied mostly.[66-72] The mechanisms by which a proper regulation is obviated are manifold.

Mutated FGFR genes are common initiators of these aberrations. Dimerisation causing mutations are the source of several developmental syndromes. Achondroplasia for example arises from a mutation in the transmembrane helix in FGFR3 leading to dimerisation and constitutive tyrosine kinase activation.[73] This

## Introduction

mutation is also often found in bladder cancer.[74] Mutations of the kinase domain itself, which result in constitutive activation, are involved in the development of childhood sarcoma RMS (rhabdomyosarcoma).[66] Interestingly, in some human cancers loss-of-function mutations are found in FGFR genes, which suggests, that they feature tumour suppressing functions.[75] Mutations in FGF ligands are also found in human disease but are mostly germline loss-of-function mutations. An FGF3 deficiency leads to deafness. Ligand mutations in cancer are quite rare and their consequences are not clear. Germline SNPs are thought to modulate malignant phenotypes in some cancer types. An SNP in the FGFR4 gene seems to be linked to a more aggressive behaviour and increased metastatic potential in a variety of cancer types, for instance in lung, breast, skin, colon, and prostate cancer.[76-80] Several SNPs in intron 2 of FGFR2 seem to increase the risk of breast cancer.[81-82] Particularly potent oncogenes are fusion proteins of dimerising protein domains with kinase domains of FGFRs caused by chromosomal translocations. They are permanently dimerised without any ligand and continuously activate signalling. Due to the fact that they are not localised at the cell surface but in the cytosol they escape any negative regulation and lysosomal degradation. SCLL (stem cell leukemia lymphoma syndrome) is often linked to a fusion protein containing the FGFR1 kinase domain.[83] Other chromosomal aberrations, for example leading to multiple copy numbers of FGFRs are also found in connection with cancer. Thus, 10% of all breast cancer patients harbour an 8p 11-12 amplicon which leads to FGFR1 over-expression.[84-86] furthermore, amplification of FGFR1 is frequently found in squamous cell lung cancer.[72] Alternative splicing in FGFR1, FGFR2 and FGFR3 leads to altered ligand specificity which can result in aberrant autocrine or paracrine signalling loops.[24] Impaired down-regulation of FGF signalling, hence defective internalisation leading to higher receptor levels and prolonged signalling is potentially caused by mutation in any involved protein and is found in many types of cancer.[87] The inactivation of negative regulators is also suggested to be involved in oncogenicity.[29] In prostate cancer, decrease of Sef and Sprouty is common.[88-89]

### 1.3.5 Targeting FGF signalling for therapy

One of the strategies to attenuate aberrant FGF signalling for cancer therapy is to develop small molecule tyrosine kinase inhibitors. [90] By targeting the ATP binding site on the intracellular tyrosine kinase domain such inhibitors have already been used successfully against other RTKs in cancer. [12-13] This type of therapy may be relevant for cancers deriving from FGFR over-expression, activating FGFR mutation, or dimerised fusion proteins. Unfortunately, due to the high degree of homologies of kinase domains within the whole RTK family, even receptor subtype-specific inhibitors may have at least some effect on other related receptors. In combination with the fact that RTKs are expressed all over the body, the high potential for systemic side effects of these small molecule tyrosine kinase inhibitors are obvious. Although there have been successful efforts targeting other RTKs, only few clinical studies targeting FGFR have been completed.

Another approach of interfering with FGF signalling for cancer therapy is the use of monoclonal antibodies. They can potentially target FGFRs as well as ligands. Blocking of receptor binding and/or dimerisation can be achieved. Additionally monoclonal antibodies may promote the removal of tumor cells by the immune system. [91] They have already been used successfully in treatment of various cancer types with deregulated RTKs. [12-13, 91] The advantage of this approach is the possibility of generating antibodies that target specific FGFs or FGFR subtypes. [92] The monoclonal antibodies act extracellularly and are therefore relevant as therapy tools for cancer types that derive from over-expression of FGFs or FGFRs or harbour activating FGFR mutations. Cytoplasmic fusion proteins cannot be targeted by this approach.

FGF ligand traps are another strategy and are most useful in cancer types that show FGF over-expression. These traps consist of FGFR ligand domains and sequester FGF ligands extracellularly and consequently prevent receptor binding on the cell membrane. A most promising FGF ligand trap, FP-1039, a soluble fusion protein

containing an FGFR1 IIIc domain and an Fc portion of IgG1 prevents FGF1, FGF2, and FGF4 binding and potentially blocks proliferation and angiogenesis. FP-1039 is being tested in phase II clinical trials.

### **1.4 FGF18**

FGF18 belongs to the FGF8 group and is, besides FGF1, 2, 9, and 22, one of the factors whose expression is not limited to embryonic development but occurs throughout life. [93]

#### **1.4.1 Structure, receptor binding and signalling pathways of FGF18**

FGF18 is a glycoprotein with two potential N-linked glycosylation sites.[94] Its structure is most similar to those of FGF8 and FGF17 since they all belong to one group. [95-96] The nucleotide sequence of the human FGF18 gene shows 90% identity with the murine gene and the FGF18 amino acid sequence of human and mouse is identical to 99%. [97-98] The first 26 amino acids form a hydrophobic tail which functions as signal peptide for secretion.[95]

FGF18 has great receptor selectivity and binds to the IIIc splicing variant of FGFR3 and to FGFR4 with high affinity and to FGFR2 IIIc modestly. [99-103] Additionally, in endochondrial development FGF18 interacts with FGFR1 in prehypertrophic and hypertrophic zones. [104] FGF18 binding and subsequent dimerisation of FGFR3, FGFR1 and FGFR2, lead to activation of MAP kinases and ERKs (extracellular signal regulated kinases).[105]

#### **1.4.2 Physiological role of FGF18**

##### ***Embryonic development***

Much of the investigation that was made on FGF18 leads to the conclusion that this factor plays a considerable role in embryonic development. In studies performed in

## Introduction

vitro and in vivo on embryos of mice, rats and chicks, FGF18 expression was found in midbrain, lungs, pancreas, muscle and the intestinal tract.[95, 101, 106-111] Furthermore, FGF18 seems to play a role in cortical neuron activity, hair growth and skin maintenance and survival differentiation and proliferation of adenohypophyseal progenitor cells.[112-114] Additionally, FGF18 expression was found in cephalic and mandibular mesenchyme and in the heart of human embryos. [98]

### ***Skeletal development***

FGF1, FGF2 and FGF18 are the most important factors of the FGF family for bone development and repair.[115-116] Accordingly, IIIc splicing variants of FGFR3 and FGFR2 are positive regulators of bone formation.[117-118] FGF18 is required for whole skeletal growth as several in vivo and in vitro studies have shown.[99-100, 118-120] FGF18 knock-out mice die within 30 minutes after birth which is thought to be caused by skeletal abnormalities that reduce thoracic volume and lead to cyanosis.

During long bone development FGF18 is expressed in the perichondrium, and during calvarial bone development it is found in mesenchyme and osteoblasts. Especially in the processes of chondrogenesis and osteogenesis, FGF18 seems to be involved. Studies with knock-out mice unravelled FGF18 as a regulator of ossification in endochondrial bone growth. FGF18 deficient mice also demonstrated the involvement of this factor in osteogenesis, since they showed delayed long bone ossification and low expression of osteopontin and osteocalcin, two osteogenic markers. Furthermore, the closure of cranial structure was retarded. Other investigations discovered some details of the involved signalling cascades within the MAPK pathway in this process. Transcription factors Cbfa1/Runx2 (core binding factor A1/runt-related transcription factor 2) which are activated via the MAPK pathway control downstream expression of the osteoblast differentiation genes osteopontin osteocalcin and collagen 1. Osteoblast proliferation was found to be mediated by ERK and osteoclasts were stimulated via RANKL (receptor activator of NF- $\kappa$ B ligand) and cyclooxygenase-2.[105] Consequently, FGF18 can be considered as a positive regulator of osteogenesis. On the other hand, since knock-out mice embryos show an increase in chondrocyte

## Introduction

proliferation, chondrogenesis seems to be negatively regulated by FGF18. This may happen by the inhibition of IHH (Indian hedgehog) signalling, a process involved in chondrocyte differentiation.[99, 116, 119] These results are consistent with the fact that FGFR3 activation was found to regulate osteogenesis positively but inhibit chondrogenesis.[99] However, the effect of FGF18 on chondrogenesis may vary, depending on the type of cartilaginous tissue it acts on. In the growth plate chondrogenesis is suppressed by FGF18, but it seems to promote cartilage repair when expressed in the periosteum during embryonic development. Furthermore, a study of an osteoarthritis rat model showed that intra articular injection of FGF18 promotes repair of damaged cartilage.[118, 121]

FGF2 is also known for its high significance in modulation of bone and cartilage functions and the mitogenic action of FGF18 towards osteoblasts and chondrocytes was found to be as strong as the one of FGF2.[105] Nevertheless, studies with mouse models showed that targeted deletions in FGF2 result in a light decrease of the number of osteoblasts and do not have an effect on chondrogenesis.[122] In contrast, FGF18 deficient mice have severe problems with ossification and long bone development, which highlights the more specific function of FGF18 on bone and cartilage cells and may be sufficient for compensating the role of FGF2 in skeletal formation. [105, 119]

Another study that displays the importance of FGF18 in bone development compared FGF18 and FGFR3 knock-out mice. Both models showed similar phenotypes of long bones and embryonic development, but compared to wild type, the FGF18 knock-out resulted in shorter bones than the FGFR3 knock-out. This suggests an involvement of interaction of FGF18 with other receptors like FGFR2 in long bone development.[99, 116]

Wnt and hedgehog signalling, which are regulated by GSK3 (glycogen-synthase kinase 3), are essential for endochondrial bone formation. Investigations with mouse embryonic cultures discovered that the repression of GSK3 results in activation of

## Introduction

FGF18 by which chondrocyte and osteoblast differentiation is influenced. This led to the suggestion that FGF18 may be regulated, by the wnt-pathway, in detail by GSK3 via upregulation of  $\beta$ -catenin.[123]

### ***Non-skeletal functions of FGF18***

FGF18 seems to act as a pleiotropic growth factor, since several mesenchymal and epithelial cells and tissues were found to be stimulated by FGF18 for proliferation, including lung, kidney, heart, testes, spleen, skeletal muscles and brain.

Especially the effect on the digestive system has been demonstrated by administration of recombinant FGF18 to mice. After only a few days, liver and small intestine showed weight gain due to high proliferation. Ectopic expression led to similar symptoms, at least in the liver. [95] FGF18 was found to be expressed in embryonic pancreas and presumably has a specific function there, which is not yet understood.[110] Increased expression of FGF18 may promote tumorigenesis in colorectal cancer.[124]

### ***Respiratory system***

FGF18 is expressed in embryonic and postnatal lungs. Studies with knock-out mice suggest that FGF18 is involved in alveolar development in a late phase of embryonic development but does not have an impact on lung branching morphogenesis. [95, 99, 109, 125]

### ***Brain***

In the course of many studies FGF18 expression was detected in brain tissue during embryonic development but also in adulthood. It seems to be involved in the organisation of the midbrain and the specification of left-right asymmetry. Furthermore FGF18 stimulates glial cells.[101-102, 106-108, 111, 126-127]

### 1.4.3 FGF18 in cancer

So far the role of FGF18 in cancer is a relatively unexplored field. However, recent studies suggest that FGF18 may contribute to tumour progression in colorectal and hepatocellular carcinoma. Analysis of colorectal tumour samples determined that 34 out of 38 tumours showed up-regulation of FGF18 and that expression levels increase with tumour progression. In this study, FGF18 was found to have pro-tumourigenic and pro-metastatic effects on tumour cells and the tumour microenvironment and may stimulate neoangiogenesis.[128] Likewise in hepatocellular carcinoma, a study unravelled the involvement of FGF18 in tumour cell survival and neovascularisation.[129]

### 1.5 Melanoma

Skin cancer is the third most common malignancy in humans and two to three million new cases are diagnosed per year. The most common forms are basal cell carcinoma, squamous cell carcinoma and melanoma. Though with 132 000 cases melanoma makes up only a small portion of new skin cancer cases each year, it is the most dangerous type, causing the most deaths (WHO). Eighty percent of melanoma cases are diagnosed at an early stage and are cured by surgery. Nevertheless, as soon as the tumour has progressed and metastasized, prognosis is very poor. The median survival rate of patients suffering from metastatic malignant melanoma is 6 months and only 5% survive 5 more years.[130]

There are 4 clinical subtypes of melanoma.[131] Nodular melanoma appears as a raised nodule without any significant flat portion. The acral lentiginous melanoma (ALM) is the only type which does not seem to be associated with UV exposure, since it occurs mainly on the palms of the hands, the soles of the feet or the nail bed. Lentigo maligna is a subtype that predominantly is found on sun-exposed regions of elderly persons. Superficial spreading melanoma (SSM) is the most common subtype and appears flat with an intra-epidermal component. Frequent severe sunburns, especially at early age seem to be in connection with the development of this disease.



### **1.5.1 Melanocytes and the development of melanoma**

Melanocytes are pigmented cells and predominantly reside in skin and eyes. Cutaneous melanocytes are found in the basal layer of skin and hair follicles where they produce pigments for skin and hair colour. A so-called epidermal melanin unit in humans consists of one melanocyte which is associated with about 36 keratinocytes that interact mainly via gap junctional intercellular communication.[132]. During childhood, the stable ratio between melanocytes and keratinocytes has to be maintained when the total skin surface expands. Proliferation of melanocytes therefore has to follow distinct steps. First the melanocytes have to decouple from the basement membrane and the keratinocytes. The melanocyte dendrites are retracted before the cell can divide. Division is followed by migration along the basement membrane in order to preserve correct distribution. Finally the melanocyte recouples to the matrix and the keratinocytes, whereby another epidermal melanin unit is formed. Not much is known about the half-life of melanocytes in adulthood but it is suggested that they have very low proliferation rates unless stimulated by sunlight or wounding.[133] Homeostasis of melanocytes is on the one hand regulated by endocrine and paracrine factors like hormones, growth factors and cytokines, and on the other hand by intercellular communication via cell-cell or cell-matrix adhesion and gap junction intercellular communication (GJIC). Keratinocytes are known to play a crucial role in several regulatory mechanisms of melanocytes. [134-135] Upon UV radiation keratinocytes secrete factors which have an impact on melanocyte survival, differentiation proliferation, motility and the production of melanin. The latter is known as tanning response, which highlights the importance of melanocytes in protection against UV radiation and skin cancer. [136]

E-cadherin is expressed on melanocytes and keratinocytes and is the major adhesion molecule between these two cell types. The loss of E-cadherin expression seems to be most critical for tumour progression since it leads to loss of keratinocyte control. In most melanomas E-cadherin is down-regulated, as well as connexin (Cx) 26, 30 and 43, which leads to the loss of GJIC and contributes to tumourigenesis.[134, 137-139] This

## Introduction

may be associated with the expression of Snail family transcription factors, which is also detected frequently in melanoma but not in melanocytes and correlates directly with the loss of E-cadherin. Experiments showed that forced expression of Snail leads to the down-regulation of E-cadherin. [140-141] The transcription factor Twist is known to be expressed in carcinomas and leads to down-regulation of epithelial markers like E-cadherin, but at the same time to up-regulation of mesenchymal markers like N-cadherin and therefore may contribute to EMT in melanoma. Generally melanomas with up-regulated Twist have poor prognosis.[142] Effectively, besides the loss of E-cadherin, a gain of N-cadherin is generally observed in melanoma. This switch in adhesion molecules leads to a change in communication partners, from keratinocytes to other N-cadherin expressing cells, like fibroblasts and vascular endothelial cells. This affects tumour stromal cell adhesion, invasion, migration and gene expression of melanoma cells. N-cadherin expression on melanoma cells changes cell morphology from a dendritic to a more rounded cell shape, thus making cells less adherent, which plays a key role in metastasis. The tight junction protein, zonula occludens protein-1 (ZO-1) is another factor found to be overexpressed in melanoma. In the course of cadherin switching, it is recruited to N-cadherin based junctions and subsequently reorganises the cytoskeleton, which leads to greater invasiveness of the melanoma cell.[143] another melanoma associated antigen is Mel-CAM, whose expression seems to be linked to down-regulation of E-cadherin.[132] It is considered to be the major part of gap junctions between melanoma cells and its ligand functions as co-receptor of N-cadherin. Mel-CAM is known to be involved in invasion and metastasis.[144] Figure 3 gives an overview of cell-cell interactions of melanocytes and melanoma cells, with the factors involved listed.

## Introduction

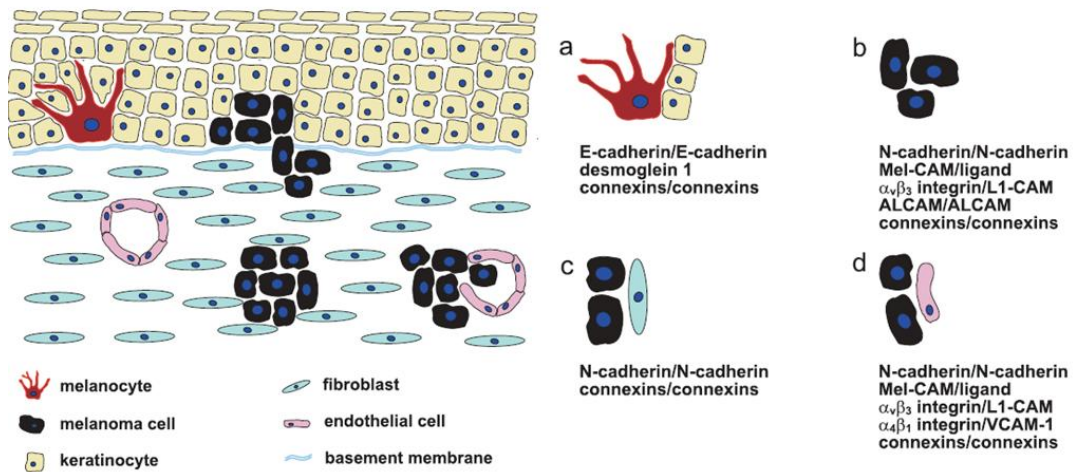


**Figure 3:**(a) Interaction between melanocytes and keratinocytes is mediated via E-cadherin, desmoglein 1 and connexins. (b) Melanoma cell-melanoma cell contacts are established by N-cadherin/N-cadherin, Mel-CAM/ligand,  $\alpha_v\beta_3$  integrin/L1-CAM, ALCAM/ALCAM and interactions of connexins. (c) The connection of melanoma cells to the basal membrane is mediated via N-cadherin and connexins and communication between melanoma cells and endothelial cells is accomplished via N-cadherin/N-cadherin, Mel-CAM/Ligand,  $\alpha_v\beta_3$  integrin/L1-CAM,  $\alpha_4\beta_1$  integrin/VCAM-1 and connexin interactions.[145-147] This figure is taken from Haass and Herlyn, 2005[148]

There is a traditional model for melanoma progression which describes six distinct steps from normal melanocytes to a metastatic malignant melanoma: development of a common nevus (1) with lentiginous melanocytic hyperplasia (2), aberrant differentiation and nuclear atypia of melanocytes (3), radial growth phase (RGP) melanoma (4), vertical growth phase (VGP) melanoma (5) and metastatic melanoma(6). [131] Figure 4 shows schematic pictures of some progression stages of melanoma.

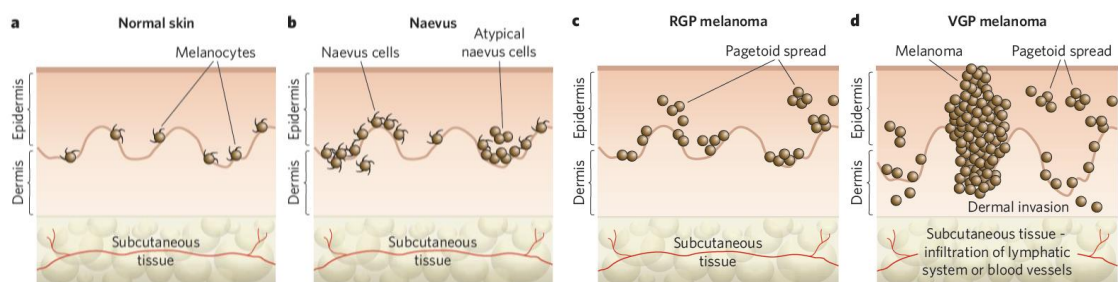


**Figure 4:** Schematic pictures of different steps in melanoma progression. (a) Normal skin. (b) Step 1: nevus. (c) Step 4: radial growth phase (RGP) melanoma. (d) Step 5: vertical growth phase (VGP) melanoma. This figure was taken from Grey-Schopfer et al., 2007.[149]

The mutation of genes involved in regulation of growth which may lead to production of autocrine growth signalling or loss of adhesion, plays a crucial role already in the first step of this progression. Especially the disruption of intercellular signalling and the consequent escape of regulation by keratinocytes enable melanocytes to proliferate and spread.[134] This seems to be the major trigger for the development of nevi and moles. Nevertheless, nevi and moles are benign and not necessarily progress to malignant tumours due to cellular senescence, a natural tumour suppressive mechanism. At the stage of radial growth phase the tumours are no longer benign, may involve micro-invasion of the dermis and can progress to VGP melanoma with metastatic potential. This progression from RGP to VGP is considered to be most critical for the outcome of the disease.[150]

However, in many cases the development of melanoma cannot be explained by this classical stepwise progression. Certainly, most melanomas arise within the epidermis and subsequently invade across the basement region, but beside these *in situ* melanomas, there are rare cases of *de novo* melanoma which originate from the dermis. Also very rarely, melanomas occur in the dermis in association with congenital nevi. Remarkably, about 50% of tumours which do not seem to have passed through the classical steps, arise without any clinical precursor lesion, suggesting that melanocyte precursor or stem cells may be another potential source for the development of melanoma.[148]

### **1.5.2 Deregulated signalling pathways in melanoma**

In order to understand the biology of melanoma, methods like comparative genomic hybridisation and analysis of mutations by gene re-sequencing have been utilised and revealed aberrant activity of several signalling pathways to be involved.

The signalling cascade along the G-protein Ras, which is attached to the inner cell membrane, and the cytosolic protein kinases RAF, MEK and ERK was found to be deregulated in a high percentage of melanoma. This pathway generally is known to regulate cell fate decisions and is activated downstream of RTKs, cytokines and

heterotrimeric G-protein-coupled receptors.[151] In normal melanocytes this cascade is activated by growth factors like FGFs, SCF (stem cell factor) and HGF (hepatocyte growth factor) which individually cause only a weak transient activation of ERK with modest mitotic effect. A combined activation of ERK by several growth factors is necessary for melanocyte proliferation [152-153] In 90% of human melanomas ERK is found to be hyper-activated and is therefore considered to be a key regulator of melanoma cell proliferation.[154] The mechanisms behind this over-activation are manifold. Frequently observed causes in melanoma are for example autocrine signals of growth factors or mutational activation of their receptors. Especially in melanoma which are not considered to arise from UV radiation exposure, like the acral and mucosal melanoma mutation or gene amplification of the RTK c-Kit, the receptor of stem cell factor, is found.[155] Furthermore, oncogenic Ras genes can be the cause for ERK hyper-activation. In about 20% of human melanomas a mutation in NRAS is found. Less frequent are mutations in one of the other two Ras genes, KRAS and HRAS, in melanoma.[156] However, the most frequently affected gene in melanoma is BRAF, which belongs besides ARAF and CRAF, to the three human RAF genes. In about 50% of all melanomas an activating BRAF mutation is found. There are 50 distinct mutations in BRAF identified but the most common is an activating substitution of valin by glutamic acid at position 600 (BRAF<sup>V600E</sup>), which accounts for 80% of all BRAF mutations in melanoma.[157-159] Besides constitutive activation of ERK, which induces proliferation and survival of the cell, BRAF<sup>V600E</sup> activates several other genes downstream like MITF (microphthalmia associated transcription factor), BRN-2 (POU domain 3 transcription factor), the cell cycle regulators cyclin D1 and P16<sup>INK4a</sup> and the tumour maintenance enzymes matrix-metalloprotease-1 and inducible nitric oxide synthetase.[149, 160] Furthermore, BRAF<sup>V600E</sup> stimulates autocrine VEGF secretion and therefore contributes to neoangiogenesis.[161] However, genetic analysis unravelled a minor subgroup of melanomas that harbour a mutation in BRAF at another position than V600, which leads to decreased activity of BRAF. This subgroup relies on CRAF activity for activation of the MAPK pathway and thereby for cell growth and survival.[159]

## Introduction

The phosphoinositide-3-OH kinase (PI3K) pathway is another signalling cascade which was frequently found deregulated in melanoma. These kinases hyper-phosphorylate membrane lipids, the phosphoinositides, which are thereby converted to second messengers and activate downstream effector pathways.[162] Several cellular conditions, like survival, proliferation, growth in respect of cell mass and motility are regulated by the PI3K pathway. In a high proportion of melanomas, this signalling cascade is hyper-activated. Mutations in PI3K itself are quite rare and occur in only 3% of metastasising melanoma.[163] Nevertheless, over-expression of Akt (PKB, PI3K effector protein kinase B) is found in 60% of melanomas.[164] PTEN (phosphate and tensin homologue) negatively regulates the PI3K pathway activity. Five to twenty percent of late stage melanomas harbour a loss-of-function mutation in PTEN that leads to hyper-activation of the pathway.[165]

Interestingly, a study of three dimensional melanoma cell cultures showed that both pathways, ERK and PI3K signalling need to be inhibited to suppress cell growth, which suggests the importance of dual inhibition in melanoma treatment.[166] Genetic analysis of melanomas unravelled that mutations of NRAS and BRAF, or NRAS and PTEN are mutually exclusive, but a combination of mutations in BRAF and PTEN occurs in 20% of the cases. This led to the conclusion that Ras must act upstream of BRAF and PTEN and therefore activate both pathways.[149]

An important feature of melanoma to enable proliferation is the sustained expression of MITF (microphthalmia-associated transcription factor). This transcription factor is the major regulator of melanocyte biology, affecting expression of melanogenic proteins, melanoblast survival and melanocyte lineage commitment. The level of expressed MITF is essential for the effect on the cells. High levels reduce cell proliferation and tumourigenicity, whilst critically low levels induce cell cycle arrest and apoptosis. Only at moderate expression levels, MITF allows proliferation.[167-168] Additionally, MITF can support melanocyte transformation in combination with BRAF.[169] However, activated ERK phosphorylates MITF which is thereby tagged for degradation. Hence, constitutively active ERK leads to constant down-regulation of

MITF. How melanomas recover MITF expression is not quite clear, since only 10-16% of metastatic melanoma show gene amplification of *MITF*. Anyway, *MITF* harbours a TCF/Lef (T-cell factor/lymphoid enhancer factor) binding site and is therefore targeted by  $\beta$ -catenin. Although stabilising  $\beta$ -catenin mutations are rare in melanoma,  $\beta$ -catenin reservoirs in cells is found in 28%.[170-172] Besides, mutations causing up-regulation of  $\beta$ -catenin are more common. These may be mutations which lead to silencing of APC (adenomous polyposis coli), over-expression of transcription factor SKI or alterations in p14<sup>ARF</sup>. [173-174]

### 1.5.3 Senescence and how it is overcome in melanoma

“Replicative senescence” is a normal process of diploid cells, by which the ability to divide is lost after a finite number of divisions. It is caused by telomere shortening and tumour suppressors are activated.[175] “Stress-induced senescence” is a similar process caused by DNA-damage, oxidative stress, or oncogenes. Accordingly, senescence represents a barrier to many types of cancer which needs to be overcome during tumour progression.[176] BRAF<sup>V600E</sup>, for example, is a typical melanocyte senescence inducing oncogene.

Senescence is a very complex mechanism, however, two central inducers are the tumour suppressors p53 and RB (retinoblastoma protein).[177] The gene locus CDKN2 (cyclin-dependent kinase 2) encodes for 3 additional tumour suppressors, p14<sup>ARF</sup>, p15<sup>INK4b</sup> and p16<sup>INK4a</sup>. p14<sup>ARF</sup> activates p53, p16<sup>INK4a</sup> inhibits deactivation of RB and p15<sup>INK4b</sup> is suggested to have a back-up function for p16<sup>INK4a</sup>. [178-179] Nevertheless, it was shown that p14<sup>ARF</sup> can induce senescence in a p53 independent manner as well. Studies with murine melanocytes and fibroblasts suggested that the importance of each of these tumour suppressors in senescence is cell type dependent and unlike fibroblasts melanocyte senescence seems to be strongly regulated by p14<sup>ARF</sup> and not by p53.[180-181] These findings are consistent with the fact that p53 mutations, frequently found in human cancers, have a rare occurrence in melanoma of about 9%. Indeed, aberrations of the CDKN2 locus are quite common in familial melanoma and

most frequently affect p16<sup>INK4a</sup>, sometimes p14<sup>ARF</sup> and rarely p15<sup>INK4b</sup>. Additionally, genetic or epigenetic inactivation of p14<sup>ARF</sup> is frequent in melanoma.[182-185]

### 1.5.4 Strategies of therapy

Due to the manifold etiologies of melanoma several approaches on targeted treatment have been tested by now.

Since BRAF is the most commonly mutated gene in melanoma, a number of small molecule BRAF inhibitors have been developed and tested *in vitro* for potential applicability in clinical studies. The first one to be extensively studied was sorafenib, a kinase inhibitor which was originally developed as CRAF inhibitor. Although tumour regression was achieved in BRAF<sup>V600E</sup> melanoma xenografts, other studies showed that sorafenib has a very weak inhibiting effect on BRAF. The tumour repressing action may rather be achieved by inactivation of other targets like VEGFR or PDGFR, and may be independent of BRAF inactivation. Clinical trials with sorafenib showed very low response rates in melanoma cases with activating BRAF mutations. Nevertheless, sorafenib showed pro-apoptotic activity on melanoma cell lines with low activity BRAF mutations which generally rely on CRAF activity.[186-188] More recently developed BRAF inhibitors were developed with higher specificity for BRAF. Preclinical studies have been undertaken of dabrafenib, vemurafenib, SB590885, AZ628, XL281 and GDC08-79.[189-192] Vemurafenib is an ATP-competitive RAF inhibitor and was found to selectively inhibit growth of BRAF<sup>V600E</sup> mutated melanoma cell lines and mouse xenografts.[190, 193-194] Forty eight percent of BRAF<sup>V600E</sup> mutated melanoma patients responded to vemurafenib treatment, which led to its rapid clinical approval and application for the treatment of BRAF<sup>V600E</sup> mutated metastatic melanoma.[195] Nevertheless, a significant percentage of BRAF<sup>V600E</sup> mutated melanoma showed intrinsic resistance to vemurafenib.[191] Retrospective genetic studies could not detect any differences between vemurafenib sensitive and resistant cell lines suggesting a quite complex mechanism of resistance.[196] Unfortunately, almost all BRAF mutated melanomas, which responded to vemurafenib ultimately developed resistance and



## Introduction

therapy failed.[197] Dabrafenib is an ATP-competitive inhibitor of BRAF mutants V600E/D/K, wild-type BRAF and CRAF and is currently clinically evaluated.[198] Unexpectedly treatment with sorafenib, vemurafenib, dabrafenib and XL281 induced proliferative squamous lesions as side effects. Clinical evidence suggests a paradoxical activation of the MAPK pathway as a result of BRAF inhibition in these lesions.[199]

The members of the Ras protein family are low-molecular-weight GTP-binding proteins and located at the plasma membrane, which are difficult to target. Farnesyl transferase inhibitors (FITs) were developed to target Ras by preventing membrane localization. Unfortunately FITs showed only weak single-agent anti-tumour activity.[200]

Consequently, attention was directed to find tractable downstream targets. Eventually, efforts to develop MEK inhibitors have been made. Although clinical responses of most of these inhibitors were disappointing, the MEK inhibitor trametinib showed a 20% response rate in BRAF<sup>V600E</sup> mutated melanoma patients.[201]

Currently there are 5 small molecular c-Kit inhibitors approved for treatment of GIST (gastrointestinal stromal tumors) and CML (chronic myeloid leukemia), imatinib, dasatinib, nilotinib, sorafenib and sunitinib. Recent studies suggest that these inhibitors may be applicable in c-Kit mutated melanoma as well and that the nature of the individual c-Kit mutation could possibly predict the response to these inhibitors, which would enable a targeted therapy matched to the mutation.[202-203]

In light of these data the benefits of combination therapies become obvious, especially in preventing the development of drug resistance of the tumour after a period of response. In most cancer types, such drug resistances can be acquired by *de novo* mutations in the drug-target gene. But there is no evidence for *de novo* mutations in relapsing melanoma. Potential resistance mechanisms of melanoma imply up-regulation of other signalling pathways, mainly PI3K or MEK/ERK.[204] Promising results have been achieved by dual treatment simultaneously inhibiting BRAF and MEK or MEK and PI3K by which the onset of resistance was overcome.[205-206]

## Introduction

Recent preclinical studies, however, unravelled data that highlight the importance of melanoma genotype analysis as basis for choosing the optimal therapy for each individual patient. One of these emerging findings is that BRAF inhibitors paradoxically activate MAPK activity in tumours which lack a BRAF activating mutation.[207] Vemurafenib and others are on the one hand able to inhibit BRAF<sup>V600E</sup> activity but on the other hand can induce CRAF homodimers in melanomas with Ras mutations leading to MEK activation.[208] In NRAS mutated melanoma vemurafenib can increase invasive potential by activation of ERK and FAK (focal adhesion kinase).[209] Several BRAF inhibitors were found to suppress apoptosis by modulating Mcl-1 (myeloid cell leukemia sequence 1) expression in NRAS mutated melanomas and thereby contribute to tumour progression.[210]

## 1.6 Aims

Previous studies [211] determined expression patterns of FGFs in melanoma. Figure 5 shows collected expression array data from 11 melanoma xenografts.

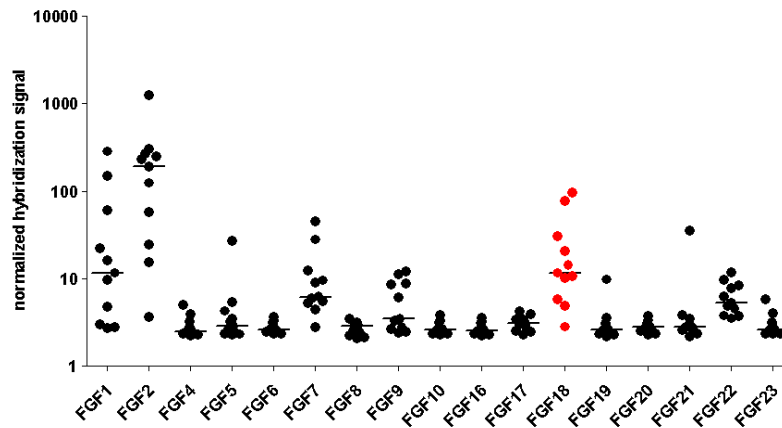


Figure 5: Collected expression array data of FGFs in melanoma.

The data shows that FGF1 and FGF2 are most prominently expressed in melanoma amongst all genuine FGFs and there have already been some efforts to unravel the distinct roles of these two ligands in melanoma. Interestingly, the median expression of FGF18, in the samples, highlighted in red in figure 1, is almost exactly the same as that of FGF1 making FGF18 one of the most highly expressed FGFs in melanoma.

Studies on colorectal cancer unravelled pro-tumourgenic effects of FGF18 via autocrine and paracrine signalling. FGF18 expression was found to be elevated in colon carcinogenesis and highly expressed in carcinoma. Up-regulation was found in 34 out of 38 colorectal tumours.[128]

Although FGF18 is expressed in quite high levels not only in melanoma but in melanocytes as well [212], the strong pro-tumourgenic action of this ligand in colorectal carcinoma provides a rationale for detailed investigation of the role of FGF18 in melanoma.

## Introduction

One main aim of this thesis was to expand the expression data of FGF18 transcript expression to a larger panel of melanoma cell lines and to investigate the expression of FGF18 protein in tissue samples of human primary and metastatic melanoma.

The role of canonical Wnt-pathway activation, in melanoma progression is so far not well understood, especially because literature reports concerning  $\beta$ -catenin expression in melanoma are quite ambiguous. On the one hand, downregulation of  $\beta$ -catenin was found in correlation with tumour progression. [213-215] On the other hand, up-regulation of phospho- $\beta$ -catenin was found to correlate with poor outcome.[216] In colorectal cancer, the elevated expression of FGF18 is based on the constitutive activation of the Wnt-pathway, and a direct correlation between Wnt-pathway activity and FGF18 expression level was found in colorectal carcinoma as shown in figure 6.[128, 217] Accordingly, another aim of this thesis was the examination of Wnt/ $\beta$ -catenin signaling activity and whether FGF18 expression is controlled by this pathway in melanoma cell lines.

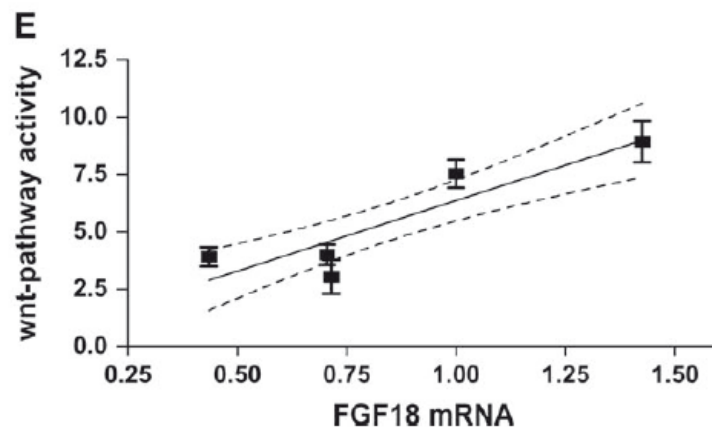


**Figure 6:** Correlation of FGF18 mRNA levels and Wnt-pathway activity was determined by linear regression and was found to be highly significant. This figure was taken from Sonvilla et al., 2008. [128]

Previous expression analysis of FGFR genes in melanoma revealed that the predominantly expressed receptors are FGFR1 and FGFR4. Collected expression array data is shown in figure 7.[211] Figure 8 shows the percentage of positive melanoma

## Introduction

cell lines for each of the FGF receptor variants. [218] Considering the fact that FGF18 is predominantly bound by FGFR3 IIIc and FGFR4, this data leads to the suggestion of autocrine signalling cascades in melanoma via FGF18.

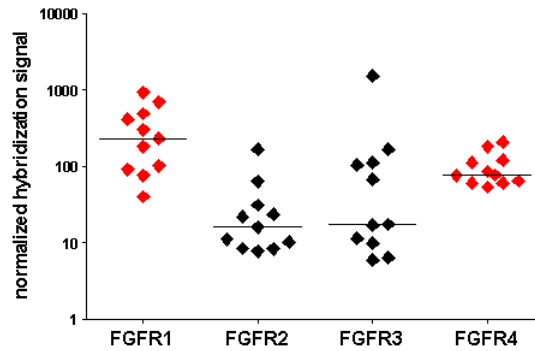


**Figure 7: Collected expression array data of FGF receptors in melanoma.**

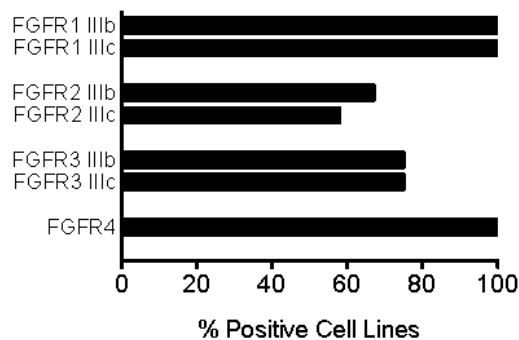


**Figure 8: Presence of all four FGF receptors and their isoforms displayed as percentage of positive melanoma cell lines. RT-PCR data of 12 cell lines. This figure was taken from Sonvilla et al., 2008.[218]**

These presumed autocrine signals were also subject of investigation in the course of this diploma thesis. Specifically, the focus was laid on examining the effects of FGF18 on viability, motility and invasion of selected melanoma cell lines.

Besides VEGFs (vascular endothelial growth factors), FGFs are known to be involved in angiogenesis during embryonal development and wound healing.[219] Sustainment of angiogenesis of lymph and blood endothelia is a major requirement for progression of

## Introduction

tumourigenesis and metastasis. So far, especially FGF2 was found to have inductive effects on angiogenesis in a paracrine manner in melanoma and other cancer types.[220-221] FGF18 was found to promote angiogenesis in hepatocellular and colorectal carcinoma.[128-129] To investigate a potential role of FGF18 in melanoma angiogenesis the ability of lymph and blood endothelial cells to receive paracrine signals via FGF18 was determined. Furthermore, in skeletal development, FGF18 is known to induce VEGF expression and thereby coordinates neovascularisation of the growth plate.[222] On these grounds, interest was laid on whether FGF18 may contribute to neoangiogenesis in melanoma by up-regulating VEGF expression.



## II. Materials and Methods

A total of 28 different lines representing different stages and types of melanoma were used for comparative analysis to unravel the role of FGF18. Table 2 gives an overview of the used cell lines with respective melanoma type and origin in terms of stage of progression and tissue of which they have been gathered from.

**Table 2: List of analysed melanoma cell lines with information about respective origin and subtype.**

cell line		origin	subtype	cell line		origin	subtype
FTSLA/a	VM-1	LN	SSM	MYAH	VM-16	ME	unknown
GCRF	VM-2	PT	NM	RALL	VM-19	PT	SSM
GLJ	VM-4	LN	NM	RHTP	VM-21	PT	NM
GTBS	VM-7	PT	NM	RKTJ	VM-23	PT	NM
GUBS/a	VM-8	LN	NM	SHTJ	VM-24	LN	unknown
GYK	VM-9	BN	SSM	TMFI	VM-28	BR	unknown
HOIN	VM-50	BR	NM	WCRE	VM-30	PT	SSM
HOST	VM-47	BR	NM	WLTJ	VM-31	ME	NM
JMUM	VM-10	PT	SSM	WPZA	VM-32	PT	NM
JTST	MV-11	ME	NM	XAPG	VM-44	PT	SSM
KAKA	VM-48	BR	NM	XBNE	VM-34	SC	unknown
KRFM	VM-13	ME	NM	XZFI		unknown	unknown
LCWC	VM-14	LN	NM	YDFR	VM-41	BR	unknown
MJZJ	VM-15	LN	unknown	skmel		unknown	unknown

**Legend: (VM) Vienna Melanoma number, official denotation; origin: (PT) primary tumour, (SC) subcutaneous, (LN) lymph node, (BN) bone metastases, (BR) brain metastases, (ME) malignant effusions. Subtypes: (NM) nodular melanoma, (SSM) superficial spreading melanoma.**

Several approaches were applied in order to reveal the expression, regulation and function of FGF18 in melanoma. One approach of investigating FGF18 expression was done on protein level by evaluation of a tissue micro-array containing samples from nevi, melanoma primary tumours and metastases. The second approach was performed on the melanoma cell lines. Via quantitative Real-Time Polymerase Chain Reaction (qRT-PCR), expression on RNA level was evaluated.

To determine whether Wnt-pathway may play a role in the regulation of expression of FGF18 in melanoma, as it was shown for colorectal cancer [128], Wnt-pathway activity



was examined in several melanoma cell lines. Subsequently, this data was tested for any correlation to the FGF18 expression data.

Melanoma cell lines with knock-down of FGF18 and FGF18 over-expressing melanoma cell lines were established, in order to examine the role of autocrine signalling of FGF18 in melanoma. A set of assays was performed to unravel effects of FGF18 on viability, motility and auxiliary skills for metastasis of these knock-down or over-expressing clones. Applied assays associated to viability were MTT assay, apoptosis assay, clonogenicity assay, cell cycle analysis and establishment of growth curves. To investigate changes in migration and metastasis auxiliary skills, scratch assay, transmigration assay, invasion assay and anchorage-independent growth assay were performed.

In order to analyze the possibility that FGF18 could contribute to angiogenesis, telomerase immortalised lymph (LECs, T1S1) and blood (BECs, G1S1) endothelial cell lines were included in the study. Expression analysis of FGF18 and the four FGF receptors in these cells was done on the RNA level. To analyse whether FGF18 contributes to angiogenesis by activating VEGF expression, correlation between expression of fGF18 and VEGF-A in melanoma cell lines was determined.

### **2.1 Cell culture**

All melanoma cell lines were cultivated at 37°C and 5% CO<sub>2</sub> atmosphere in RPMI-1640 medium containing 10% foetal calf serum (FCS), abbreviated R10. According to requirements either T25 or T75 cell culture flasks were used. Approximately twice a week, confluent cells were washed with 1 x Dulbecco's PBS +/- purchased from PAA then treated with trypsin/EDTA from Sigma and then passaged at a ratio of 1:10.

## 2.2 Expression analysis on protein level - Tissue Micro Array

A tissue micro array containing 100 nevi or melanoma tissue samples plus a negative control of hepatocellular carcinoma was purchased from Biomax. Twenty four of these 100 samples were from benign nevi and 56 from primary tumours, of which one sample was stage 1, 48 stage 2, 5 stage 3 and 2 were stage 4 tumours. The residual 20 samples were metastases. The immunohistochemical staining of this tissue micro array was carried out by my colleague Andreas Lackner. Three different genes were detected and analysis was performed with primary antibody, enhancers and HRP (horse reddish peroxidase) polymer tertiary antibodies (UltraVision, Thermo Scientific). For staining of FGF18 a goat anti-human antibody, that had already been evaluated in previous studies (Sonvilla *et.al.* 2008 [128]) was used in combination with DAB+ (3,3' Diaminobenzidine ) chromogen. S100B antibody was applied in combination with AEC (3-Amino-9-Ethylcarbazole) chromogen. Staining of the proliferation marker Ki67 was also performed but proved not to be beneficial for the evaluation. Haematoxylin was used as counterstain. S100B is an antigen found on benign melanocytic lesions and in malignant melanomas, although the latter show decreased S100B antibody staining in correlation with low proliferation rates.[223] This staining served to distinguish melanocytic tissue from other epidermal tissue. The control samples were stained solely with blue haematoxylin but also display the brown melanin pigments which are produced by melanocytes. This is very important for the evaluation of the intensity of the brown FGF18 staining, whereat the pigment staining needs to be subtracted. FGF18 staining in hair follicles was also not comprised in the evaluation. By comparing the control staining, the FGF18 staining and the S100B staining the intensity of the melanocytic tissue of all 100 samples was comparatively evaluated. Each sample was assessed with a number between 0 and 3, whereby 0 stands for no visible staining, 1 for slight, 2 for distinct, and 3 for intense staining by FGF18 antibody. Figure 9 shows the different stainings of one sample.

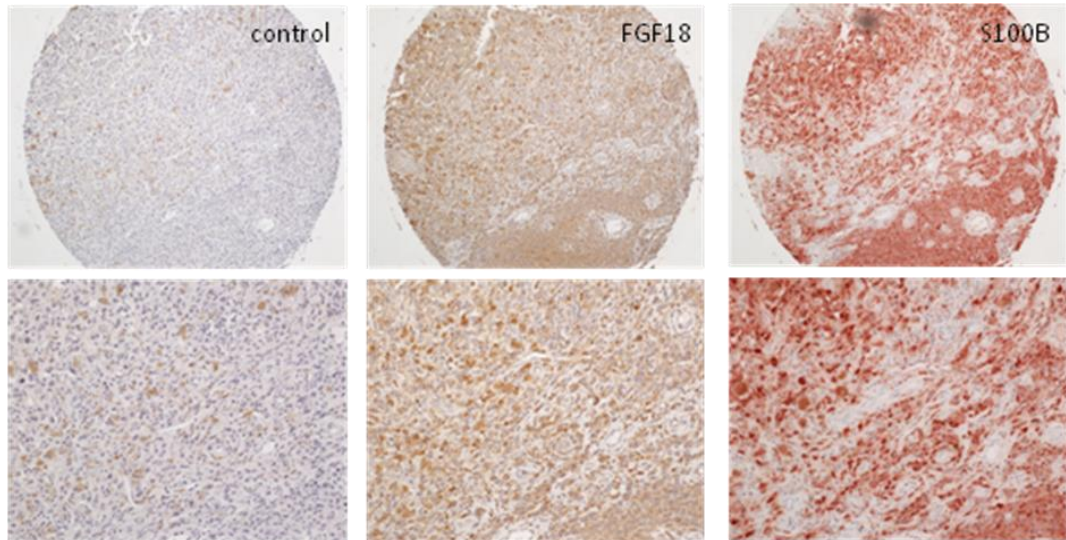


**Figure 9: Exemplary pictures of control staining, FGF18 and S100B antibody staining of tissue samples of a primary tumour stage 2 in 10x and 20x magnification.**

### 2.3 Expression analysis on RNA level

In this analysis of expression level of a certain gene, the relative amount of mRNA of the respective gene compared to a housekeeping gene was measured by qRT-PCR. Therefore, the first step was to extract RNA from the cells to be analysed. In order to increase stability of the genetic sequences of the RNA and thus making applicable for qRT-PCR the synthesis of cDNA was necessary. RT-PCR was performed in an ABI 7500 Real-Time PCR system. This method was applied for analysis of FGF18 and VEGF-A expression in melanoma cell lines as well as of FGF18 and FGFR 1-4 expression in LECs and BECs.

#### ***RNA extraction***

A T25 flask containing the required cell line at a confluence of 80% was used for this RNA extraction protocol. After removing the growth medium from the flask and washing the cells with 1 x PBS, 3 ml of guanidinium-thiocyanate-chloroform-phenol (TRIzol) were added. After 5 minutes of incubation at room temperature the lysate was transferred to a tube. Point two ml of chloroform were added per ml TRIzol.

## Materials and Methods

Guanidinium-thiocyanate denatures proteins and releases rRNA from ribosomes. After vortexing, the lysate was centrifuged at 12000 g for 15 minutes at a temperature between 2-8°C. A biphasic-mixture developed. The lower organic phase mainly consisted of chloroform and contained all proteins. The nucleic acids were dissolved in the upper aqueous phase which was collected in a new tube for further purification. Point five ml isopropanol were added per ml TRIzol, which precipitates RNA. After mixing vigorously and incubating for 10 minutes at room temperature, the mixture was again centrifuged at 13000 g for 10 minutes at a temperature between 2-8°C. The supernatant was discarded and the pellet was washed with 1 ml 75% ethanol by vortexing and was subsequently centrifuged at 7500 g for 5 minutes. The ethanol supernatant was again discarded and the pellet was air-dried, then resuspended in 15 µl RNase-free ddH<sub>2</sub>O. Concentration and purity of the RNA were measured with a NanoDrop spectrophotometer. Nucleic acids show absorbance at 260 nm by which the amount of RNA can be determined. The ratio of absorbance at 260 nm and 280 nm indicates the grade of contamination by proteins. The value 260 nm / 230 nm shows contamination by other organic compounds. Pure RNA shows ratio values of 260 nm / 280 nm between 1.8 and 2 and of 260 nm / 230 nm above 1. Only samples meeting these criteria were used for further analysis. After measurement of purity and concentration, integrity of the RNA was examined by agarose-gel electrophoresis. One µg of each RNA sample was taken up in 5 µl RNase-free ddH<sub>2</sub>O and 5 µl of urea buffer were added. After denaturing the RNA at 70°C for 3 minutes the RNA was stained with 2 µl of the fluorescence stain Vista Green. The mixture was loaded onto a 1.5% agarose-gel. Gel electrophoresis was performed at a voltage of 80 V for 30 minutes. The RNA was examined via a fluorescence detecting imager. Intact RNA shows two distinct bands of 28S ribosomal RNA and 18S rRNA. Degraded RNA would appear as smear on the gel. The RNA was stored at -80 °C.

### ***cDNA synthesis***

Two µg RNA were filled up to 13 µl with RNase-free H<sub>2</sub>O. For denaturation the RNA was heated up to 70°C for 10 minutes. For each RNA sample to be transcribed, 4 µl of 5

## Materials and Methods

x buffer RT, 1 µl dNTPs (10mM each), 1µl reverse transcriptase (200 u/µl), 0.5 µl Riboblock RNase inhibitor (40 u/µl) and 1 µl random primers (0.2 µg/µl) were used. After adding the 13 µl RNA, the mix was incubated at 42 °C for 1 hour. In order to stop the reaction, the mixture was heated up to 70°C for 10 minutes again. Finally 20 µl of RNase-free H<sub>2</sub>O were added and the synthesised cDNA was stored at -20°C.

### **qRT-PCR**

For normalization of all different melanoma cell lines the mRNA amount of the housekeeping gene GAPDH was synchronously measured with FGF18. In the same manner, analysis of VEGF-A in melanoma cells and FGFR1-4 and FGF18 in LECs and BECs was performed. Individual TaqMan probes (TaqMan® Gene Expression Assays, AppliedBiosystems™), for each of the analysed genes, were used for qRT-PCR. Per sample 6.25 µl polymerase and nucleotides mix (Maxima™ Probe/ROX qPCR Master Mix, Fermentas), 0.625 µl of the respective TaqMan probe, and 0.625 µl ddH<sub>2</sub>O were used and prepared in a Master Mix. After pipetting 7.5 µl of Master Mix into the 96 well plate and adding 5 µl of the fivefold diluted cDNA, the amplification was started (see table 3). All analyses were performed in duplicates.









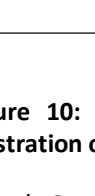
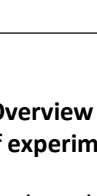
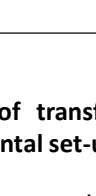
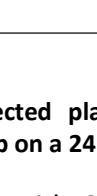
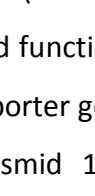
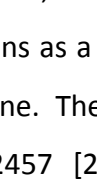
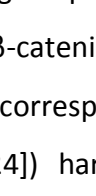
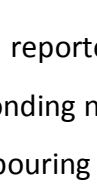
**Table 3: Programmed stages for Taqman qRT-PCR**

	temperature	time	repetitions
stage 1	50 °C	2'	1x
stage 2	95 °C	10'	1x
stage 3	95 °C	15''	40x
	60 °C	1'	

## 2.4 Determination of the impact of Wnt-pathway activity on FGF18 expression

### Analysis of Wnt-pathway activity in melanoma cell lines

For this intent the use of a reporter gene system, referred to as TOP/FOP assay was chosen. Cells were seeded into 24 well plates and each cell line was transfected with four different combinations of 5 different plasmids. All combinations were tested in duplicates. Figure 10 shows an overview of the plasmid combinations and the respective functions.

24 well-plate					transfected plasmids	function
				combination „TOP“	TOP A87 A16	$\beta$ -catenin reporter internal luciferase standard examination of transfection efficacy
				combination „FOP“	FOP A87 A16	negative control for $\beta$ -catenin reporter internal luciferase standard examination of transfection efficacy
				combination „luciferase“	A115 A87	positive control for luciferase detection internal luciferase standard
				combination „EGFP“	A16	examination of general transfection efficacy Luciferase negative, blank values

**Figure 10: Overview of transfected plasmid combinations and their functions with schematic illustration of experimental set-up on a 24 well plate.**

TOP (TOPFlash, Addgene plasmid 12456 [224]) is a plasmid with 7 TCF/Lef binding sites and functions as a  $\beta$ -catenin reporter plasmid. TOP also encodes a firefly luciferase as reporter gene. The corresponding negative control plasmid is FOP (FOPFlash, Addgene plasmid 12457 [224]) harbouring mutated TCF/Lef binding sites and the firefly luciferase gene. Reporter gene activity of FOP therefore displays false positive signals of TOP. A plasmid called pLUC encoding the firefly-luciferase gene controlled by a CMV (cytomegalovirus) promoter was used as positive control for luciferase activity (pLuc-IRESe-EGFPneo). pEGFP (pEGFP-N3, Clontech) is a plasmid that encodes an enhanced

## Materials and Methods

green fluorescent protein (EGFP) and was transfected into separate cell layers on the one hand, and on the other hand co-transfected with the plasmids TOP and FOP, which enables quick examination of general transfection efficacy by fluorescence microscopy. Figure 11 shows two examples of cell lines with different transfection efficacies visible by fluorescence microscopy. Additionally, pEGFP transfected samples functioned as luciferase negative blanks. To create an internal standard for luciferase activity and avoid erroneous evaluation due to differences in transfection efficacy amongst samples and cell lines, the plasmid pRL (Promega), harbouring a *Renilla*-luciferase gene was co-transfected.

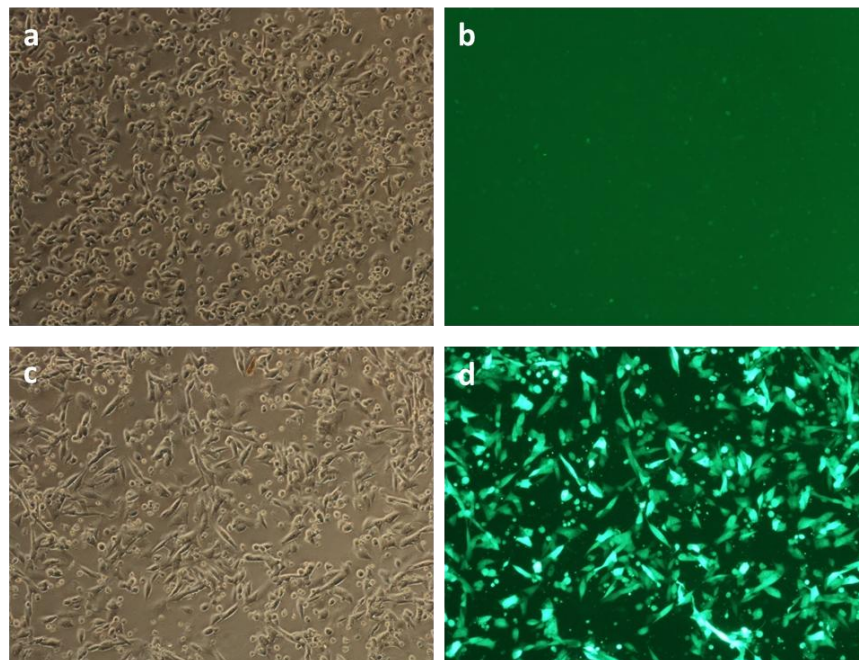


**Figure 11: Examples of two melanoma cell lines with different transfection efficacies. (a) FTSLA phase contrast image, (b) FTSLA fluorescence microscopy, EGFP signal; (c) MJZJ phase contrast image, (d) MJZJ fluorescence microscopy, EGFP signal.**

For analysis, the Dual-Luciferase® Reporter Assay kit (Promega) was applied. This kit consists of a Passive Lysis Buffer to lyse the cells, a Luciferase Assay Reagent II (LARII) which contains beetle luciferin - the substrate for firefly-luciferase -and a Stop&Glo Reagent which arrests firefly-luciferase activity and contains Coelenterazine, the substrate for *Renilla*-luciferase. When adding these substrates subsequently to the cell

lysate, activity and therefore amount of both luciferases can be measured easily by luminescence. The measurement was done with a TECAN Injector Luminometer.

### ***TOP/FOP Assay – protocol***

In the evening of day 1, 2 wells of a 24 well plate were seeded with  $1.88 \times 10^5$  cells in 500  $\mu$ l R10 medium per plasmid combination, per cell line. In the morning of day 2, when the cells had reached about 50% confluence, the transfection was performed. For each well, 2  $\mu$ l Lipofectamine® 2000 (Invitrogen) were mixed with 48  $\mu$ l OPTI-MEM® I Reduced Serum Medium (Gibco) and incubated for 5 minutes at room temperature. In the meantime the plasmid combinations were mixed and filled up to 50  $\mu$ l per well with OPTI-MEM®. Table 4 shows the applied amount of each plasmid in the respective plasmid combination. Each plasmid/ OPTI-MEM® solution was then mixed 1:1 with Lipofectamine® 2000 / OPTI-MEM® solution and incubated for 20 minutes at room temperature. In each well medium was exchanged for 300  $\mu$ l fresh R10 before 100  $\mu$ l of the respective transfection mixture were added to the cells. See figure 10 for experimental set-up.

**Table 4: Applied amounts of plasmids in the respective combinations.**

	plasmid 1	plasmid 2	plasmid 3
plasmid combination „TOP“	100 ng pRL	800 ng TOP	800 ng pEGFP
plasmid combination „FOP“	100 ng pRL	800 ng FOP	800 ng pEGFP
plasmid combination „luciferase“	100 ng pRL	800 ng pLUC	
plasmid combination „EGFP“	800 ng pEGFP		

After 6 hours, medium was removed and 500  $\mu$ l fresh R10 medium were added. Twenty-four hours later all wells were treated with 10 mM lithium chloride. Another 24 hours later, on day 4, transfection efficacy was checked for GFP fluorescence by microscopy in order to decide whether further analysis was expedient. Since luciferase assays are very sensitive in principle, analysis was continued even with very low GFP signals. The cells were washed with 1 x PBS before 100  $\mu$ l of 1 x Passive Lysis Buffer were added. After incubation for 15 minutes at room temperature while shaking, the



cell lysates were transferred into 1.5 ml tubes and treated with ultra sound for 10 minutes. In order to separate cell debris from protein solution the samples were centrifuged for 10 minutes at 14000 rpm. Duplicates, in each case 10 µl of supernatant of the sample, were transferred to a white 96 well OptiPlate™-96 (Packard). The analysis was performed by an Injector Luminometer. The chosen program conducted injection of 50 µl of LARII in one well followed by measurement of luminescence for 10 seconds before carrying on with the next well. When all wells were measured for firefly-luciferase in this way, the program was repeated with Stop&Glo Reagent instead of LARII, producing values for *Renilla*-luciferase activity.

The collected data of luminescence measurements were calculated as follows. First values of blanks, hence of samples with plasmid combination “EGFP”, were subtracted from all other values. Next, values of firefly-luciferase activity of samples with combinations “TOP” and “FOP” were divided by respective values of *Renilla*-luciferase activity, leading to a normalisation to enable comparative analysis of different cell lines. Last, a relative value of  $\beta$ -catenin activity to the negative control samples was calculated by dividing the normalised firefly-luciferase values of combination “TOP” by the normalised firefly-luciferase values of combination “FOP”. The result is the ratio between the false positive signal intensity of the combination “FOP” and the actual  $\beta$ -catenin reporter signal intensity of the combination “TOP”.

### **2.5 Potential of autocrine signalling of FGF18 in melanoma**

In order to investigate autocrine signalling of FGF18 in melanoma cells, two cell lines were chosen for exemplary analysis. The cell line FTSL/a expresses FGF18 on a moderate level and was utilised to examine the effects of FGF18 knock-down. In parallel, overexpression of FGF18 was induced in this cell line. MJZJ is the second cell line, chosen for analysis. Since MJZJ has a very low endogenous expression level of

FGF18, establishment of a knock-down was not considered reasonable, but the cell line was suitable for experiments with induced overexpression.

### 2.5.1 Establishment of FGF18 knock-down in FTSL/a

RNA interference was the chosen method to silence gene expression of FGF18 in FTSL/a. Stable knock-down clones were created by stable transfection via lentiviral particles carrying small hairpin RNA (Thermo Scientific, Open Biosystems, Expression Arrest GIPZ Lentiviral shRNAmir) . These replication incompetent lentiviral particles carry several sequences on their genome to facilitate simple application for the user as well as efficient generation of knock-down clones as figure 12 shows.

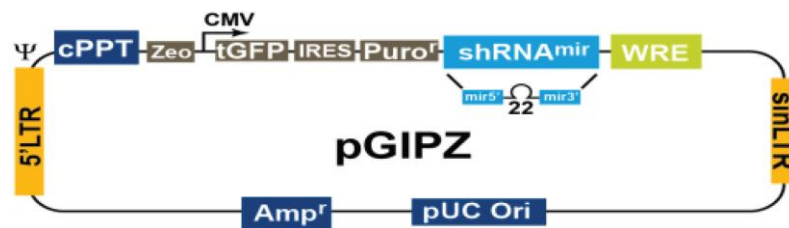
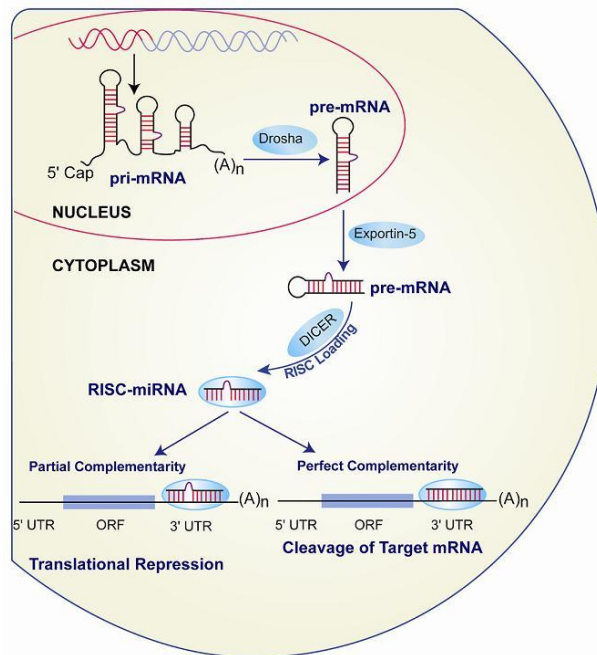


Figure 12: Lentiviral vector plasmid (Thermo Scientific, Open Biosystems Expression Arrest GIPZ Lentiviral shRNAmir Technical Manual).

### RNA interference

RNA interference by small hairpin RNA is a natural mechanism of eukaryotic cells and functions in post-transcriptional gene silencing. This process (see figure 13) starts with the expression of a primary micro RNA that forms a hairpin structure. In the nucleus, the dsRNA specific ribonuclease Drosha processes the pri-miRNA to pre-miRNA. Subsequently the pre-miRNA is delivered into the cytoplasm by Exportin-5 where Dicer cleaves off the hairpin-loop, separates the complementary strands of the dsRNA and enables the formation of a complex with RISC. Depending on whether the complementary sequence matches the target mRNA perfectly or partially, the binding of the RISC complex to the target leads to translational repression or degradation of

the mRNA. In both cases, no protein is produced from the targeted mRNA and the gene is silenced.[225-226]



**Figure 13: RNA interference** ([http://www.genscript.com/siRNA\\_technology.html](http://www.genscript.com/siRNA_technology.html) accessed on 9/26/12)

The special design of Thermo Scientific Open Biosystems Expression Arrest GIPZ Lentiviral shRNAmir leads to expression of human micro RNA 30 (miR30) primary transcripts in the transfected cell. These miR30 sequences provide recognition sites for the dsRNA specific ribonuclease Drosha. Due to this miR30 design the processing efficiency by Drosha in the nucleus and Dicer in the cytoplasm is 10 times higher than in other shRNA designs [227]. Consequently, more siRNA/miRNA is produced and the knock-down ability is potentially higher. Another design feature of the construct provides strand specific incorporation into the RISC (RNA induced silencing complex), which also increases efficacy. The complementary target sequence itself shows more than three mismatches to any other human or murine genome sequence.

A set of three FGF18 knock-down viruses differing in their small hairpin target sequences within the human FGF18 gene, referred to as “6”, “7” and “8”, was applied. Additionally, a positive and a negative control knock-down virus were used. The

positive control virus targets the housekeeping gene GAPDH and the negative control a non-silencing construct, carrying a small hairpin which is not complementary to any human sequence.

### ***Procedure of lentiviral transduction***

Sixteen thousand cells were seeded per well of a 96 well-plate in 100  $\mu$ l of R10. After incubation of 20 hours at 37°C and 5% CO<sub>2</sub> the transfection was started. For that purpose the medium was changed to 110  $\mu$ l of fresh medium containing 8  $\mu$ g/ml polybrene. Virus particles of an MOI (multiplicity of infection) of 10, hence ten viral particles for each seeded cell, were added. Triplicates for each viral construct were applied. After another 20 hours of incubation at 37 °C and 5% CO<sub>2</sub> the medium containing the viral particles was taken off and 120  $\mu$ l fresh R10 were added. Two days after transfection, the selection with puromycin was started. In addition to fresh R10, 0.8  $\mu$ g/ml puromycin was added to two of the three wells containing transduced cells of each viral construct. Additionally, untransduced control cells were treated, to determine the efficacy of puromycin selection. One well per viral construct was not treated with puromycin and received fresh R10 only, in order to create clones which would be selected subsequently via Fluorescent Activated Cell Sorting (FACS) on the basis of GFP expression. On day 3 after transfection, the cells, which had not received puromycin were expanded to a 6 well plate in 2 ml of R10. After five days the medium was changed. Another 8 days later, a big part of the cells were not attached to the bottom of the well but still alive, which was why the supernatant of the wells was transferred to another 6 well plate. The cells in the old well as well as the transferred ones received fresh R10. Six days after starting the antibiotic selection, the concentration of puromycin was raised to 2  $\mu$ g/ml, since the survival of untransfected, but treated cells indicated 0.8  $\mu$ g/ml as an insufficient amount. Additionally, the cells received fresh R10. Sixteen days after transfection, cells of one of the two wells per viral construct were expanded to a 6 well plate and received 2 ml of fresh R10 with 2  $\mu$ g/ml puromycin. The remaining wells on the 96 well plate also received 100  $\mu$ l fresh R10 containing 2  $\mu$ g/ml puromycin. Twice a week the cells received fresh medium. The

## Materials and Methods

ones on selection were always treated with 2 µg/ml puromycin additionally. Thirty one days after transfection, the cells treated with the viral constructs GAPDH shRNA and sh non-silencing control, which did not receive puromycin, had built a stable layer in the 6 well and were expanded to a T25 Flask. Two days later, the unselected FGF18 knock-down clones were also ready for such an expansion. The puromycin treated cell lines generally showed lower proliferation velocity and were cultured for further 14 days before they were ready for expansion into a T25 flask. Again the cells received fresh R10 and respectively 2 µg/ml puromycin twice a week till they formed a confluent layer. Next the unselected but transfected cell layers of each virus construct were split and partitioned to two T25 flasks, of which one was sorted by FACS. Afterwards the cells were partitioned to two T25 flasks again. The cells of one flask were frozen for backup as soon as the layer was confluent again. The transfected and puromycin selected cells were also frozen for storage, but not used for further experiments, since the unselected cells were preferred for examination.

### Freezing living cells

To freeze backups of the stably transduced cells, DMSO, dimethyl sulfoxide, was added to the medium and functions as cryoprotectant.

The medium was removed from the T25 flask and the cells were washed with 1 x PBS, before 700 µl of trypsin were added. After 5 minutes of incubation at 37°C and 5% CO<sub>2</sub> it was checked microscopically, whether the cells had detached from the flask ground before 4.3 ml 10% serum medium were added and the cells were collected in a 15 ml tube. The cells were centrifuged at 700 rpm for 5 minutes and the supernatant was discarded. The cell pellet was resuspended in 3 ml R10 and 150 µl DMSO were added dropwise. One ml aliquots were then carried over into cryotubes (Greiner bio-one). In order to freeze the cells slowly, the aliquots were stored in styrofoam boxes at -80 °C overnight before storing them in liquid N<sub>2</sub>.

### **Evaluating the efficiency of the FGF18 knock-down**

The relative amount of the respective mRNA present in the transfected cells correlates with the knock-down efficacy of the hairpin. Therefore, RNA was isolated from cells and cDNA was synthesised. Evaluation was done by quantitative real-time PCR. See chapter 2.3 for qRT-PCR details. The clones which received the virus with the highest efficacy were chosen for further analysis.

### **2.5.2 Inducing overexpression of FGF18 in FTSLA/a and MJZJ**

The chosen method for inducing FGF18 overexpression was adenoviral transduction (AdEasy) with a construct carrying the FGF18 under control of a CMV promotor, referred to as adFGF18. A negative control virus construct featuring a GFP gene, called adGFP, was applied simultaneously.

#### ***Testing the efficacy of adenovirally-induced FGF18 overexpression***

The increase of FGF18 expression resulting from adenoviral transfection was kindly evaluated by my colleague Lukas Ratzinger by qRT-CR analysis. Three different virus concentrations, MOI 3, MOI 10 and MOI 30 were tested. Already at the lowest concentration of MOI 3, an elevation of FGF18 expression higher than 11 000 fold in FTSLA and 6 000 fold in MJZJ was reached and considered to be sufficient for further application. Figure 14 shows expression levels of FGF18 after adenoviral transfection.

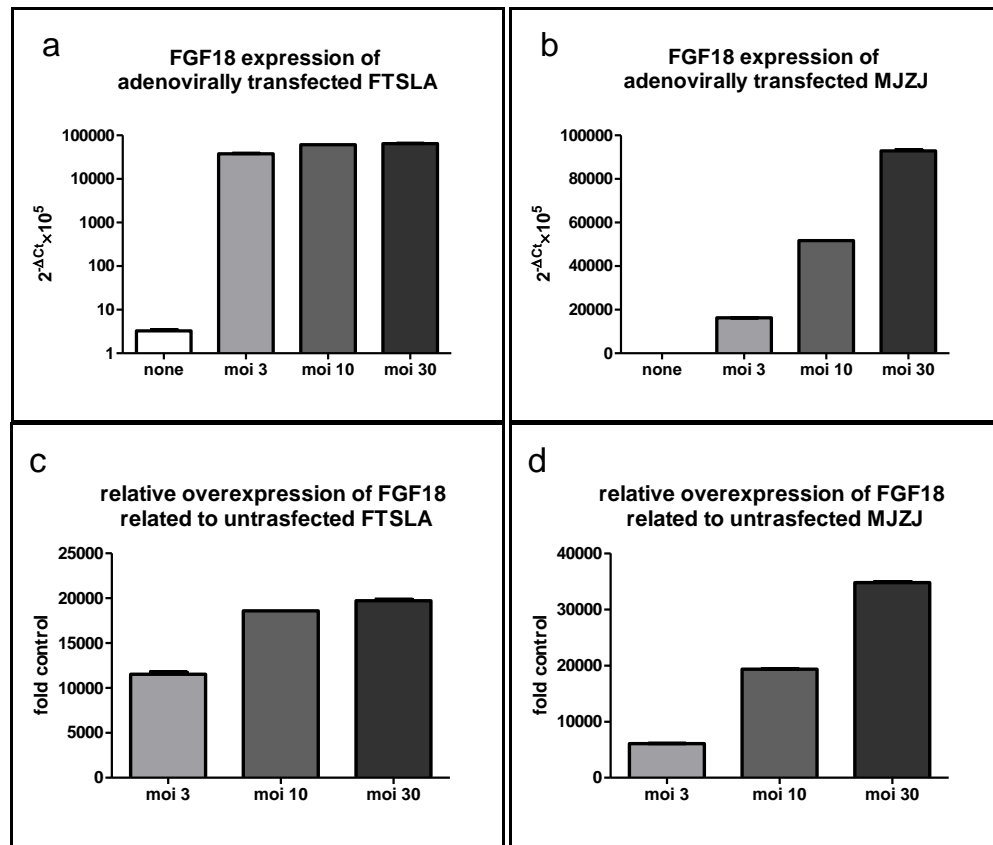


Figure 14: Expression levels of FGF18 in FTSL/a and MJZJ after adenoviral transduction. (a) and (b) show  $2^{-\Delta C_t} \times 10^5$  values of qRT-PCR. (c) and (d) display the respective fold expression compared to untransduced cells.

### ***Adenoviral transduction protocol***

Due to the very high titers of the adenoviral stocks, and the small numbers of cells required for several of the implemented assays, effective individual transduction in each well was not feasible. Therefore many of the assays, namely MTT, transmigration, invasion, clonogenicity, anchorage independent growth assay, apoptosis test and growth curve establishment, were generally performed synchronously allowing antecedent transduction of a higher number of cells. Transduction for scratch assay was performed directly in the 6 well-plates which were used for further analysis.

Per cell line in each case 1.2 million cells were seeded into 3 T25 flasks. After 6 hours of incubation in the incubator, when the cells had attached to the bottom of the flask, adenoviral particles adGFP or adFGF18 were added at an MOI of 3 to each flask. The

cells in the third flask were used as untransduced control group and were also subjected to the subsequent experiments. On the next day the transduced cells were washed 3 times with 1 x PBS in order to remove remaining viral particles from the medium. The FGF18 over-expressing cells were then seeded out for further analysis.

## Analysis of viability and growth

### 2.5.3 Viability test - MTT assay

MTT (3-(4,5-Dimethylthiazol-2-yl)-2,5-diphenyltetrazolium bromide) is a yellow tetrazol, which is reduced to formazan by reductases like succinate-dehydrogenase, or reduction equivalents like NADH or NADPH. Since these substances are produced by viable cells, the amount of produced formazan correlates with the number of living cells. Formazan has an absorption maximum at 550 nm and can therefore easily be quantified by spectrometry. The OD of formazan indirectly reflects the number of living cells.

For MTT assays, 96 well plates were used and for each sample 3000 cells were seeded out in 100 µl R10 per well. Triplicates were applied. After 5 days of incubation at 37°C and 5% CO<sub>2</sub> atmosphere, the growth medium was removed and a tenfold dilution of the MTT reagent in R10 was added. Synchronously three wells without cells were also treated with the MTT solution, which functioned as blanks. When the colouring of the samples was optimal to detect differences, which was decided by visual judgement, the absorption at 550 nm was measured.

### 2.5.4 Apoptosis test – caspase assay

Caspases are proteases that play a key role in inducing apoptosis in mammalian cells.[228] Thus, analysis of caspase activity is an adequate way to determine the rate



of apoptosis initiation in cells. The applied Caspase-Glo® 3/7 Reagent (Caspase-Glo® 3/7, Promega) contains, besides an appropriate cell lysis buffer, luminogenic substrates for caspase 3 and 7. This allows quantitative detection of the activity of these two caspases in cell lysate by luminometric measurement.

For each approach 4 wells were seeded with 15 000 cells in R10 on a 96 well plate. After 24 hours cells were washed with 1 x PBS. Two wells of each approach received 50 µl starving medium containing 0.1% serum. The residual two wells served as control for starvation and received normal R10. For each serum concentration, two wells were filled with 50 µl of the respective medium, which later on served as blanks, since the amount of serum was found to have much influence on the measurement of luminescence, in such an amount as that 0.1 % serum gives values between 50 – 150 emission, whereas 10 % serum show much more Caspase activity with values between 450 – 650. After 48 hours of starvation, analysis was performed. 50 µl of Caspase-Glo® 3/7 reagent were added to each well and incubated for 1 hour and 30 minutes at room temperature. Then, 90 µl from each well were transferred to a white OptiPlate™-96 (Packard) and luminescence was measured with a TECAN Luminometer.

For calculation of the results the blanks of the respective serum concentration were subtracted.

### **2.5.5 Clonogenicity assay**

This assay tests the ability to form clonogenic cell aggregates arising from a single cell, in other words the ability of a single cell to multiply without any cell-cell contacts.

One thousand cells per well were seeded in 2 ml R10 on a 6 well plate. Henceforth, the progression of clones was inspected from time to time by transmission light microscopy. Medium was changed every 7 days. When the clones had reached an appropriate size and eventual differences to control groups were obvious, the cells

were washed with 1 x PBS and then fixed with 1 ml 1:3 methanol:acetic acid. After 30 minutes incubation time, while shaking, the fixed cells were again washed with 1 x PBS, then stained with 500 µl crystal violet solution. Duration of the staining was cell line-dependent and lasted from 20 minutes up to several hours. Afterwards the staining solution was removed and the cells were washed once with ddH<sub>2</sub>O. When the wells were dry again, pictures were taken.

### ***Analysis of crystal violet staining intensity in clonogenic, transmigration and invasion assay***

In order to measure the intensity of the staining, which correlates with the number of stained cells, the crystal violet was eluted again with 2% SDS destaining solution. The amount of applied destaining solution was dependent on the staining intensity and was chosen, so that the most intensively stained sample was eluted completely. Usually 250 – 1000 µl were applied on 6 well plates and 100 – 300 µl in 24 well plates. From each well, duplicates of 50 µl of destaining solution were transferred onto a 96 round bottom well-plate. The intensity of crystal violet in the destaining solution was measured spectrometrically at its absorption maximum of 550 nm.

### **2.5.6 Growth curve establishment**

On day 1, in each case 70 000 cells were seeded into 8 wells of 6 well plates. Henceforth, every second day, the cells of two wells were collected and counted. To collect the cells 300 µl of trypsin were applied per well and after short incubation in the incubator trypsin was inactivated by adding 950 µl R10. The counting was performed via a CASY cell counting system.

### **2.5.7 Cell cycle analysis**

This analysis determines the percentage of cells in each cell cycle stage. The fraction of cells in one stage reflects the duration of this stage. Determination of the stage was done by evaluating the DNA amount in the cell via propidium iodide (PI) DNA staining and subsequent measurement by FACS (fluorescence activated cell sorting). In stage G0/G1, cells show normal diploid DNA content. Cells with doubled diploid chromosomes and thus twice the diploid DNA content reside in stage G2/M. When cells show a DNA amount in between these two values they were in S-phase at the time of fixation.

#### ***DNA staining protocol***

First the PI staining solution, containing 50 µg PI and 50 µg RNase A in 1 x PBS, was prepared. A confluent cell layer of a T25 flask was gathered for cell cycle analysis. After applying trypsin/EDTA the cells were resuspended in 5 ml 1 x PBS and transferred into a 15 ml tube. The cells were centrifuged at 600-1200 rpm and the pellet resuspended in 3 ml cold 70% ethanol for fixation. Incubation for 30 minutes at 4°C followed. Alternatively, the cells could be stored at -20°C in 70% ethanol. After another centrifugation the cells were resuspended in 2-3 ml 1 x PBS and transferred into a round bottom tube suitable for FACS. Again the cells were centrifuged and after removing the PBS, resuspended in 0.5 ml staining solution. At least for 10 minutes the staining was incubated at 4°C before analysis by FACS.

## **Analysis of migration and metastasis auxiliary skills**

### **2.5.8 Scratch assay**

The ability of cells to migrate is a very important feature for metastasis and therefore indicates the aggressiveness of the original tumour. This assay tests the ability of

## Materials and Methods

confluent cells to close a scratch wound induced by with a pipette tip on a culture surface.

Per well, 500 000 cells in 2 ml R10 were seeded on a 6 well pate. As soon as the cells had formed a confluent layer, a cell-free space was introduced into the cell layer by precise scratching with a 200  $\mu$ l tip. Four scratches were made per well. Eventual unattached cells were removed by washing with 1 x PBS. Pictures were taken of each scratch after 0, 4, 8, 24 and 48 hours.

### **2.5.9 Transmigration assay**

In this assay special membranes with 8  $\mu$ m pores, so-called trans-well inserts, are used to test the cells' ability to migrate through this barrier. Hence, here as well, the aggressiveness of the original tumour is analysed.

For this assay 24 well plate trans-well inserts were needed. First 800  $\mu$ l of R10 were added to each well. Then the trans-well inserts were put into the wells and 40 000 cells were seeded onto the trans-well inserts in 200  $\mu$ l R10. After 72 hours of incubation at 37°C and 5% CO<sub>2</sub> atmosphere the inserts were removed and the medium in the wells was changed. When the clones had grown to a proper size and eventual differences between the samples were evident, the growth medium was removed and the cells were washed with 1 x PBS before they were fixed stained with crystal violet and analysed as described above for the clonogenic assays.

### **2.5.10 Invasion Assay**

This assay differs from transmigration assay by an additional collagen layer on the filter of the trans-well insert, which the cells needed to invade to migrate through the filter. This is supposed to simulate the invasion of surrounding tissue in metastasis.

First, 800  $\mu$ l of 20% serum medium were added per well of a 24 well plate. The higher serum concentration in the lower well was applied in order to achieve an enticing

effect towards the cells. Trans-well inserts were put into the well and 28 µl of a cold collagen/PBS solution (1:12.25) were pipetted onto the filters of the trans-well inserts. The collagen layer was hardened in the incubator overnight. On the next day 40 000 cells were seeded onto the layer in 200 µl of R10. After 72 hours the trans-well inserts were removed and analysis was performed in the same way as in transmigration assay.

### **2.5.11 Anchorage independent growth – soft agar assay**

This assay tests, similar to the clonogenic assay, the ability of single cells to form cell clones without cell-cell contacts. Additionally, the cells are embedded in a three dimensional nutrient agar and anchorage of any kind is thereby prevented.

One point five ml of a 1:1 mixture of agar (12 mg/ml in ddH<sub>2</sub>O) and 2 x medium with additives of glutamine, NaHCO<sub>3</sub>, folic acid, FCS and penicillin/streptomycin were poured into wells of a 6 well plate and stored in the incubator overnight. On the next day, 30 000 cells in 750 µl R10 were mixed with the above described 1:1 mixture of agar and 2 x medium and seeded onto the prepared soft agar in the 6 well plate. By incubating the plate at 4°C for 3 minutes the liquids hardened quickly so that the cells were three dimensionally distributed in the soft agar. Henceforth, the progression of clone formation was inspected from time to time by transmission light microscopy. When clones in the soft agar had reached a certain size and eventual differences to control groups were visible, pictures were taken from all clones within exemplary vertical areas. The evaluation was made by counting the clones in the pictures and measuring their diameters.

### III. Results

#### 3.1 FGF18 protein expression in melanoma tissue samples - Tissue Microarray

Analysis of FGF18 expression in tissue samples was done by evaluation of a tissue microarray. Immunohistochemical staining of each core was assigned a value between 0 and 3, whereat 0 stands for no visible staining, 1 for weak, 2 for distinct, and 3 for intense staining. Table 5 lists staining intensities for the different categories of tissue samples.

**Table 5: Overview of all samples analysed in this tissue array. The numbers of samples of each melanoma stage showing no (0), weak (1), distinct (2) and intense (3) staining are listed. The bottom line shows the sum of analysed samples of each stage.**

staining intensity (assessment number)	nevi	primary tumors				metastases	
		stage 1	stage 2	stage 3	stage 4		
0	8		8	1		3	
1	11	1	20	2		10	
2	5		20	2	1	7	
3					1	0	
total number of samples	24	1	48	5	2	20	100

In order to illustrate any differences of FGF18 expression between the represented stages, mean values and standard error of the assessments of each stage were calculated and are displayed in figure 15. Overall there was a slight increase in FGF18 expression in melanoma tissue compared to nevi. Since there were only 1, 5, and 2 samples in stage 1, stage 3, and stage 4 melanomas, respectively, the apparent increase of mean staining intensity with tumour stage needs further evaluation. There was no significant difference between primary tumours and metastatic lesions as it can be seen in figure 16a. Comparison of non-malignant nevi to all malignant samples, hence primary tumours and metastases, showed a significant increase of FGF18 expression ( $p = 0.0269$ ), which is displayed in figure 16 b.

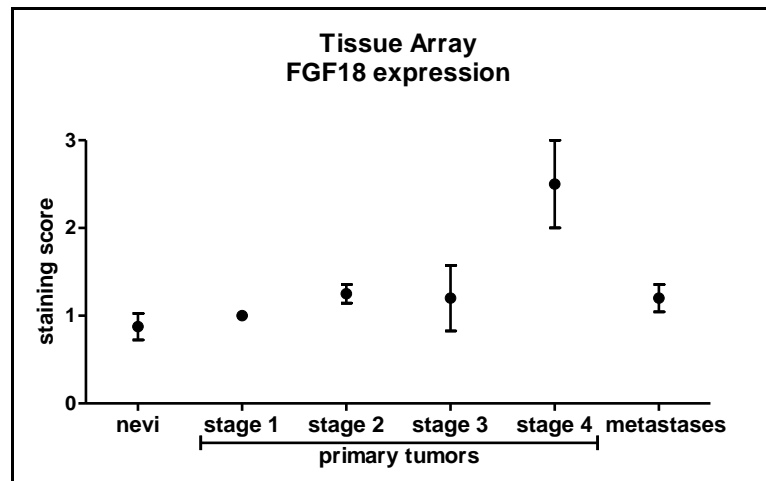


Figure 15: Mean values (with SEM) of staining intensity assessments of each represented stage.

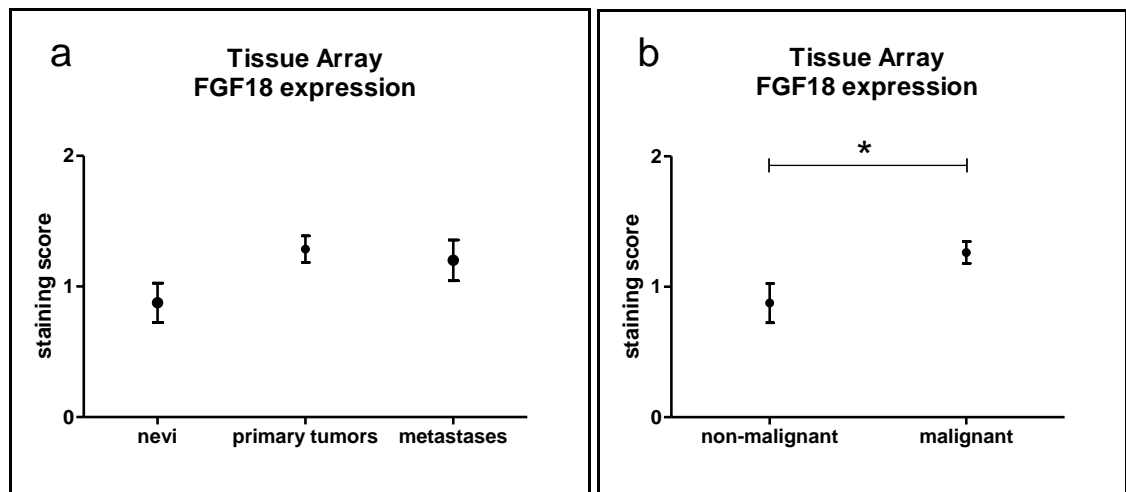


Figure 16: comparison of mean values (with SEM) of staining intensity assessments of (a) nevi, all primary tumours and metastases and (b) non-malignant lesions (nevi) and malignant lesions (all primary tumours and metastases). The asterisk indicates a significant difference of  $p = 0.0269$ .

### 3.2 FGF18 gene expression in melanoma cell models

For analysis of expression of FGF18 in melanoma cell lines, mRNA levels were measured by qRT-PCR. Therefore RNA was extracted from each cell line. For evaluation of RNA amount the RNA extracts were transcribed into cDNA and then analysed via qRT-PCR. Expression of GAPDH was analysed as well, in order to establish an internal standard. To normalise the FGF18  $C_T$  values, the corresponding GAPDH  $C_T$

## Results

values were subtracted. Since these  $dC_T$  values are indirectly proportional to the original amount of cDNA in the sample, they are converted into  $2^{-dC_T}$ .

Figure 17 and 18 display  $2^{-dC_T}$  values of all tested melanoma cell lines arranged according to expression level. The colour code of figure 17 assigns the types of melanoma of each sample, whereas figure 18 denotes the respective origin.

Studies of Thomas Metzner showed that FGF18 expression level of melanocytes would be integrated into these graphs (figure 17 and 18) somewhere in the midfield. Consequently, it can be assumed that about half of the analysed melanoma cell lines show increased levels of FGF18 expression, in some cases, like JTST or XAPG, extremely high over-expression, whereas the other half express decreased levels, whereat none has lost expression completely. The distribution of melanoma subtypes along FGF18 expression levels does not indicate any correlation between subtype and FGF18. Also the respective origins of the cell lines do not seem to be linked to a specific FGF18 expression level, with the notable exception of malignant effusions which tend to have very high levels. Of the 5 cell lines with the highest FGF18 expression 4 were derived from malignant effusions.

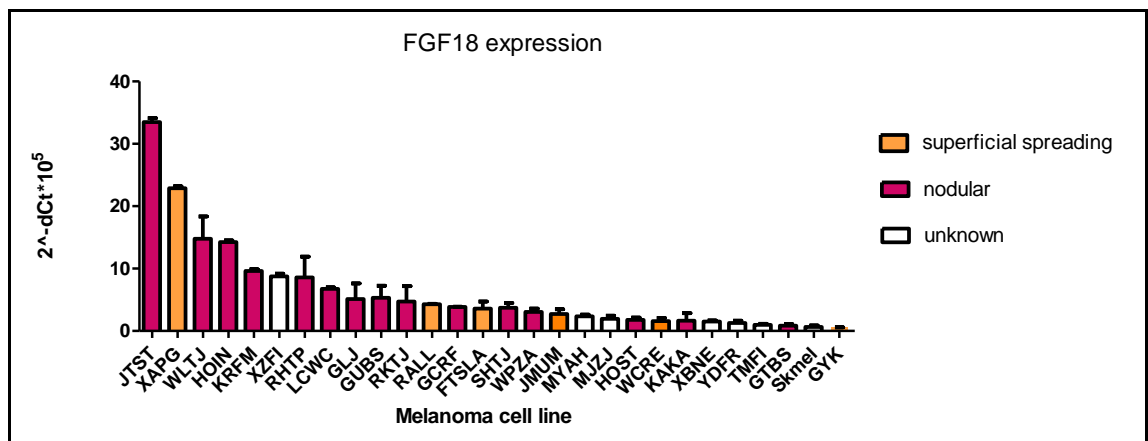


Figure 17: Mean qRT-PCR FGF18 expression data (with SEM) of melanoma cell lines with colour code representing the type of melanoma



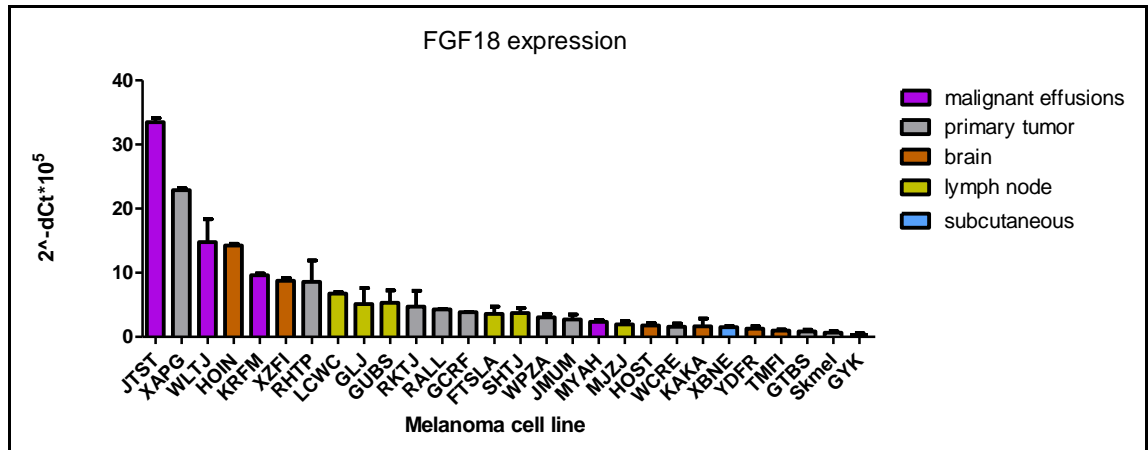


Figure 18: Mean qRT-PCR FGF18 expression data (with SEM) of melanoma cell lines with colour code representing the origin of the cell line.

### 3.3 Contribution of FGF18 to neoangiogenesis in melanoma

For verification of the potential for paracrine effects of FGF18 on lymph and blood endothelial cells, expression analysis of FGFR 1-4 in these cells was done. To test for the potential of autocrine FGF18 signalling in these cells or the possibility that melanoma cells could be influenced by FGF18 secreted by endothelial cells, these cells were also tested for FGF18 expression.

Evaluation of expression levels of FGF18 and the FGF receptors 1-4 was performed in the same manner as expression analysis of melanoma cell lines.

Expression levels of FGF18 were quite low in both lymphendothelial cells (LECs, T1S1) and blood endothelial cells (BECs, G1S1) as figure 19 shows. The comparison in figure 20 of FGF18 expression in LECs and BECs to the melanoma cell lines accentuates this. Figure 19 furthermore displays expression of FGFRs of the respective cell lines. Both show very high levels of FGFR1 expression and more moderate expression of FGFR4. Very slight expression of FGFR3 was found in T1S1. G1S1 showed very slight expression of FGFR2 and somewhat higher but still very low levels of FGFR3.

## Results

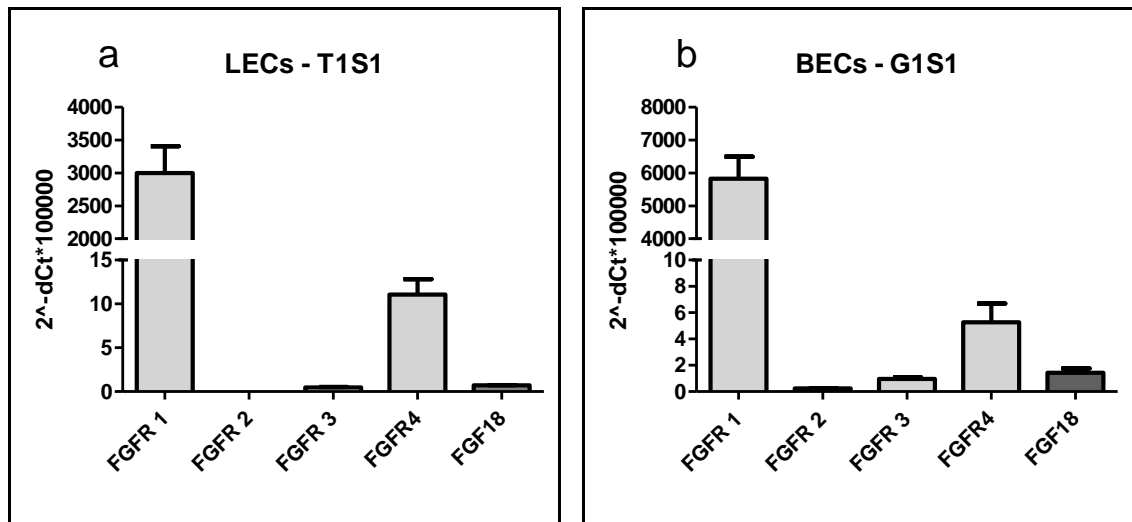


Figure 19: Mean expression data (with SEM) of immortalised lymph (a) and blood (b) endothelial cells for FGFR1-4 and FGF18.

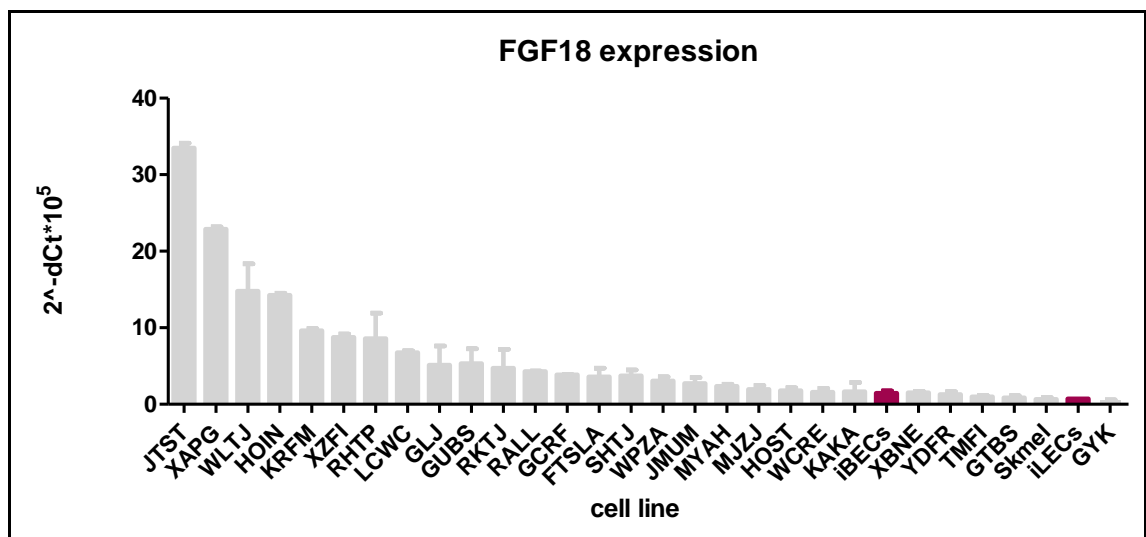


Figure 20: Mean expression data (with SEM) of FGF18 in LECs and BECs and melanoma cell lines.

Additionally, VEGF-A expression was analysed in melanoma cell lines and correlation to FGF18 expression was determined in order to clarify whether FGF18 regulates VEGF expression in melanoma and thereby contributes to neoangiogenesis. Figures 21 and 22 show VEGF-A expression data of melanoma cell lines. Here as well, the colour code of figure 21 assigns the types of melanoma of each sample, whereas figure 22 denotes the respective origin.

## Results

Correlation between expression levels of FGF18 and VEGF-A was determined by calculation of a regression curve. Figure 23 shows VEGF-A expression values plotted against FGF18 expression values and the calculated regression curve in red. A good portion of melanoma cell lines have high expression levels of VEGF-A. Especially the cell lines MJZJ and GUBS, which derive from lymph node metastases show very high expression of VEGF-A. However, significant correlation to FGF18 expression could not be found.

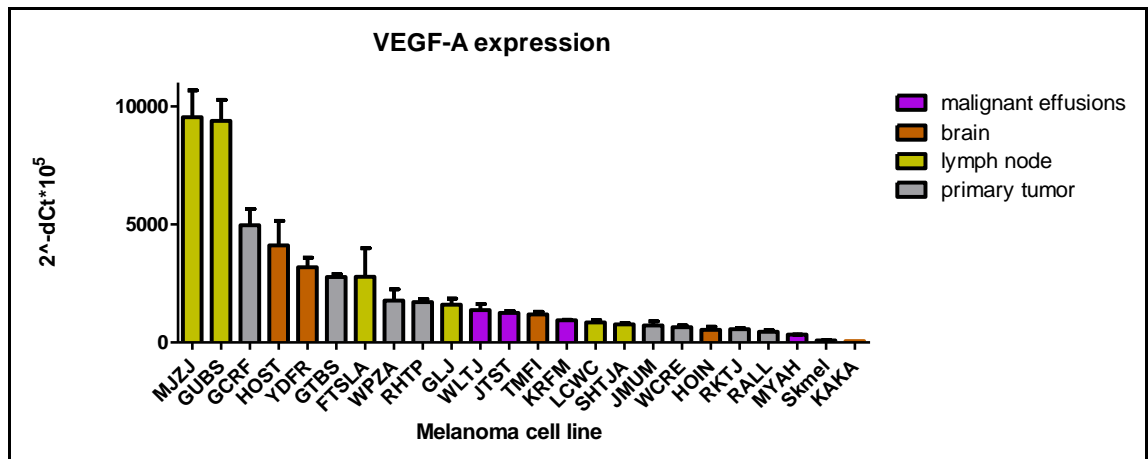


Figure 21: VEGF-A expression data of melanoma cell lines with colour code representing the subtype of melanoma.

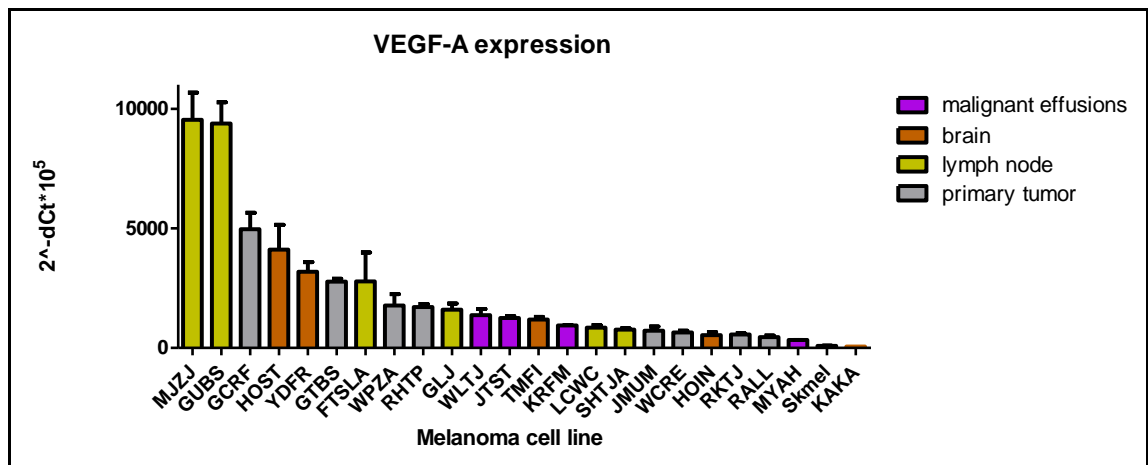


Figure 22: qRT-PCR VEGF-A expression data of melanoma cell lines with colour code representing the origin of the cell line.

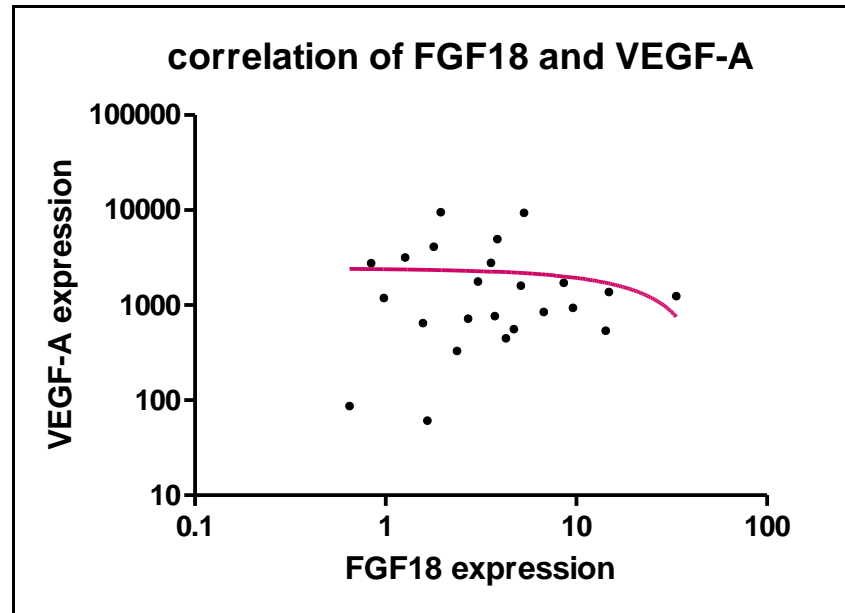


Figure 23: Correlation between FGF18 and VEGF-A expression plus regression curve in red. qRT-PCR  $2^{-\Delta\Delta CT}$  FGF18 values were plotted along the x-axis and the respective VEGF-A values along the y-axis.

### 3.4 Determination of the impact of endogenous Wnt-pathway activity on FGF18 expression in melanoma cells

#### Analysis of Wnt-pathway activity in melanoma cell lines

Via transfection of a  $\beta$ -catenin reporter plasmid, carrying a firefly luciferase reporter gene, activity of Wnt-pathway activity was analysed. Co-transfection of a *Renilla* luciferase plasmid was performed to establish an internal standard for luciferase activity, in order to normalize differences in transfection efficacy amongst samples and cell lines. Each approach was performed three times and analysed via an injection Luminometer.

Figures 24 and 25 display Wnt-pathway activity values of each melanoma cell line, calculated as ratio between the false positive signal and the actual  $\beta$ -catenin activity signal with respective colour codes for melanoma subtypes and histologic origins from which the cell lines were established. In 12 out of 22 analysed cell lines  $\beta$ -catenin activity was detected. Independent of original melanoma subtypes, values of Wnt-pathway activity are widely different amongst melanoma cell lines. However, cell lines

## Results

derived from primary tumours show no  $\beta$ -catenin activity, apart from RHTP which has very low activity. In contrast, in all tested cell lines which were established from malignant effusions, Wnt-pathway activity was detected.

Correlation between Wnt-pathway activity and expression level of FGF18 was determined by calculation of a regression curve. Figure 26 shows FGF18 expression values plotted against  $\beta$ -catenin activity values and the calculated regression curve. No correlation could be observed in the collected data set, suggesting that FGF18 expression in melanoma cells is independent of Wnt pathway activity.

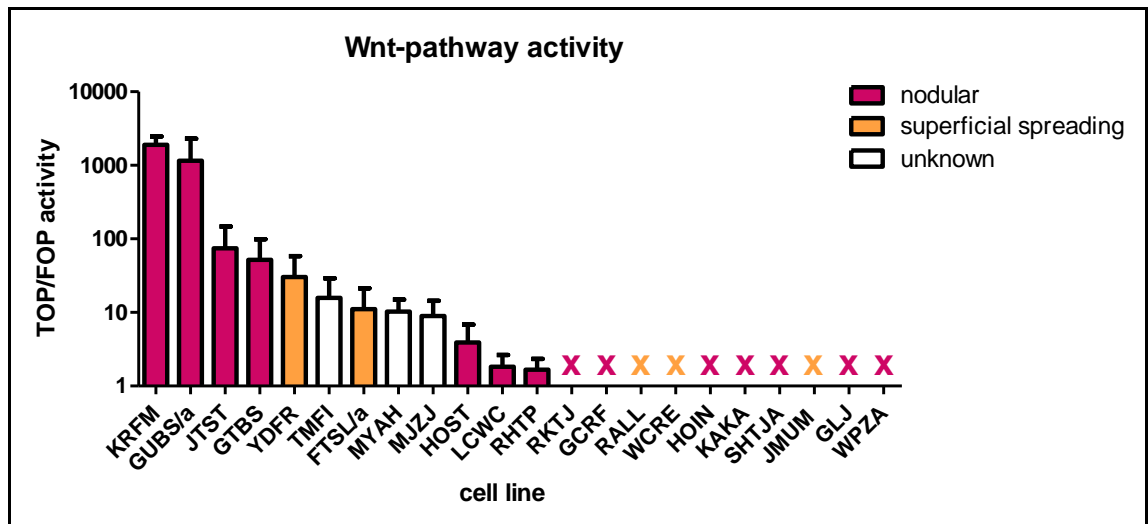


Figure 24: Mean TOP/FOP values (with SEM) represent Wnt-pathway activity of each cell line. Melanoma subtype, from which the cell lines were established, are indicated by the colour code. Lowest possible value is 1, which denotes no detectable  $\beta$ -catenin activity and is marked with X.

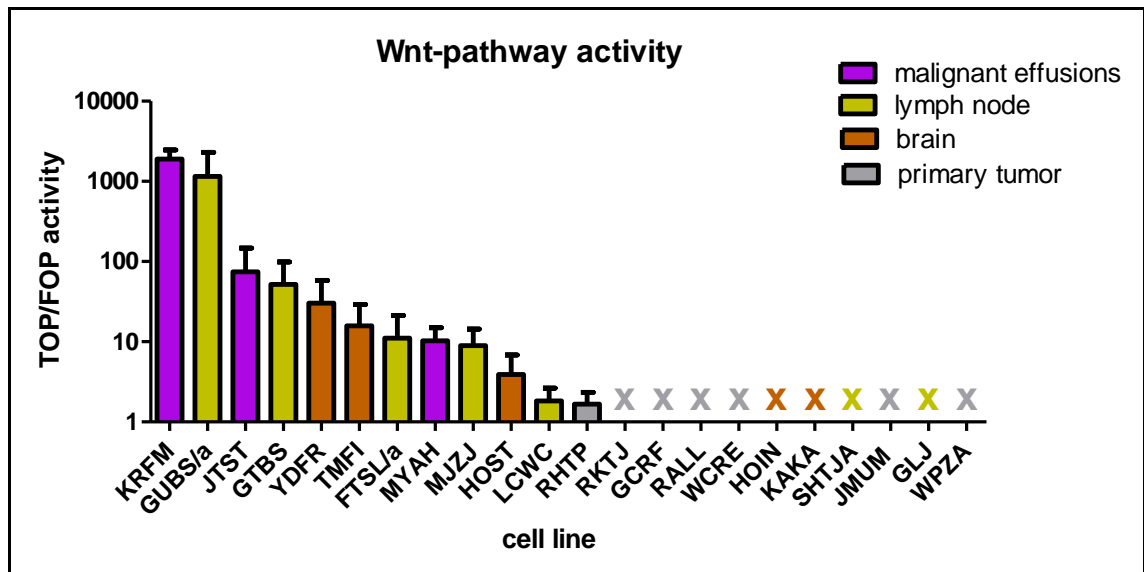


Figure 25: Mean TOP/FOP values (with SEM) represent Wnt-pathway activity of each cell line. Histological origin, from which the cell lines were established, are indicated by the colour code. Lowest possible value is 1, which denotes no detectable  $\beta$ -catenin activity and is marked with X.

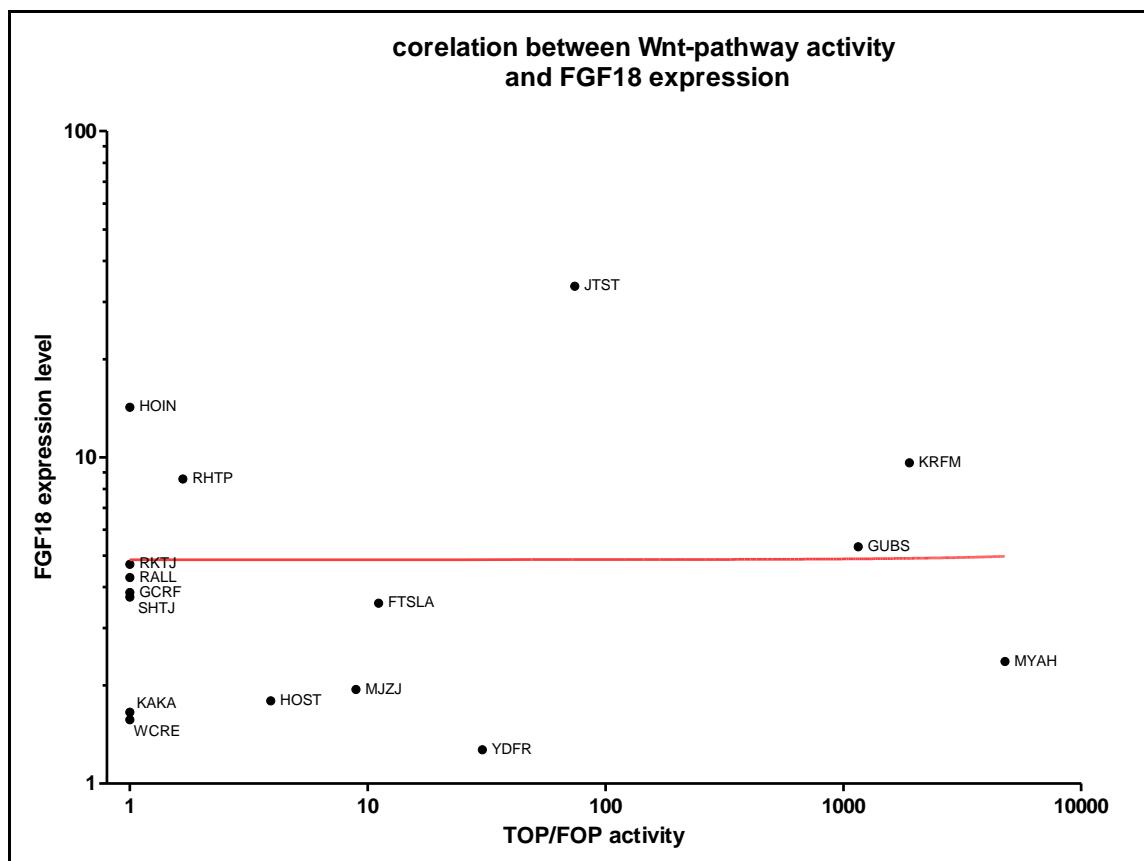


Figure 26: Correlation between Wnt-pathway activity and FGF18 expression plus regression curve in red. TOP/FOP values were plotted along the x-axis and the respective FGF18 qRT-PCR  $2^{-\Delta CT}$  values along the y-axis.

### 3.5 Potential of autocrine signalling of FGF18 in melanoma

#### 3.5.1 Evaluation of the lentiviral transfection efficacy

After FTSL/a cells were transduced with the three different FGF18-targeting small hairpin lentiviral particles (shRNA 6-8) and the non-silencing control virus, RNA was extracted from the resulting stable sublines to investigate the gene expression levels of GAPDH and FGF18 via qRT-PCR.

#### qRT-PCR

In order to test the efficacy of knock-down by the applied shRNAs, qRT-PCR analysis was done. Again FGF18 and GAPDH were analysed simultaneously. An internal standard was created by the GAPDH values, to normalise FGF18 expression to the general expression activity of the respective cell line. Thereby the FGF18 values of the different cell lines could be compared. Further calculation was performed in the same manner as for all the other qRT-PCR results in chapter 3.2 and  $2^{-\Delta\Delta CT}$  values were determined. Additionally, this value of each sample was calculated relatively to the value of the cell line which received the non-silencing shRNA construct. This displays the fold expression of the gene in each cell line compared to the non-silencing control, which can be seen in figure 27

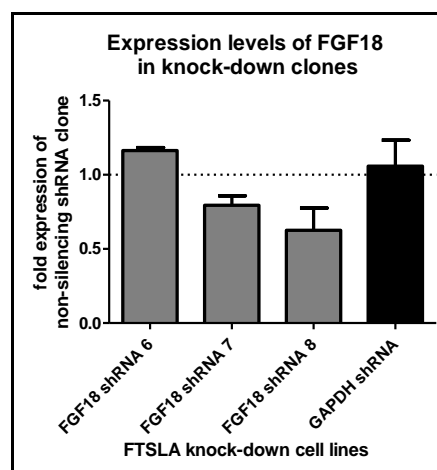


**Figure 27:** Mean fold expression (with SEM) of FGF18 of each subline compared to the non-silencing control.

## Results

The relative expression levels of FGF18 in figure 27 show that the shRNA constructs FGF18 shRNA “7” and FGF18 shRNA “8” have a knock-down effect on FGF18 expression. The cells which received shFGF18 “6” do not show a decrease in FGF18 expression levels compared to the negative control clone. The construct FGF18 shRNA “8” shows the highest FGF18 knock-down efficacy, which however was still below 50%. This cell line was chosen for further tests.

In addition to the established stable knock-down clone of FTSL/a, two cell lines, MJZJ and FTSL/a received adenovirally-mediated induction of FGF18 over-expression. Efficacy of adenovirally induced FGF18 over-expression had already been determined before and reached very high levels. See Materials and Methods section for details. These three approaches were used to test effects of altered FGF18 expression on viability and growth as well as migration and auxiliary features for metastasis of melanoma cells.

## Analysis of viability and growth

### 3.5.3 Viability test – MTT assay

In order to test a potential effect of the FGF18 knock-down or over-expression on the viability of the cells, an MTT assay was performed. Higher deltaOD values of formazan indicate more living cells. Each approach was performed at least two times in triplicates. For accentuation of potential differences of deltaOD values to the respective negative controls, results were calculated as fold of the control and significance was evaluated as it is displayed in figure 28. The two cell lines in which FGF18 over-expression was induced did not show significant increase or decrease in viability, yet the FTSL/a knock-down clones show significantly increased viability ( $p = 0.0042$ ).



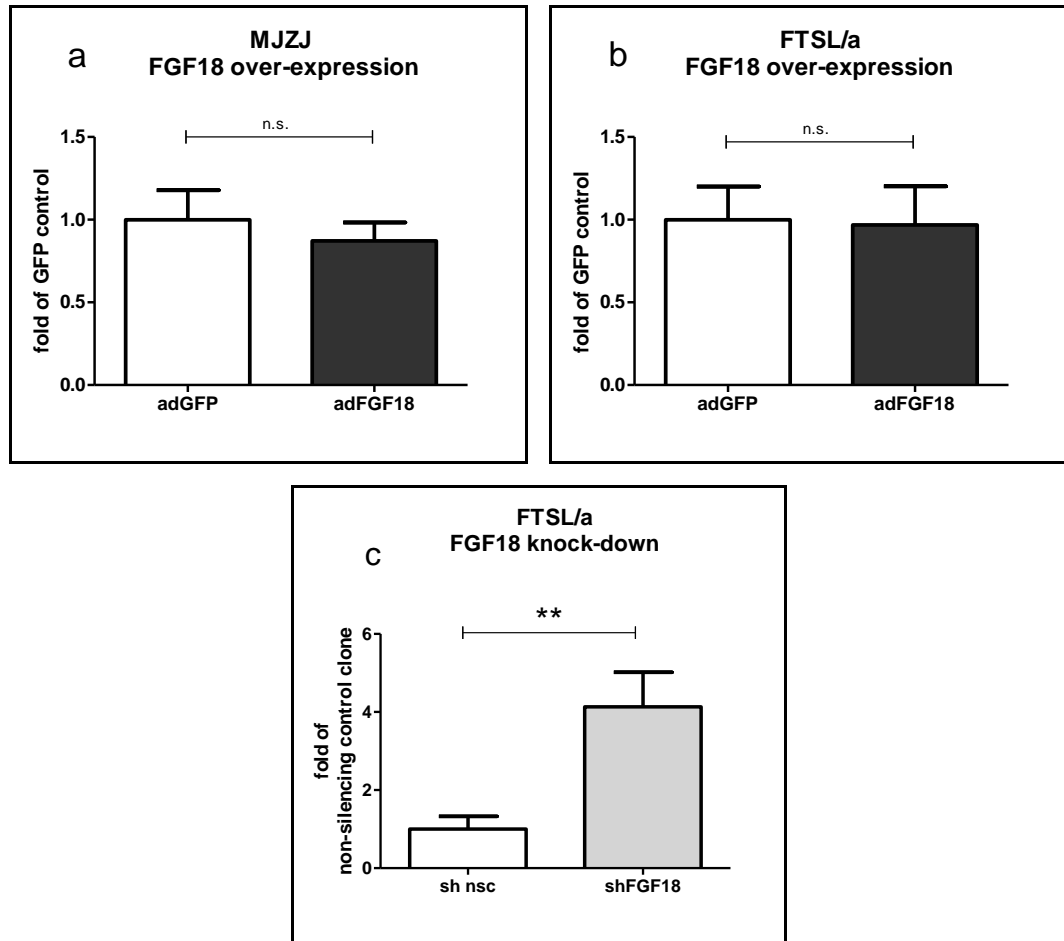


Figure 28: MTT-Assay. Fold control values of (a) MJZJ with induced FGF18 over-expression (adFGF18), (b) FTSL/a with induced FGF18 over-expression (adFGF18) and (c) FTSL/a with induced FGF18 knock-down (shFGF18) plus respective negative control values (adGFP; sh nsc, non-silencing control). Significance is indicated as either n.s. (not significant) or \*\* (p=0.0042).

### 3.5.4 Apoptosis test – caspase assay

By evaluating caspase activity via a luminogenic caspase substrate, initiation of apoptosis was analysed in melanoma cell lines. Measurements were taken at starving conditions in 0.1% serum medium and control conditions in normal 10% serum medium. Each approach was carried out at least two times in duplicates. For calculation of the results the blanks of the respective serum concentration were subtracted. Here as well, results were calculated as fold of the control in order to accentuate differences of the values to the respective negative controls. Results are shown in figure 29. Neither of the cell lines with induced FGF18 over-expression, nor

## Results

the FTSL/a knock-down clones showed significant changes of caspase activity to their respective controls.

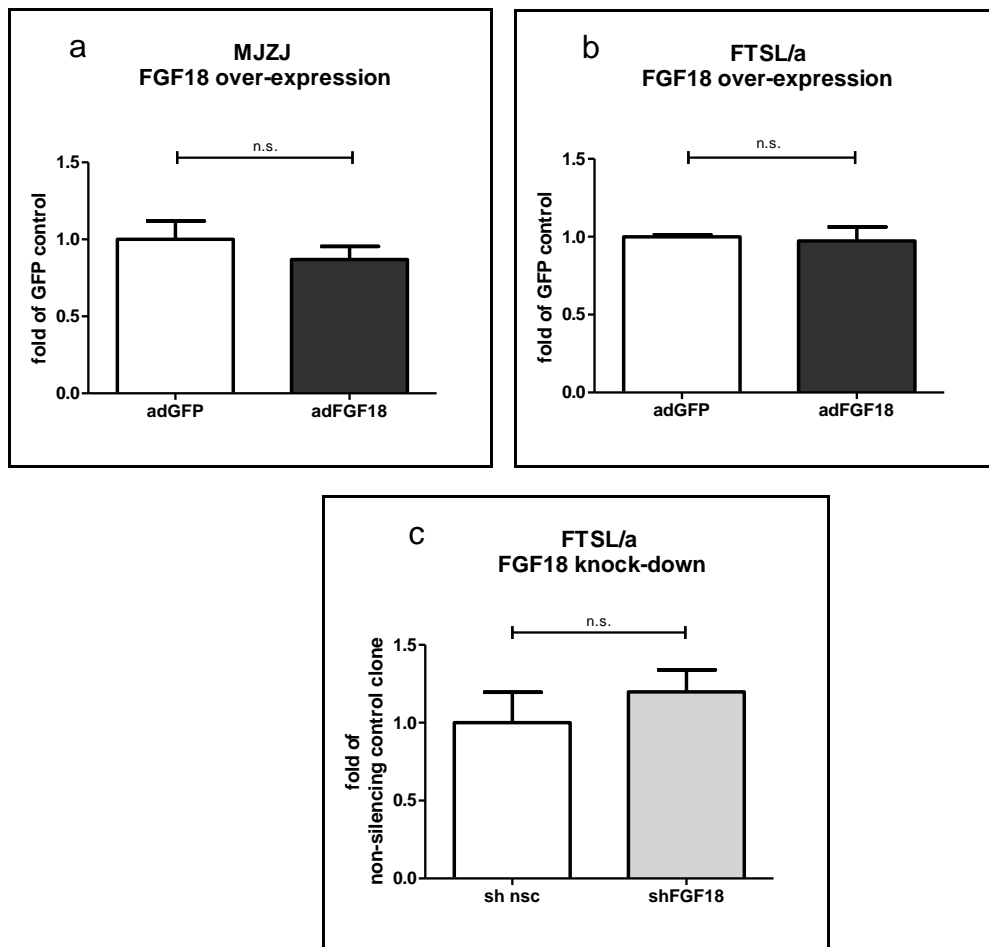


**Figure 29: Fold control values (with SEM) of caspase activity measured by luminescence assay of (a) MJZJ with induced FGF18 over-expression (adFGF18; adGFP – control), (b) FTSL/a with induced FGF18 over-expression (adFGF18; adGFP – control) and (c) FTSL/a with induced FGF18 knock-down (shFGF18; sh nsc – non-silencing control) under starving conditions with 0.1% serum medium. Non-significant values are indicated with n.s.**

### 3.5.5 Clonogenicity assay

This assay was performed in order to test the ability of single sells to form cell clones. For analysis, clones were fixed and stained with crystal violet. Pictures were taken and the crystal violet of each sample was afterwards eluted and intensity of the staining was measured photospectrometrically at 550 nm. Each approach was carried out at least three times in duplicates. Figure 30 displays representative wells after crystal violet staining of each of the approaches plus controls. Again results were calculated as

## Results

fold of the control, to highlight differences of values to the control and significance was evaluated. Figure 31 displays the results. Over-expression of FGF18 did not induce any significant change in clonogenicity of the cell lines. The FTSL/a FGF18 knock-down clones have increased ability to form clones compared to the non-silencing control ( $p = 0.0066$ ).

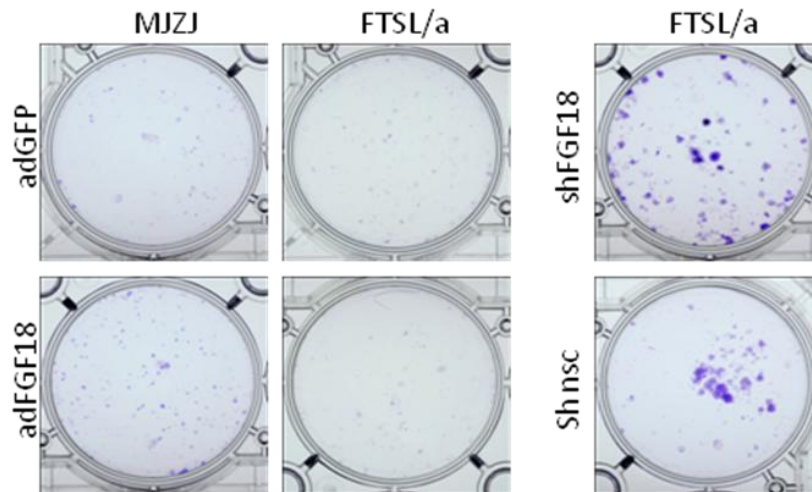


**Figure 30: Clonogenicity assay: Pictures of stained cell aggregates of MJZJ with induced FGF18 over-expression and control, FTSL/a with induced FGF18 over-expression and control and FTSL/a knock-down clones and control.**

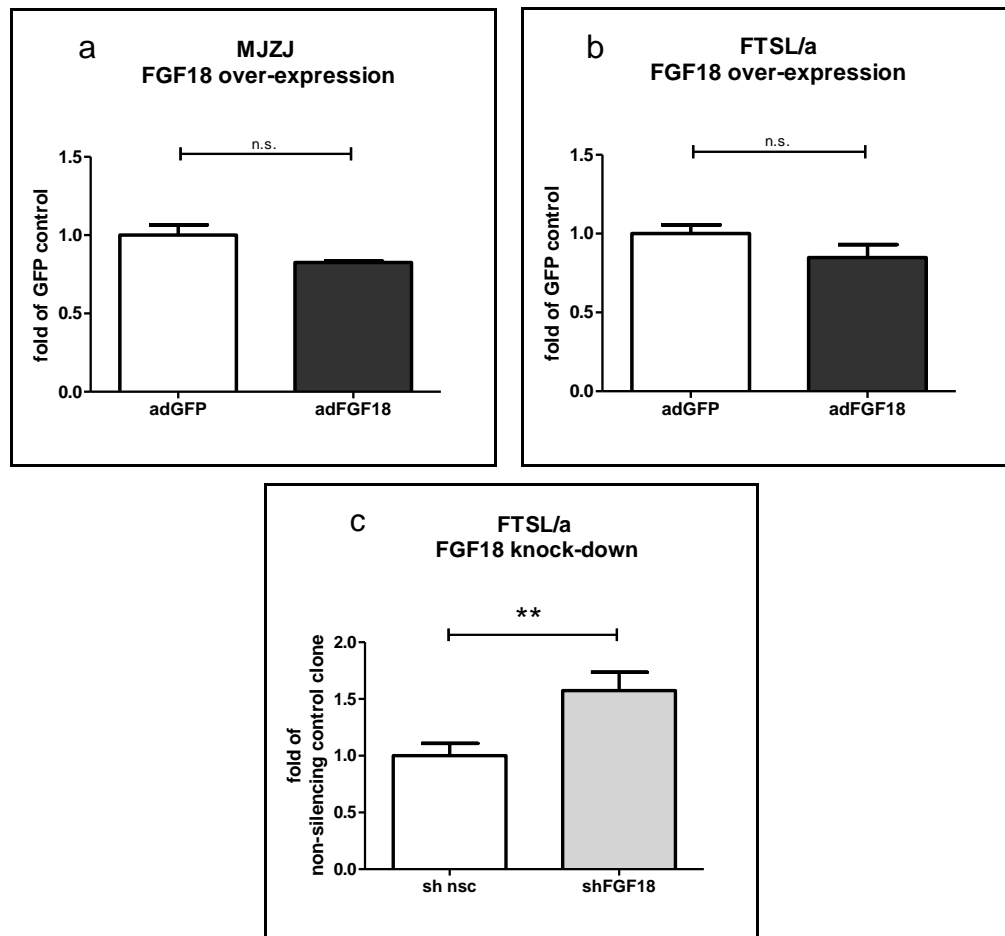


**Figure 31: Clonogenicity assay: Fold control values of crystal violet staining of (a) MJZJ with induced FGF18 over-expression (adFGF18), (b) FTSL/a with induced FGF18 over-expression (adFGF18) and (c) FTSL/a with induced FGF18 knock-down (asFGF18) plus respective controls (adGFP; sh nsc, non-silencing control). Significance is indicated as either n.s. (not significant) or \*\* ( $p = 0.0066$ ).**

### 3.5.6 Growth curve establishment

To compare velocity of growth of cell populations with altered FGF18 expression with the respective control, growth curves were established. All measurements of each point of time were performed in duplicates. Figure 32 displays growth curves of the three approaches in comparison with their controls. Statistically relevant change of growth velocity could neither be found in the FGF18 over-expressing cells nor in the knock-down clones compared to respective controls.

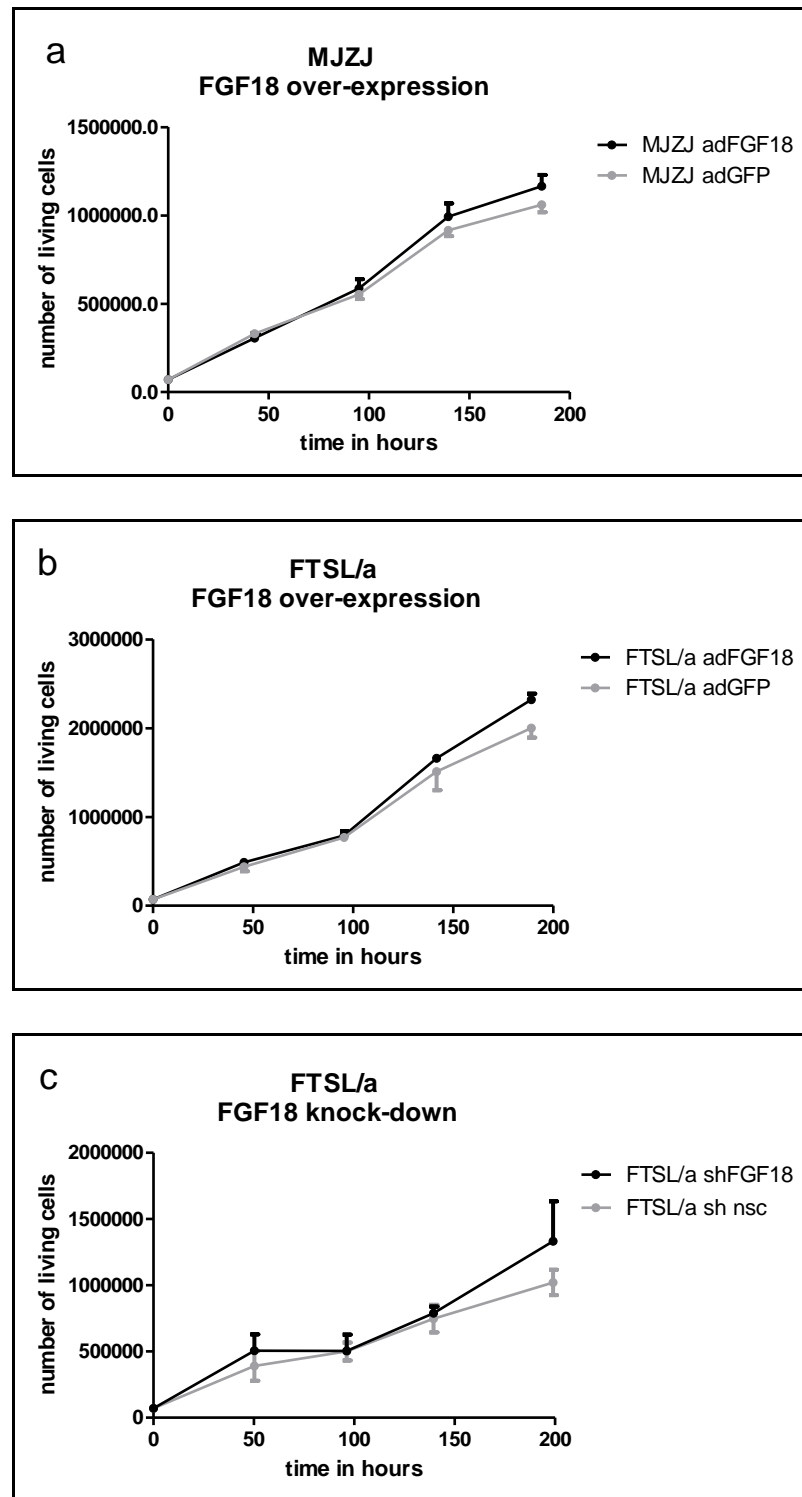


Figure 32: Growth curves of mean values (with SEM) of (a) MJZJ with induced FGF18 over-expression (adFGF18), (b) FTSL/a with induced FGF18 over-expression (adFGF18) and (c) FTSL/a with induced FGF18 knock-down (shFGF18) plus respective controls (adGFP; sh nsc, non-silencing control).

### 3.5.7 Cell cycle analysis

This analysis determines the percentage of duration of each cell cycle stage within one cycle. Each approach was analysed two times in duplicates. Figure 33 displays the portion of each stage in one cell cycle in terms of percentage of cells residing in the specific stage at time of fixation. No significant changes in cell cycle were found in FGF18 over-expressing MJZJ and FTSL/a or FTSL/a FGF18 knock-down clones.

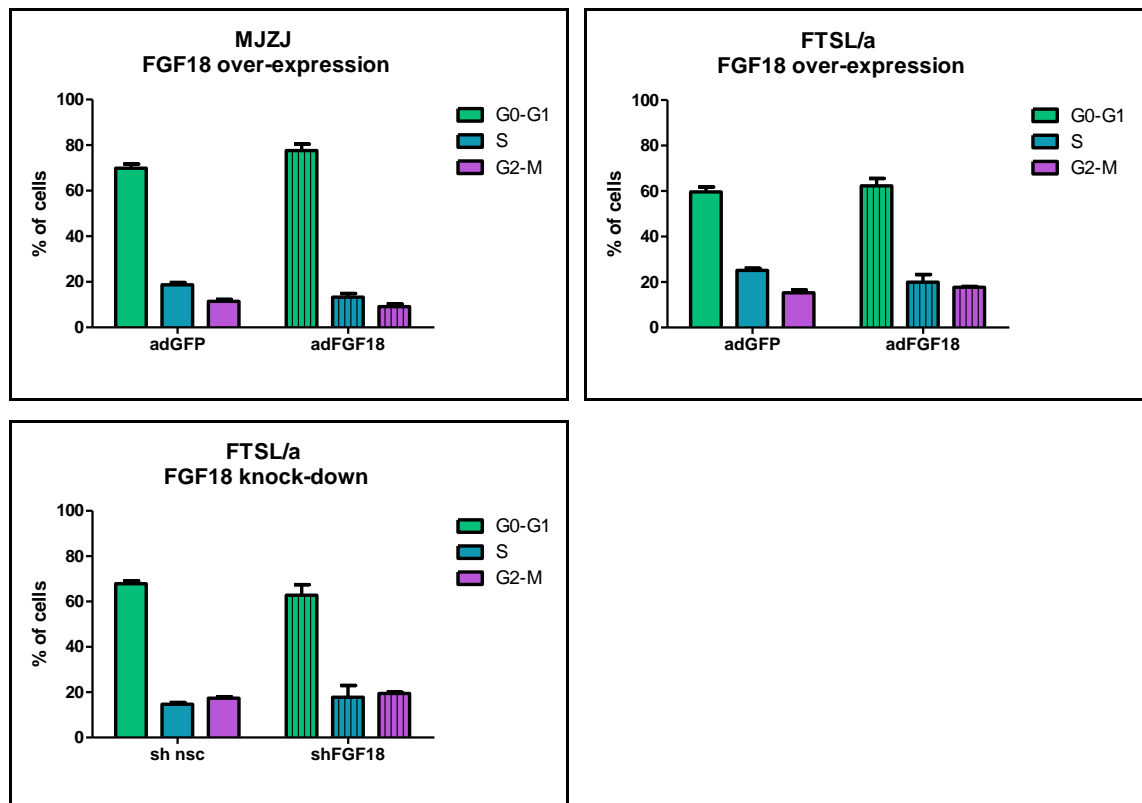


Figure 33: Cell cycle analysis: Percentage of cells, residing in each of the three cell cycle stages, reflects temporal division of the cell cycle. Mean values (with SEM) for MJZJ with induced FGF18 over-expression (adFGF18) and control (adGFP) are shown in (a), for FTSL/a with induced FGF18 over-expression (adFGF18) and control (adGFP) in (b) and for FTSL/a with induced FGF18 knock-down (shFGF18) and control (sh nsc, non-silencing control) in (c).

### Analysis of migration and metastasis auxiliary skills

#### 3.5.8 Scratch assay

In this assay, the ability of remigration of cells into free space on a culture surface is tested. Scratches were induced and the progression of remigration was noted by

## Results

taking pictures after 0, 4, 8, 24 and 48 hours. Gap widths of each picture were then measured and evaluated in terms of percentage of total scratch closure. Since FTSL/a FGF18 knock-down clones generally did not form cell layers but rather grew in clones, this assay could not be performed for this approach. The non-silencing control clones also hardly formed cell layers but did not show such distinctive clone formation as the FGF18 knock-down clones. For the two approaches with induced FGF18 over-expression the test was performed at least two times in quadruplicates. Figure 34 shows exemplary pictures of the assay of FTSL/a and MJZJ with induced FGF18 over-expression plus respective controls. Figure 35 displays mean values with standard errors of evaluated scratch closure. No statistically relevant changes by FGF18 over-expression were found in general ability or velocity of scratch closure in the two tested cell lines.

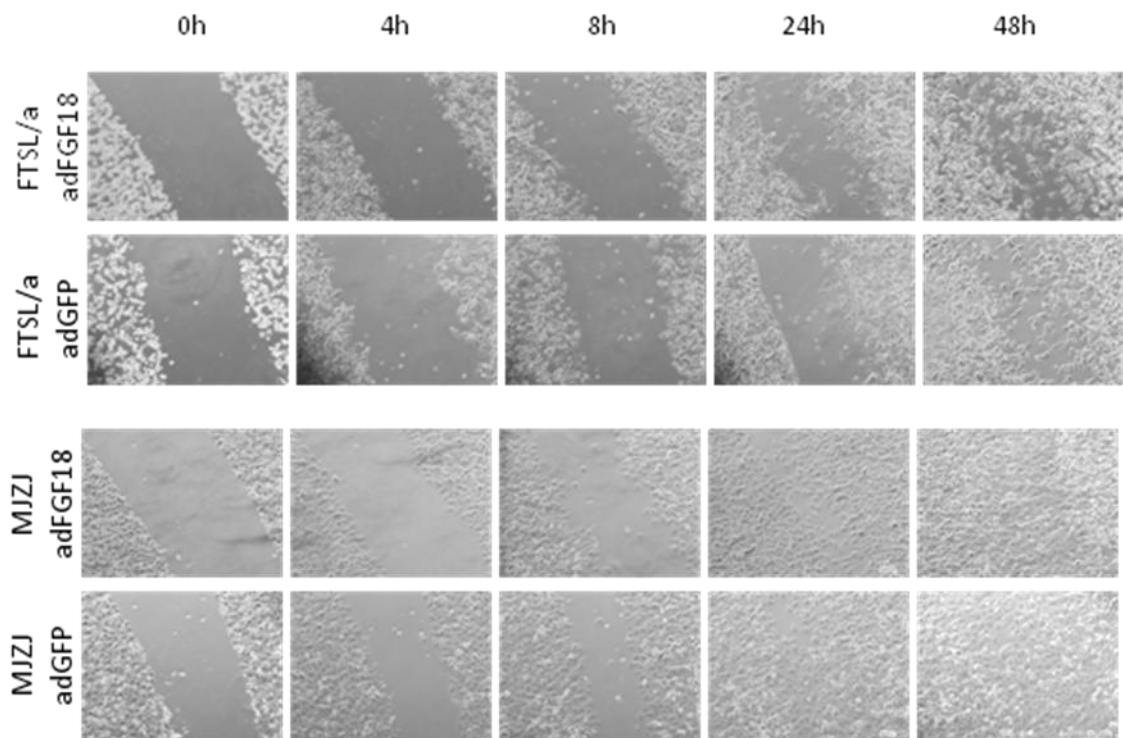


**Figure 34:** Exemplary pictures of scratch assays of FTSL/a and MJZJ with induced FGF18 over-expression (adFGF18) and the corresponding control (adGFP) at 0, 4, 8, 24 and 48 hours.

## Results

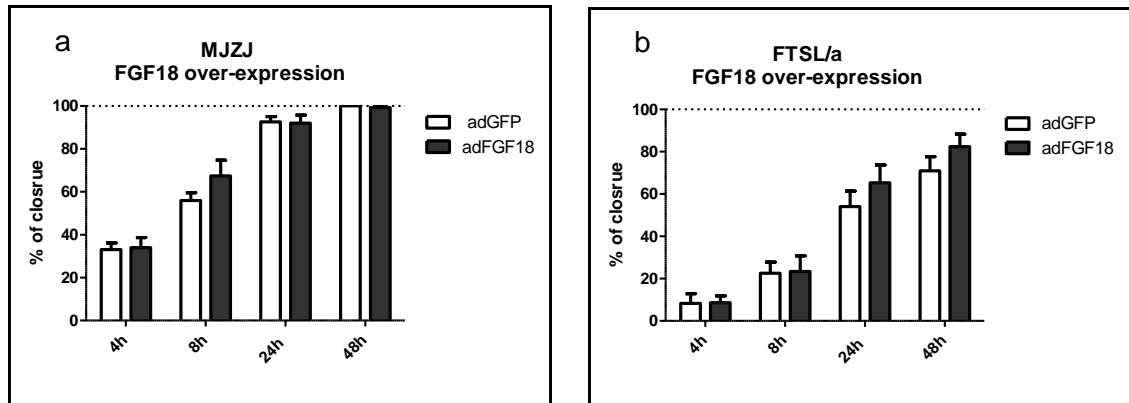


**Figure 35: Scratch assay: mean percentages (with SEM) of scratch closure of (a) MJZJ with induced FGF18 over-expression (adFGF18) and (b) FTSL/a with induced FGF18 over-expression (adFGF18) at 0, 4, 8, 24 and 48 hours plus respective control (adGFP).**

### 3.5.9 Transmigration assay

This assay tests migration through barriers. This was accomplished by determining the ability of cells to migrate through a filter with 8  $\mu$ m pores. Analysis was, like in clonogenicity assays, performed via fixation and crystal violet staining of cells that had formed clones in the lower chamber. Pictures were taken and the crystal violet was eluted again. Photometric measurement of crystal violet in the destaining solution correlated with the amount of cells which surmounted the filter and survived. Figure 36 shows pictures of stained cell aggregates of each approach plus the respective control. The assay was carried out at least two times in duplicates. Absorption values were calculated as fold of control and displayed in figure 37. FGF18 over-expression significantly induced transmigration in the usually low expressing cell line MJZJ ( $p=0.0425$ ). Transmigrating ability of the normally moderate expressing cell line FTSL/a was not significantly affected by FGF18 over-expression, but knock-down lead to a significant decrease ( $p=0.0419$ ).



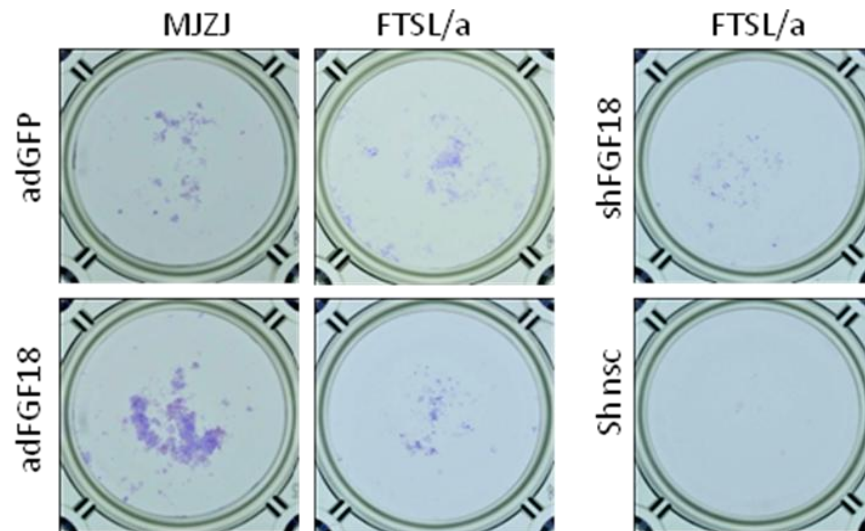


Figure 36: Transmigration assay: Pictures of stained cell aggregates of MJZJ with induced FGF18 over-expression (adFGF18) and control (adGFP), FTSL/a with induced FGF18 over-expression (adFGF18) and control (adGFP) and FTSL/a with induced FGF18 knock-down (shFGF18) and control (sh nsc).

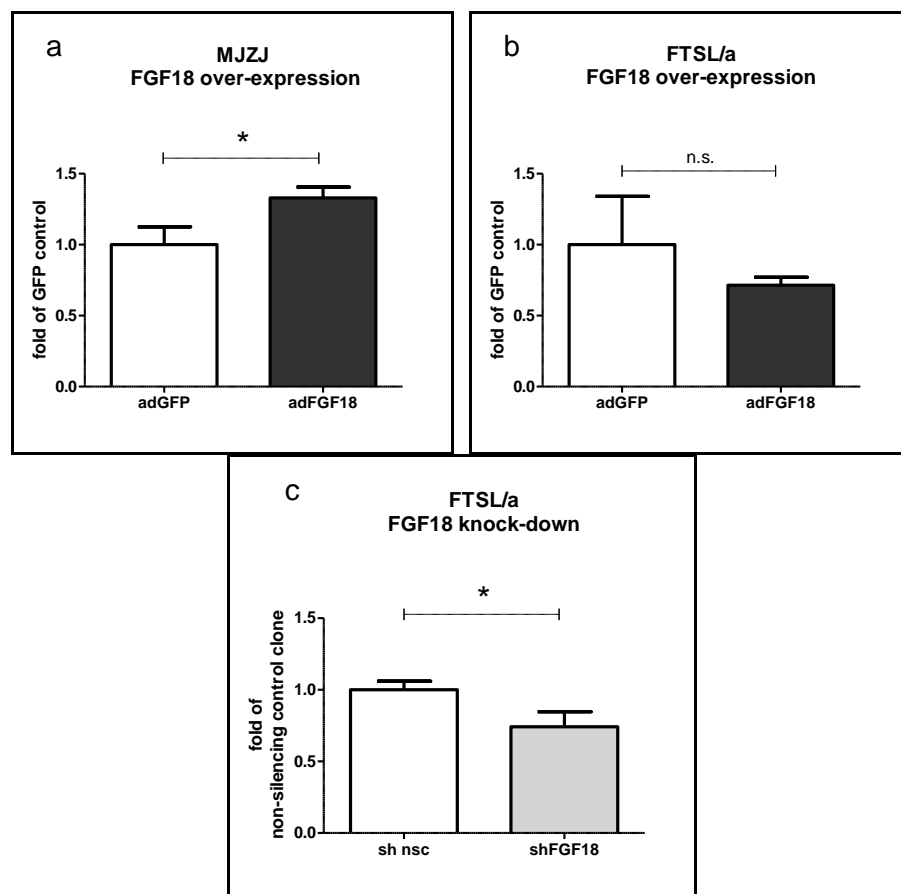
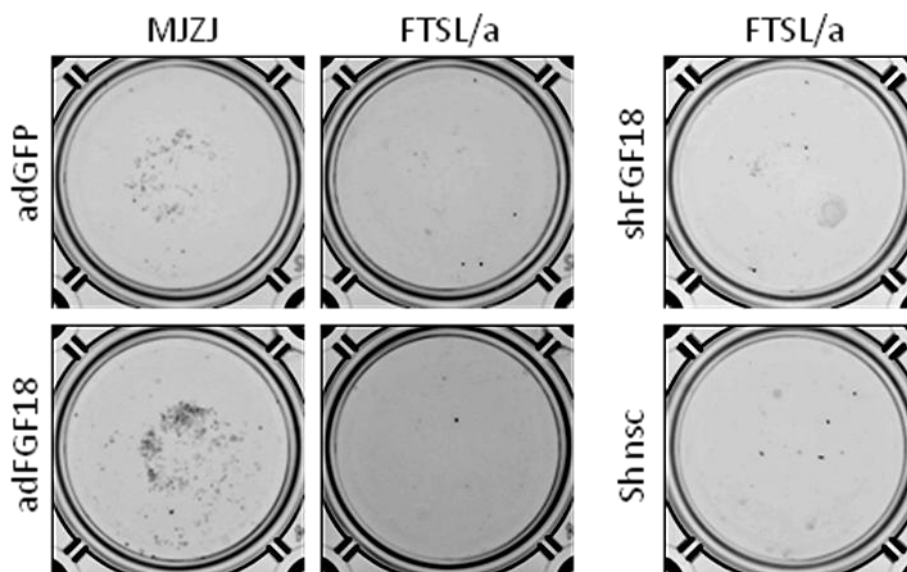


Figure 37: Transmigration assay: Fold control values for crystal violet staining intensity (with SEM) of (a) MJZJ with induced FGF18 over-expression (adFGF18; adGFP - control) (p=0.0425), (b) FTSL/a with induced FGF18 over-expression (adFGF18; adGFP - control) (n.s. p=0.5141) and (c) FTSL/a with induced FGF18 knock-down (shFGF18; sh nsc – non-silencing control) (p=0.0419).

### 3.5.10 Invasion assay

In this assay invasion was tested by seeding cells on a collagen coated filter with 8  $\mu\text{m}$  pores. The relative amount of cells which were able to surmount this barrier and furthermore progressed to proliferate on the bottom of the well was analysed by staining cell clones with crystal violet. Pictures were taken and dye was eluted. Photometric measurement of the crystal violet amount in the destaining solution corresponds with the number of stained cells and was therefore applied for evaluation. Figure 38 shows pictures of stained clones of each approach and respective control. Absorption values calculated as fold of the respective control are displayed in Figure 39. FGF18 over-expression in the usually low expressing MJZJ induced a significant increase of invasion ( $p = 0.0177$ ). FTSL/a did not show any significant change of invasiveness, neither when FGF18 was over-expressed nor knocked-down.



**Figure 38: Invasion assay: Pictures of stained cell aggregates of MJZJ with induced FGF18 over-expression and control, FTSL/a with induced FGF18 over-expression and control and FTSL/a knock-down clones and control.**

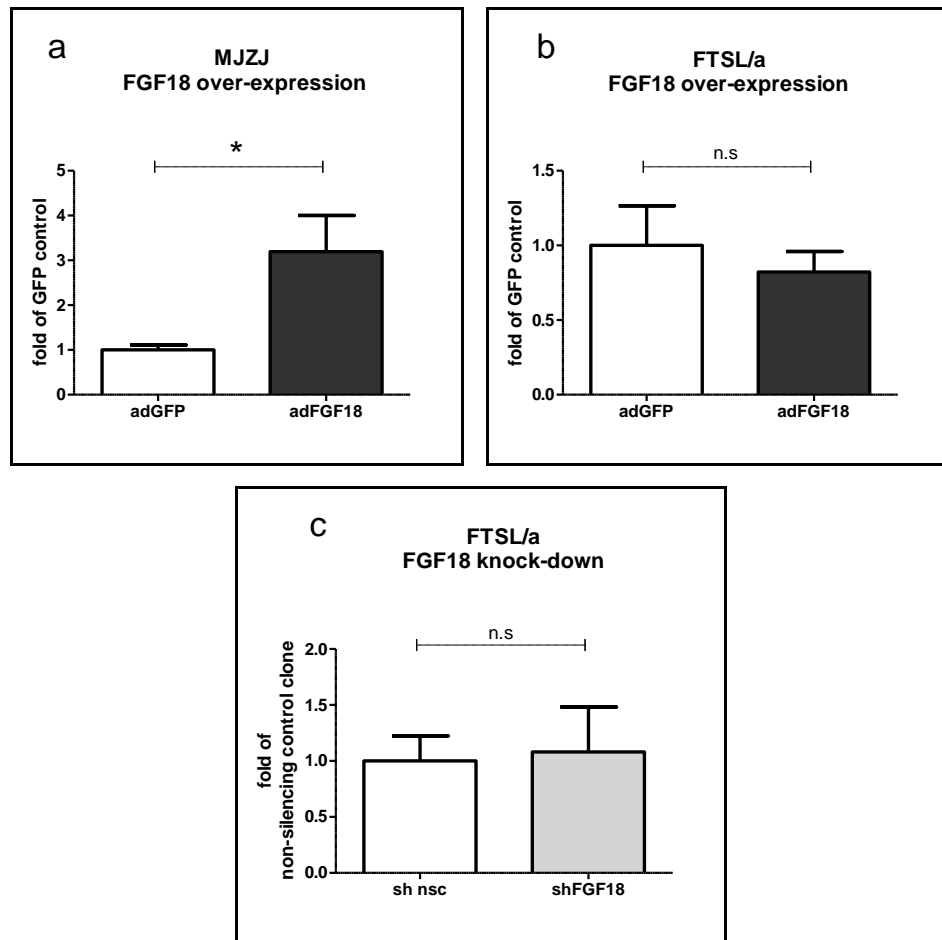


**Figure 39: Invasion assay:** Fold control values for crystal violet staining intensity (with SEM) of (a) MJZJ with induced FGF18 over-expression (adFGF18; adGFP - control) ( $p=0.0177$ ), (b) FTSL/a with induced FGF18 over-expression (aFGF18; adGFP - control) (n.s.  $p=0.5612$ ) and (c) FTSL/a with induced FGF18 knock-down (shFGF18; sh nsc – non-silencing control) ( $p=0.87$ ).

### 3.5.11 Anchorage-independent growth – soft agar assay

This assay tests the ability of single cells to form clones independent of anchorage of any kind. Cells were seeded into 3D soft agar. For analysis, pictures were taken from all clones within exemplary vertical areas. For evaluation, the clones were counted and diameters were measured. Tables 6, 7 and 8 give an overview of collected data. Figure 40 displays scatter plots of evaluated clone data which were analysed for significance.

## Results

**Table 6: Anchorage-independent growth assay: Evaluation of clones and measurement of clone diameters of MJZJ with induced FGF18 over-expression (adFGF18) and respective control (adGFP).**

	<b>MJZJ adFGF18</b>	<b>MJZJ adGFP</b>
<b>total number of clones</b>	<b>62</b>	<b>43</b>
<b>average diameter</b>	<b>45.0 <math>\mu\text{m}</math></b>	<b>38.1 <math>\mu\text{m}</math></b>
<b>% of clones bigger than 30 <math>\mu\text{m}</math> in diameter</b>	<b>48.39</b>	<b>60.47</b>

**Table 7: Anchorage-independent growth assay: Evaluation of clones and measurement of clone diameters of FTSL/a with induced FGF18 over-expression (adFGF18) and respective control (adGFP).**

	<b>FTSL/a adFGF18</b>	<b>FTSL/a adGFP</b>
<b>total number of clones</b>	<b>141</b>	<b>160</b>
<b>average diameter</b>	<b>31.93 <math>\mu\text{m}</math></b>	<b>29.02 <math>\mu\text{m}</math></b>
<b>% of clones bigger than 30 <math>\mu\text{m}</math> in diameter</b>	<b>42.55</b>	<b>31.25</b>

**Table 8: Anchorage-independent growth assay: Evaluation of clones and measurement of clone diameters of FTSLA/a with induced FGF18 knock-down (shFGF18) and respective control (sh nsc – non-silencing control).**

	<b>FTSL/a shFGF18</b>	<b>FTSL/a sh nsc</b>
<b>total number of clones</b>	<b>120</b>	<b>162</b>
<b>average diameter</b>	<b>48.86 <math>\mu\text{m}</math></b>	<b>35.21 <math>\mu\text{m}</math></b>
<b>% of clones bigger than 30 <math>\mu\text{m}</math> in diameter</b>	<b>76.67</b>	<b>57.41</b>

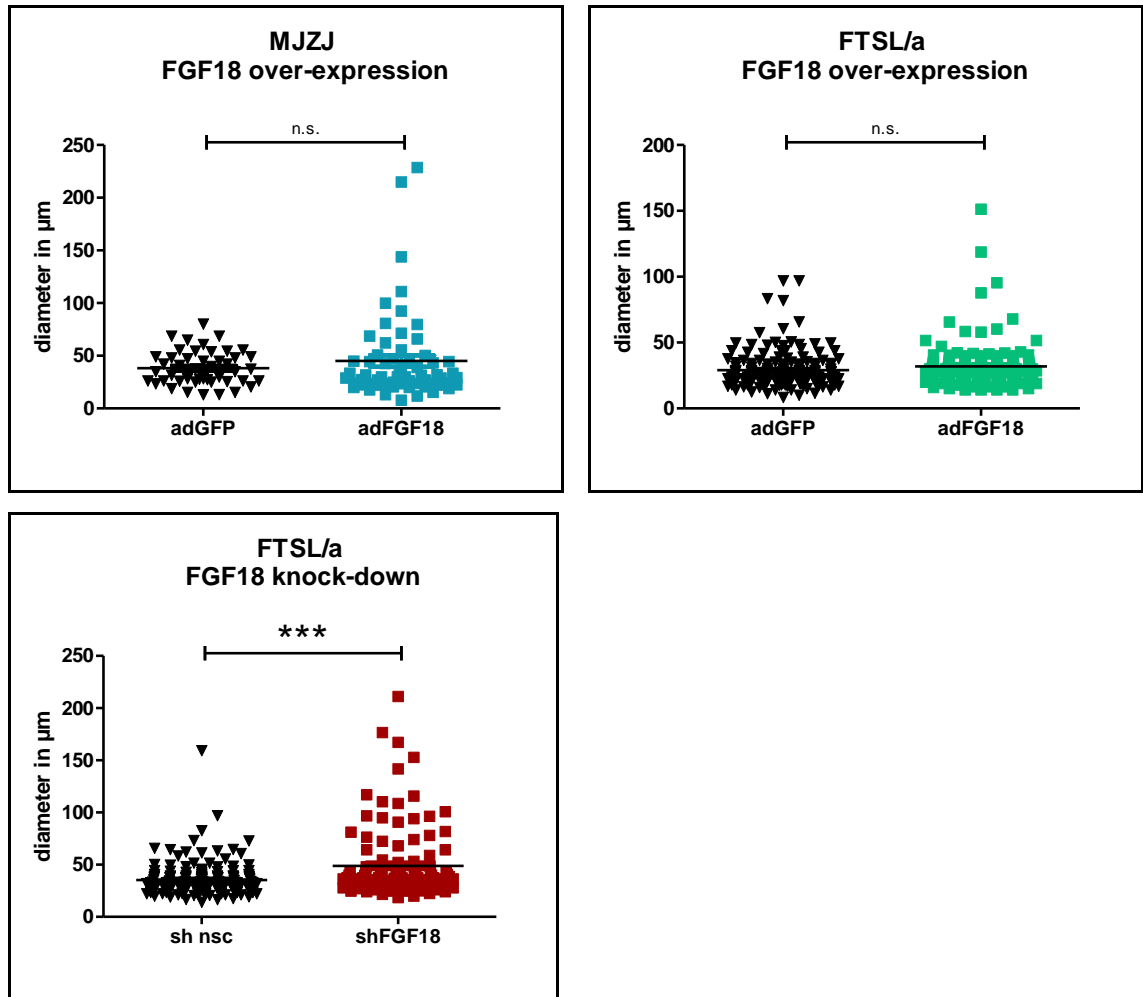


Figure 40: Anchorage-independent growth assay: Scatter plots of evaluated clones of (a) MJZJ with induced FGF18 over-expression (adFGF18) plus control (adGFP), (b) FTSL/a with induced FGF18 over-expression (adFGF18) plus control (adGFP) and (c) FTSL/a with induced FGF18 knock-down (shFGF18) plus control (sh nsc).

## IV. Discussion

Only a few studies were devoted to the role of FGF18 in cancer. What has been found so far is that FGF18 seems to be overexpressed in hepatocellular and colorectal carcinoma. Analysis of colorectal tumours detected FGF18 over-expression in 34 out of 38 tumour samples and progressive increase of FGF18 levels in colorectal cancer along with tumourigenesis. [128] In hepatocellular carcinoma one of the three FGF8 family members, FGF8, FGF17 and FGF18, was found to be elevated in 59%. [129] Recent studies on melanoma unravelled that expression levels of FGF18 are, besides FGF1 and 2, the highest amongst FGFs.[211] In this diploma thesis FGF18 expression levels in melanoma were analysed on protein level in tissue samples via tissue microarray and on RNA level in melanoma cell lines via qRT-PCR. Comparison of tissue array values of each progression stage revealed no differences of FGF18 expression levels, except of primary tumours stage 4 which seem to have elevated FGF18 expression. But since there were not more than two stage 4 samples analysed this result needs further confirmation. However, the comparison of non-malignant nevi and the total of malignant lesions revealed increased expression of FGF18 in malignant melanoma. Expression data of melanoma cell lines also show elevated levels of FGF18 in about half of the samples. However, a big portion of cell lines also seem to have down-regulated FGF18. A correlation between FGF18 expression levels and melanoma subtypes could not be found. Comparison of origins of the respective cell lines, which also reflect cancer progression stage, with FGF18 expression did not reveal any correlation as well, though malignant effusions may tend to have very high levels of FGF18. However, gradual up-regulation of FGF18 along progression of carcinogenesis, like it was found in colorectal carcinoma, could not be detected in melanoma.[128] Additionally, elevated levels of FGF18 in the majority of samples, was not found in melanoma, at least not as distinct as in colorectal carcinoma.

The widely differing FGF18 levels in melanoma cell lines as well as in tissue samples gave reason for further analysis regarding regulation mechanisms of FGF18 expression. Studies on colon cancer identified FGF18 as a downstream target of Wnt-pathway with

putative  $\beta$ -catenin target promotor regions harbouring Tcf4 binding sites. Activation of FGF18 via Wnt-pathway in colorectal carcinoma was further demonstrated by revelation of highly significant correlation between  $\beta$ -catenin activity and FGF18 expression.[124, 128] Such correlation was not found in melanoma cell lines. Therefore it can be precluded, that FGF18 expression is regulated by canonical Wnt-pathway in melanoma. Concerning the general role of Wnt/ $\beta$ -catenin pathway in melanoma, literature reports are quite ambiguous. Some studies observed gradual loss of nuclear  $\beta$ -catenin during tumour progression, which is associated with decrease of expression of melanocyte differentiation genes. It is suggested that Wnt-pathway activity has a homeostatic effect in melanocytes and accordingly its down-regulation promotes the development of malignancies.[213-214] However, other studies detected up-regulation of phospho- $\beta$ -catenin in association with melanoma progression.[216] Analysis of Wnt-pathway activity detected active  $\beta$ -catenin in 12 of 22 analysed cell lines. The fact that all cell lines derived from malignant effusions show very high  $\beta$ -catenin activity and those originating from primary tumours very low or no activity, indicate that this activity increases along tumour progression. These findings stand in contrast with prior reports about progressing loss of  $\beta$ -catenin in melanoma progression.[213-214] The evaluated data, in this thesis, actually reflect the amount of active  $\beta$ -catenin. Therefore the observed increase from primary tumours to malignant effusions also does not accord with the increasing levels of phospho- $\beta$ -catenin along tumor progression reported by Kielhorn et.al. 2003.[216] Phospho- $\beta$ -catenin is not active and targeted for degradation.[216, 229-230] The obtained data which suggest a pro-tumorigenic action of Wnt activity in melanoma rather falls into place with what was found in several other cancer types. Thus deregulated Wnt-pathway activity may contribute to development of colon adenocarcinoma, colorectal and hepatocellular carcinoma, as well as leukemia and hair follicle tumours.[231-237]

Previous studies in hepatocellular and colorectal carcinoma unravelled FGF18 generally as tumourigenesis promoting factor. Thus, administration of recombinant FGF18 had an impairing effect on apoptosis in hepatocellular carcinoma cell lines and stimulated

growth and survival in colorectal carcinoma cell lines. [128-129] In this diploma thesis, analysis of melanoma cell lines with adenoviral mediated over-expression of FGF18 did not reveal comparable function of FGF18 in melanoma. Neither MJZJ, a cell line with low expression of FGF18, nor FTSL/a, which usually expresses FGF18 in moderate levels showed any significant effect of induced FGF18 over-expression on viability and growth. Results from MTT-tests, apoptosis tests, clonogenicity assays and growth curves revealed no statistically significant differences to respective control groups.

Experiments with RNA interference of FGF18 in hepatocellular and colorectal carcinoma cell lines further confirmed its pro-tumourgenic effects. FGF18 knock-down in hepatocellular carcinoma led to decrease of viability, clonogenicity and growth in soft agar. Likewise, in colon carcinoma, clonogenicity and growth was reduced by FGF18 knock-down.[124, 128-129] The gathered results of this study, about the effect of FGF18 knock-down in the melanoma cell line FTSL/a are quite ambiguous. On the one hand, results of MTT-tests show a highly significant increase in FGF18 knock-down clones compared to the non-silencing control clones. Caspase assays, on the other hand, revealed no statistically significant differences. However, these results are not necessarily contradictory, since MTT-assays measure the amount of available reductases and reduction equivalents, which rather reflects metabolic activity than general viability, and caspase assays directly measure apoptosis. Establishment of growth curves and cell cycle analysis did not reveal any effect of FGF 18 knock-down on growth in FTSL/a. However, clonogenicity was increased in knock-down clones with high significance.

Research concerning migration revealed some effect of FGF18 on low expressing MJZJ. Thus, significant increase of transmigration and invasion was detected in FGF18 over-expressing MJZJ. However, scratch assays and anchorage-independent growth assays did not produce statistically relevant results with this cell line. FTSL/a, which usually have moderate expression levels of FGF18, did not show any impact on migration and metastasis auxiliary skills in response to induced over-expression. Neither scratch-, transmigration-, invasion, nor anchorage-independent growth assays detected



## Discussion

significant differences to the non-silencing control. However, FGF18 knock-down in this cell line resulted in significant decrease of the ability to transmigrate. Interestingly, FGF18 knock-down in FTSL/a turned out to be of advantage when cultivated in a soft agar. Anchorage-independent growth assay results showed a significant increase of clone size compared to non-silencing control clones. This finding is consistent with the increased clonogenicity when FGF18 is knocked-down in this cell line. This promoting effect of FGF18 knock-down on clonogenicity and growth in soft agar in melanoma cell lines is exactly the opposite to the effects of FGF18 knock-down in hepatocellular carcinoma cell lines where clonogenicity and growth in soft agar is decreased.[129] Likewise in colorectal carcinoma cell lines, FGF18 knock-down lead to reduced clonogenicity.[128]

Generally, analysis of melanoma cell lines with induced over-expression and knock-down of FGF18 did not reveal an explicit picture of its function in melanoma. Neither MJZJ, nor FTSL/a, showed an effect of FGF18 over-expression on viability and growth. Yet, on MJZJ, which have low FGF18 expression levels, the over-expression seems to have a promoting effect on migration and invasion. FGF18 over-expression in the already moderate expressing cell line FTSL/a does not seem to have any effect at all. Interestingly, FGF18 knock-down seems to have an advantageous effect on the viability of FTSL/a at least in some respect and a negative impact on migration. A general assessment of FGF18 being a tumourigenesis promoting factor, as it is suggested in hepatocellular and colorectal carcinoma, could not be concluded from these data. The role of FGF18 in melanoma seems to be very complex and further studies on this topic may be beneficial.

Besides VEGFs (vascular endothelial growth factors), some FGFs, especially FGF2, are known to be involved in angiogenesis during embryonic development and wound healing. [219] FGF18 in the growth plate is known to induce VEGF expression and thereby regulates skeletal neovascularisation.[222] Additionally, FGF18 showed neoangiogenesis promoting effects in hepatocellular and colorectal carcinoma.[128-129] Consequently, the potential for paracrine effects of FGF18 on immortalised lymph

## Discussion

and blood endothelial cell lines was analysed. The finding of low FGF18 expression in these cells gives reason to preclude effective autocrine signalling of FGF18 in these cells. The expression levels of FGFR4 and FGFR3 indicate potential FGF18 signal reception especially via FGFR4 in both LECs and BECs. Thus, paracrine FGF18 signalling mediated by melanoma cells towards lymph and blood endothelial cells is theoretically possible which leads to the suggestion that FGF18 may be involved in neovascularisation in melanoma as it was already shown in hepatocellular and colorectal carcinoma.[128] Furthermore, expression of VEGF-A and correlation to FGF18 expression was analysed in melanoma cell lines. All cell lines showed VEGF-A expression and in some cases in very high levels. However, no correlation to FGF18 expression was found. Thereby, regulation of VEGF-A expression by FGF18, as it appears in the growth plate, can be precluded.

## Conclusion

FGF18 expression was found to be elevated in malignant melanoma tissue samples and in a big portion of melanoma cell lines. However, this elevation of FGF18 in melanoma is not as distinct as it was found in colorectal carcinoma, and gradual increase of FGF18 with malignant progression could not be found. Increased levels were neither limited to melanoma subtypes nor to histologic origins of samples. Expression regulation of FGF18 by Wnt-pathway activity could not be confirmed in melanoma, whereas it was formerly demonstrated in colorectal carcinoma. However, analysis of  $\beta$ -catenin activity hints at a possible contribution of increased Wnt-pathway activity to melanoma progression. Autocrine effects of FGF18 in melanoma proofed to be widely different from those in hepatocellular and colorectal carcinoma. On the one hand, promoting effects of FGF18 on migration and invasion could be found in a normally low expressing cell line. But on the other hand, FGF18 knock-down lead to increased viability, clonogenicity and anchorage independent growth, which demonstrates the exact opposite effect than shown in hepatocellular and colorectal cancer cells. In melanoma FGF18 seems to have much more complex effects than any distinct function can be adumbrated. However, a paracrine effect of FGF18 towards lymph and blood

## Discussion

endothelial cells mediated by melanoma cells is definitely possible and could thereby contribute to neoangiogenesis, as it was already shown in hepatocellular and colorectal carcinoma.

## V. List of Abbreviations

AEC	3-Amino-9-Ethylcarbazole
Akt	PKB, PI3K effector protein kinase B
ALM	acral letiginous melanoma
APC	adenomous polyposis coli
ATP	adenosine triphosphate
BECs	blood endothelial cells
BRAF <sup>V600E</sup>	BRAF with an activating substitution of valin by glutamic acid at position 600
BRN-2	POU domain 3 transcription factor
Cbfa1/Runx2	core binding factor A1/runt-related transcription factor 2
CDKN2	cyclin-dependent kinase 2
CML	chronic myeloid leukemia
Cx	connexin
DAB+	3,3' Diaminobenzidine
DAG	diacylglycerol
DMSO	dimethyl sulfoxide
EDTA	ethylene diamine tetraacetic acid
EMT	epithelial-mesenchymal transition
ERK	extracellular signal-regulated kinase
ESCRT	endosomal sorting complex required for transport
FACS	fluorescent activated cell sorting
FAK	focal adhesion kinase
FCS	foetal calf serum
FGF	fibroblast growth factor
FGF-BP	FGF binding protein
FGFR	fibroblast growth factor receptor
FHF	FGF homologous factor
FIT	franesyl transferase inhibitors
FLRT3	fibronectin-leucine-rich transmembrane protein 3
FRS2	FGFR substrate 2
GAB1	GRB2 associated binding protein 1
GAPDH	glyceraldehyde 3-phosphate dehydrogenase
GIST	gastrointestinal stromal tumors
GJIC	gap junction intercellular communication
GRB2	growth-factor-receptor-bound protein 2
GSK3	glycogen-synthase kinase 3
GTP	guanosine triphosphate
HGF	hepatocyte growth factor
HRP	horse reddish peroxidise
HSPG	heparan sulphate proteoglycan
Ig-like	immunoglobulin-like

## List of Abbreviations

IHH	Indian hedgedog
LECs	lymph endothelial cells
MAPK	mitogen-activated protein kinase
Mcl-1	myeloid cell leukemia sequence 1
MITF	microphthalmia associated transcription factor
MKP3	MAPK phosphatase 3
MTT	3-(4,5-Dimethylthiazol-2-yl)-2,5-diphenyltetrazolium bromide
NADH	reduced nicotineamide adenine dinucleotide
NADPH	reduced nicotineamide adenine dinucleotide phosphate
N-CAM	neural cell adhesion molekule
OD	optical density
PBS	phosphate buffered saline
PDGFR	platelet-derived growth factor receptor
PI	probidium iodide
PI <sub>3</sub>	inositol 1, 4, 5-triphosphate
PI3K	phosphoinositide-3-OH kinase
PI3K/Akt	phosphatidylinositol-3 kinase/protein kinase B
PIP <sub>2</sub>	phosphatidylinositol 4, 5-triphosphate
PKC	protein kinase C
PLC $\gamma$	phospholipase C $\gamma$
PTEN	phosphate and tensin homologue
qRT-PCR	quantitative Real-Time Polymerase Chain Reaction
R10	RPMI + 10% FCS
RAF	rat fibrosarcoma
RANKL	receptor activator of NF- $\kappa$ B ligand
Ras	rat sarcoma
RB	retinoblastoma protein
RGP	radial growth phase
RISC	RNA induced silencing complex
RMS	rhabdomyosarcoma
RPMI	Roswell Park Memorial Institute Medium
RSK2	p90 ribosomal protein S6 kinase 2
RTK	receptor tyrosine kinase
SCF	stem cell factor
SCLL	stem cell leukemia lymphoma syndrome
SDS	sodium dodecyl sulfate
Sef	similar expression of FGF
shRNA	small hairpin RNA
SPRED2	Sprouty related protein
SSM	superficial spreading melanoma
STATs	signal transducers and activators of transcription

## List of Abbreviations

TCF/Lef	T-cell factor/lymphoid enhancer factor
TRIzol	guanidinium-thiocyanate-chloroform-phenol
VEGF	vascular endothelial growth factor
VEGFR	vascular endothelial growth factor receptor
VGP	vertical growth phase
ZO-1	zonula occludens protein-1

## List of Abbreviations

## VI. List of Figures

Figure 1: Structure of FGFRs, taken from Heinzle et al., 2011[25].....	4
Figure 2: Downstream signalling of FGFs, taken from Wesche et al., 2011 [30] .....	6
Figure 3:(a) Interaction between melanocytes and keratinocytes is mediated via E-cadherin, desmoglein 1 and connexins. (b) Melanoma cell-melanoma cell contacts are established by N-cadherin/N-cadherin, Mel-CAM/ligand, $\alpha\beta 3$ integrin/L1-CAM, ALCAM/ALCAM and interactions of connexins. (c) The connection of melanoma cells to the basal membrane is mediated via N-cadherin and connexins and communication between melanoma cells and endothelial cells is accomplished via N-cadherin/N-cadherin, Mel-CAM/Ligand, $\alpha\beta 3$ integrin/L1-CAM, $\alpha 4\beta 1$ integrin/VCAM-1 and connexin interactions.[145-147] This figure is taken from Haass and Herlyn, 2005[148] .....	18
Figure 4: Schematic pictures of different steps in melanoma progression. (a) Normal skin. (b) Step 1: nevus. (c) Step 4: radial growth phase (RGP) melanoma. (d) Step 5: vertical growth phase (VGP) melanoma. This figure was taken from Grey-Schopfer et al., 2007.[149].....	18
Figure 5: Collected expression array data of FGFs in melanoma. ....	26
Figure 6: Correlation of FGF18 mRNA levels and Wnt-pathway activity was determined by linear regression and was found to be highly significant. This figure was taken from Sonvilla et al., 2008. [128] .....	27
Figure 7: Collected expression array data of FGF receptors in melanoma.....	28
Figure 8: Presence of all four FGF receptors and their isoforms displayed as percentage of positive melanoma cell lines. RT-PCR data of 12 cell lines. This figure was taken from Sonvilla et al., 2008.[218] .....	28
Figure 9: Exemplary pictures of control staining, FGF18 and S100B antibody staining of tissue samples of a primary tumour stage 2 in 10x and 20x magnification. ....	34



## List of Figures

Figure 10: Overview of transfected plasmid combinations and their functions with schematic illustration of experimental set-up on a 24 well plate.....	37
Figure 11: Examples of two melanoma cell lines with different transfection efficacies. (a) FTSLA phase contrast image, (b) FTSLA fluorescence microscopy, EGFP signal; (c) MJZJ phase contrast image, (d) MJZJ fluorescence microscopy, EGFP signal. ....	38
Figure 12: Lentiviral vector plasmid (Thermo Scientific, Open Biosystems Expression Arrest GIPZ Lentiviral shRNAmir Technical Manual). ....	41
Figure 13: RNA interference ( <a href="http://www.genscript.com/siRNA_technology.html">http://www.genscript.com/siRNA_technology.html</a> accessed on 9/26/12).....	42
Figure 14: Expression levels of FGF18 in FTSL/a and MJZJ after adenovial transduction. (a) and (b) show $2^{-\Delta C_{t105}}$ values of qRT-PCR. (c) and (d) display the respective fold expression compared to untransduced cells. ....	46
Figure 15: Mean values (with SEM) of staining intensity assessments of each represented stage.....	54
Figure 16: comparison of mean values (with SEM) of staining intensity assessments of (a) nevi, all primary tumours and metastases and (b) non-malignant lesions (nevi) and malignant lesions (all primary tumours and metastases). The asterisk indicates a significant difference of $p = 0.0269$ . ....	54
Figure 17: Mean qRT-PCR FGF18 expression data (with SEM) of melanoma cell lines with colour code representing the type of melanoma.....	55
Figure 18: Mean qRT-PCR FGF18 expression data (with SEM) of melanoma cell lines with colour code representing the origin of the cell line. ....	56
Figure 19: Mean expression data (with SEM) of immortalised lymph (a) and blood (b) endothelial cells for FGFR1-4 and FGF18. ....	57

## List of Figures

Figure 20: Mean expression data (with SEM) of FGF18 in LECs and BECs and melanoma cell lines. ....	57
Figure 21: VEGF-A expression data of melanoma cell lines with colour code representing the subtype of melanoma. ....	58
Figure 22: qRT-PCR VEGF-A expression data of melanoma cell lines with colour code representing the origin of the cell line. ....	58
Figure 23: Corelation between FGF18 and VEGF-A expression plus regression curve in red. qRT-PCR $2^{-\Delta\Delta CT}$ FGF18 values were plotted along the x-axis and the respective VEGF-A values along the y-axis. ....	59
Figure 24: Mean TOP/FOP values (with SEM) represent Wnt-pathway activity of each cell line. Melanoma subtype, from which the cell lines were established, are indicated by the colour code. Lowest possible value is 1, which denotes no detectable $\beta$ -catenin activity and is marked with X. ....	60
Figure 25: Mean TOP/FOP values (with SEM) represent Wnt-pathway activity of each cell line. Histological origin, from which the cell lines were established, are indicated by the colour code. Lowest possible value is 1, which denotes no detectable $\beta$ -catenin activity and is marked with X. ....	61
Figure 26: Correlation between Wnt-pathway activity and FGF18 expression plus regression curve in red. TOP/FOP values were plotted along the x-axis and the respective FGF18 qRT-PCR $2^{-\Delta\Delta CT}$ values along the y-axis.....	61
Figure 27: Mean fold expression (with SEM) of FGF18 of each subline compared to the non-silencing control. ....	62
Figure 28: MTT-Assay. Fold control values of (a) MJZJ with induced FGF18 over-expression (adFGF18), (b) FTSL/a with induced FGF18 over-expression (adFGF18) and (c) FTSL/a with induced FGF18 knock-down (shFGF18) plus respective negative control	

## List of Figures

values (adGFP; sh nsc, non-silencing control). Significance is indicated as either n.s. (not significant) or ** (p=0.0042). .....	64
Figure 29: Fold control values (with SEM) of caspase activity measured by luminescence assay of (a) MJZJ with induced FGF18 over-expression (adFGF18; adGFP – control), (b) FTSL/a with induced FGF18 over-expression (adFGF18; adGFP – control) and (c) FTSL/a with induced FGF18 knock-down (shFGF18; sh nsc – non-silencing control) under starving conditions with 0.1% serum medium. Non-significant values are indicated with n.s. ....	65
Figure 30: Clonogenicity assay: Pictures of stained cell aggregates of MJZJ with induced FGF18 over-expression and control, FTSL/a with induced FGF18 over-expression and control and FTSL/a knock-down clones and control. ....	66
Figure 31: Clonogenicity assay: Fold control values of crystal violet staining of (a) MJZJ with induced FGF18 over-expression (adFGF18), (b) FTSL/a with induced FGF18 over-expression (adFGF18) and (c) FTSL/a with induced FGF18 knock-down (asFGF18) plus respective controls (adGFP; sh nsc, non-silencing control). Significance is indicated as either n.s. (not significant) or ** (p = 0.0066). ....	67
Figure 32: Growth curves of mean values (with SEM) of (a) MJZJ with induced FGF18 over-expression (adFGF18), (b) FTSL/a with induced FGF18 over-expression (adFGF18) and (c) FTSL/a with induced FGF18 knock-down (shFGF18) plus respective controls (adGFP; sh nsc, non-silencing control). ....	68
Figure 33: Cell cycle analysis: Percentage of cells, residing in each of the three cell cycle stages, reflects temporal division of the cell cycle. Mean values (with SEM) for MJZJ with induced FGF18 over-expression (adFGF18) and control (adGFP) are shown in (a), for FTSL/a with induced FGF18 over-expression (adFGF18) and control (adGFP) in (b) and for FTSL/a with induced FGF18 knock-down (shFGF18) and control (sh nsc, non-silencing control) in (c). ....	69

## List of Figures

Figure 34: Exemplary pictures of scratch assays of FTSL/a and MJZJ with induced FGF18 over-expression (adFGF18) and the corresponding control (adGFP) at 0, 4, 8, 24 and 48 hours. ....	70
Figure 35: Scratch assay: mean percentages (with SEM) of scratch closure of (a) MJZJ with induced FGF18 over-expression (adFGF18) and (b) FTSL/a with induced FGF18 over-expression (adFGF18) at 0, 4, 8, 24 and 48 hours plus respective control (adGFP). ....	71
Figure 36: Transmigration assay: Pictures of stained cell aggregates of MJZJ with induced FGF18 over-expression (adFGF18) and control (adGFP), FTSL/a with induced FGF18 over-expression (adFGF18) and control (adGFP) and FTSL/a with induced FGF18 knock-down (shFGF18) and control (sh nsc). ....	72
Figure 37: Transmigration assay: Fold control values for crystal violet staining intensity (with SEM) of (a) MJZJ with induced FGF18 over-expression (adFGF18; adGFP - control) (p=0.0425), (b) FTSL/a with induced FGF18 over-expression (adFGF18; adGFP - control) (n.s. p=0.5141) and (c) FTSL/a with induced FGF18 knock-down (shFGF18; sh nsc – non-silencing control) (p=0.0419). ....	72
Figure 38: Invasion assay: Pictures of stained cell aggregates of MJZJ with induced FGF18 over-expression and control, FTSL/a with induced FGF18 over-expression and control and FTSL/a knock-down clones and control. ....	73
Figure 39: Invasion assay: Fold control values for crystal violet staining intensity (with SEM) of (a) MJZJ with induced FGF18 over-expression (adFGF18; adGFP - control) (p=0.0177), (b) FTSL/a with induced FGF18 over-expression (aFGF18; adGFP - control) (n.s. p=0.5612) and (c) FTSL/a with induced FGF18 knock-down (shFGF18; sh nsc – non-silencing control) (p=0.87). ....	74
Figure 40: Anchorage-independent growth assay: Scatter plots of evaluated clones of (a) MJZJ with induced FGF18 over-expression (adFGF18) plus control (adGFP), (b)	

## List of Figures

FTSL/a with induced FGF18 over-expression (adFGF18) plus control (adGFP) and (c)	
FTSL/a with induced FGF18 knock-down (shFGF18) plus control (sh nsc). ....	76

## VII. List of Tables

Table 1: FGF receptor isoforms and their binding ligands [25].....	5
Table 2: List of analysed melanoma cell lines with information about respective origin and subtype. ....	31
Table 3: Programmed stages for Taqman qRT-PCR.....	36
Table 4: Applied amounts of plasmids in the respective combinations. ....	39
Table 5: Overview of all samples analysed in this tissue array. The numbers of samples of each melanoma stage showing no (0), weak (1), distinct (2) and intense (3) staining are listed. The bottom line shows the sum of analysed samples of each stage. ....	53
Table 6: Anchorage-independent growth assay: Evaluation of clones and measurement of clone diameters of MJZJ with induced FGF18 over-expression (adFGF18) and respective control (adGFP). ....	75
Table 7: Anchorage-independent growth assay: Evaluation of clones and measurement of clone diameters of FTSL/a with induced FGF18 over-expression (adFGF18) and respective control (adGFP). ....	75
Table 8: Anchorage-independent growth assay: Evaluation of clones and measurement of clone diameters of FTSLA/a with induced FGF18 knock-down (shFGF18) and respective control (sh nsc – non-silencing control). ....	75

## References

## VIII. References

1. Bissell, M.J. and D. Radisky, *Putting tumours in context*. Nat Rev Cancer, 2001. **1**(1): p. 46-54.
2. Hanahan, D. and R.A. Weinberg, *The hallmarks of cancer*. Cell, 2000. **100**(1): p. 57-70.
3. Hanahan, D. and R.A. Weinberg, *Hallmarks of cancer: the next generation*. Cell, 2011. **144**(5): p. 646-74.
4. Kroemer, G. and J. Pouyssegur, *Tumor cell metabolism: cancer's Achilles' heel*. Cancer Cell, 2008. **13**(6): p. 472-82.
5. Luo, J., N.L. Solimini, and S.J. Elledge, *Principles of cancer therapy: oncogene and non-oncogene addiction*. Cell, 2009. **136**(5): p. 823-37.
6. Negrini, S., V.G. Gorgoulis, and T.D. Halazonetis, *Genomic instability--an evolving hallmark of cancer*. Nat Rev Mol Cell Biol, 2010. **11**(3): p. 220-8.
7. Colotta, F., et al., *Cancer-related inflammation, the seventh hallmark of cancer: links to genetic instability*. Carcinogenesis, 2009. **30**(7): p. 1073-81.
8. Hahn, W.C. and R.A. Weinberg, *Rules for making human tumor cells*. N Engl J Med, 2002. **347**(20): p. 1593-603.
9. Stratton, M.R., P.J. Campbell, and P.A. Futreal, *The cancer genome*. Nature, 2009. **458**(7239): p. 719-24.
10. Weinstein, I.B. and A. Joe, *Oncogene addiction*. Cancer Res, 2008. **68**(9): p. 3077-80; discussion 3080.
11. Schlessinger, J., *Cell signaling by receptor tyrosine kinases*. Cell, 2000. **103**(2): p. 211-25.
12. Lemmon, M.A. and J. Schlessinger, *Cell signaling by receptor tyrosine kinases*. Cell, 2010. **141**(7): p. 1117-34.
13. Witsch, E., M. Sela, and Y. Yarden, *Roles for growth factors in cancer progression*. Physiology (Bethesda), 2010. **25**(2): p. 85-101.
14. Yilmaz, M. and G. Christofori, *EMT, the cytoskeleton, and cancer cell invasion*. Cancer Metastasis Rev, 2009. **28**(1-2): p. 15-33.
15. Ornitz, D.M. and N. Itoh, *Fibroblast growth factors*. Genome Biol, 2001. **2**(3): p. REVIEWS3005.
16. Olsen, S.K., et al., *Fibroblast growth factor (FGF) homologous factors share structural but not functional homology with FGFs*. J Biol Chem, 2003. **278**(36): p. 34226-36.
17. Itoh, N., *Hormone-like (endocrine) Fgfs: their evolutionary history and roles in development, metabolism, and disease*. Cell Tissue Res, 2010. **342**(1): p. 1-11.
18. Itoh, N. and D.M. Ornitz, *Evolution of the Fgf and Fgfr gene families*. Trends Genet, 2004. **20**(11): p. 563-9.
19. Beenken, A. and M. Mohammadi, *The FGF family: biology, pathophysiology and therapy*. Nat Rev Drug Discov, 2009. **8**(3): p. 235-53.
20. Aigner, A., et al., *An FGF-binding protein (FGF-BP) exerts its biological function by parallel paracrine stimulation of tumor cell and endothelial cell proliferation through FGF-2 release*. Int J Cancer, 2001. **92**(4): p. 510-7.
21. Johnson, D.E. and L.T. Williams, *Structural and functional diversity in the FGF receptor multigene family*. Adv Cancer Res, 1993. **60**: p. 1-41.
22. Olsen, S.K., et al., *Insights into the molecular basis for fibroblast growth factor receptor autoinhibition and ligand-binding promiscuity*. Proc Natl Acad Sci U S A, 2004. **101**(4): p. 935-40.



## References

23. Eswarakumar, V.P., I. Lax, and J. Schlessinger, *Cellular signaling by fibroblast growth factor receptors*. Cytokine Growth Factor Rev, 2005. **16**(2): p. 139-49.
24. Zhang, X., et al., *Receptor specificity of the fibroblast growth factor family. The complete mammalian FGF family*. J Biol Chem, 2006. **281**(23): p. 15694-700.
25. Heinzel, C., et al., *Targeting fibroblast-growth-factor-receptor-dependent signaling for cancer therapy*. Expert opinion on therapeutic targets, 2011. **15**(7): p. 829-46.
26. Mohammadi, M., et al., *Identification of six novel autophosphorylation sites on fibroblast growth factor receptor 1 and elucidation of their importance in receptor activation and signal transduction*. Mol Cell Biol, 1996. **16**(3): p. 977-89.
27. Mohammadi, M., et al., *A tyrosine-phosphorylated carboxy-terminal peptide of the fibroblast growth factor receptor (Flg) is a binding site for the SH2 domain of phospholipase C-gamma 1*. Mol Cell Biol, 1991. **11**(10): p. 5068-78.
28. Klint, P. and L. Claesson-Welsh, *Signal transduction by fibroblast growth factor receptors*. Front Biosci, 1999. **4**: p. D165-77.
29. Turner, N. and R. Grose, *Fibroblast growth factor signalling: from development to cancer*. Nat Rev Cancer, 2010. **10**(2): p. 116-29.
30. Wesche, J., K. Haglund, and E.M. Haugsten, *Fibroblast growth factors and their receptors in cancer*. The Biochemical journal, 2011. **437**(2): p. 199-213.
31. Dikic, I. and S. Giordano, *Negative receptor signalling*. Curr Opin Cell Biol, 2003. **15**(2): p. 128-35.
32. Chambers, D. and I. Mason, *Expression of sprouty2 during early development of the chick embryo is coincident with known sites of FGF signalling*. Mech Dev, 2000. **91**(1-2): p. 361-4.
33. Edwin, F., et al., *Intermolecular interactions of Sprouty proteins and their implications in development and disease*. Mol Pharmacol, 2009. **76**(4): p. 679-91.
34. Mason, J.M., et al., *Sprouty proteins: multifaceted negative-feedback regulators of receptor tyrosine kinase signaling*. Trends Cell Biol, 2006. **16**(1): p. 45-54.
35. Minowada, G., et al., *Vertebrate Sprouty genes are induced by FGF signaling and can cause chondrodysplasia when overexpressed*. Development, 1999. **126**(20): p. 4465-75.
36. Martinez, N., et al., *Sprouty2 binds Grb2 at two different proline-rich regions, and the mechanism of ERK inhibition is independent of this interaction*. Cell Signal, 2007. **19**(11): p. 2277-85.
37. Li, C., et al., *Dusp6 (Mkp3) is a negative feedback regulator of FGF-stimulated ERK signaling during mouse development*. Development, 2007. **134**(1): p. 167-76.
38. Tsang, M. and I.B. Dawid, *Promotion and attenuation of FGF signaling through the Ras-MAPK pathway*. Sci STKE, 2004. **2004**(228): p. pe17.
39. Kovalenko, D., et al., *Sef inhibits fibroblast growth factor signaling by inhibiting FGFR1 tyrosine phosphorylation and subsequent ERK activation*. J Biol Chem, 2003. **278**(16): p. 14087-91.
40. Lax, I., et al., *The docking protein FRS2alpha controls a MAP kinase-mediated negative feedback mechanism for signaling by FGF receptors*. Mol Cell, 2002. **10**(4): p. 709-19.
41. Bottcher, R.T., et al., *The transmembrane protein XFLRT3 forms a complex with FGF receptors and promotes FGF signalling*. Nat Cell Biol, 2004. **6**(1): p. 38-44.
42. Haines, B.P., et al., *Regulated expression of FLRT genes implies a functional role in the regulation of FGF signalling during mouse development*. Dev Biol, 2006. **297**(1): p. 14-25.

## References

43. Wong, A., et al., *FRS2 alpha attenuates FGF receptor signaling by Grb2-mediated recruitment of the ubiquitin ligase Cbl*. Proc Natl Acad Sci U S A, 2002. **99**(10): p. 6684-9.
44. Jean, S., et al., *Extended-synaptotagmin-2 mediates FGF receptor endocytosis and ERK activation in vivo*. Dev Cell, 2010. **19**(3): p. 426-39.
45. Haugsten, E.M., et al., *Different intracellular trafficking of FGF1 endocytosed by the four homologous FGF receptors*. J Cell Sci, 2005. **118**(Pt 17): p. 3869-81.
46. Belleudi, F., et al., *Hrs regulates the endocytic sorting of the fibroblast growth factor receptor 2b*. Exp Cell Res, 2009. **315**(13): p. 2181-91.
47. Haugsten, E.M., et al., *Ubiquitination of fibroblast growth factor receptor 1 is required for its intracellular sorting but not for its endocytosis*. Mol Biol Cell, 2008. **19**(8): p. 3390-403.
48. Mardakheh, F.K., et al., *Spred2 interaction with the late endosomal protein NBR1 down-regulates fibroblast growth factor receptor signaling*. J Cell Biol, 2009. **187**(2): p. 265-77.
49. Belleudi, F., et al., *Keratinocyte growth factor receptor ligands target the receptor to different intracellular pathways*. Traffic, 2007. **8**(12): p. 1854-72.
50. Francavilla, C., et al., *The binding of NCAM to FGFR1 induces a specific cellular response mediated by receptor trafficking*. J Cell Biol, 2009. **187**(7): p. 1101-16.
51. Chambers, S.M., et al., *Highly efficient neural conversion of human ES and iPS cells by dual inhibition of SMAD signaling*. Nat Biotechnol, 2009. **27**(3): p. 275-80.
52. Rathjen, J., et al., *Formation of a primitive ectoderm like cell population, EPL cells, from ES cells in response to biologically derived factors*. J Cell Sci, 1999. **112** ( Pt 5): p. 601-12.
53. Braun, S., et al., *Fibroblast growth factors in epithelial repair and cytoprotection*. Philos Trans R Soc Lond B Biol Sci, 2004. **359**(1445): p. 753-7.
54. Podolsky, D.K., *Healing the epithelium: solving the problem from two sides*. J Gastroenterol, 1997. **32**(1): p. 122-6.
55. Abuharbeid, S., F. Czubyko, and A. Aigner, *The fibroblast growth factor-binding protein FGF-BP*. Int J Biochem Cell Biol, 2006. **38**(9): p. 1463-8.
56. Beer, H.D., et al., *The fibroblast growth factor binding protein is a novel interaction partner of FGF-7, FGF-10 and FGF-22 and regulates FGF activity: implications for epithelial repair*. Oncogene, 2005. **24**(34): p. 5269-77.
57. Ornitz, D.M., et al., *Receptor specificity of the fibroblast growth factor family*. J Biol Chem, 1996. **271**(25): p. 15292-7.
58. Orr-Urtreger, A., et al., *Developmental localization of the splicing alternatives of fibroblast growth factor receptor-2 (FGFR2)*. Dev Biol, 1993. **158**(2): p. 475-86.
59. Sinha, J., et al., *beta-Klotho and FGF-15/19 inhibit the apical sodium-dependent bile acid transporter in enterocytes and cholangiocytes*. Am J Physiol Gastrointest Liver Physiol, 2008. **295**(5): p. G996-G1003.
60. Tomlinson, E., et al., *Transgenic mice expressing human fibroblast growth factor-19 display increased metabolic rate and decreased adiposity*. Endocrinology, 2002. **143**(5): p. 1741-7.
61. Nakayama, Y., et al., *Fgf19 is required for zebrafish lens and retina development*. Dev Biol, 2008. **313**(2): p. 752-66.
62. Vincentz, J.W., et al., *Fgf15 is required for proper morphogenesis of the mouse cardiac outflow tract*. Genesis, 2005. **41**(4): p. 192-201.

## References

63. Badman, M.K., et al., *Fibroblast growth factor 21-deficient mice demonstrate impaired adaptation to ketosis*. Endocrinology, 2009. **150**(11): p. 4931-40.
64. *Autosomal dominant hypophosphataemic rickets is associated with mutations in FGF23*. Nat Genet, 2000. **26**(3): p. 345-8.
65. Presta, M., et al., *Fibroblast growth factor/fibroblast growth factor receptor system in angiogenesis*. Cytokine Growth Factor Rev, 2005. **16**(2): p. 159-78.
66. Taylor, J.G.t., et al., *Identification of FGFR4-activating mutations in human rhabdomyosarcomas that promote metastasis in xenotransplanted models*. J Clin Invest, 2009. **119**(11): p. 3395-407.
67. Elbauomy Elsheikh, S., et al., *FGFR1 amplification in breast carcinomas: a chromogenic in situ hybridisation analysis*. Breast Cancer Res, 2007. **9**(2): p. R23.
68. Ding, L., et al., *Somatic mutations affect key pathways in lung adenocarcinoma*. Nature, 2008. **455**(7216): p. 1069-75.
69. Turner, N., et al., *FGFR1 amplification drives endocrine therapy resistance and is a therapeutic target in breast cancer*. Cancer Res, 2010. **70**(5): p. 2085-94.
70. Beroukhim, R., et al., *The landscape of somatic copy-number alteration across human cancers*. Nature, 2010. **463**(7283): p. 899-905.
71. Dutt, A., et al., *Drug-sensitive FGFR2 mutations in endometrial carcinoma*. Proc Natl Acad Sci U S A, 2008. **105**(25): p. 8713-7.
72. Weiss, J., et al., *Frequent and focal FGFR1 amplification associates with therapeutically tractable FGFR1 dependency in squamous cell lung cancer*. Sci Transl Med, 2010. **2**(62): p. 62ra93.
73. Naski, M.C., et al., *Graded activation of fibroblast growth factor receptor 3 by mutations causing achondroplasia and thanatophoric dysplasia*. Nat Genet, 1996. **13**(2): p. 233-7.
74. Pandith, A.A., Z.A. Shah, and M.A. Siddiqi, *Oncogenic role of fibroblast growth factor receptor 3 in tumorigenesis of urinary bladder cancer*. Urol Oncol, 2010.
75. Gartside, M.G., et al., *Loss-of-function fibroblast growth factor receptor-2 mutations in melanoma*. Mol Cancer Res, 2009. **7**(1): p. 41-54.
76. Bange, J., et al., *Cancer progression and tumor cell motility are associated with the FGFR4 Arg(388) allele*. Cancer Res, 2002. **62**(3): p. 840-7.
77. Sugiyama, N., et al., *Fibroblast growth factor receptor 4 regulates tumor invasion by coupling fibroblast growth factor signaling to extracellular matrix degradation*. Cancer Res, 2010. **70**(20): p. 7851-61.
78. Spinola, M., et al., *Functional FGFR4 Gly388Arg polymorphism predicts prognosis in lung adenocarcinoma patients*. J Clin Oncol, 2005. **23**(29): p. 7307-11.
79. Spinola, M., et al., *FGFR4 Gly388Arg polymorphism and prognosis of breast and colorectal cancer*. Oncol Rep, 2005. **14**(2): p. 415-9.
80. Thussbas, C., et al., *FGFR4 Arg388 allele is associated with resistance to adjuvant therapy in primary breast cancer*. J Clin Oncol, 2006. **24**(23): p. 3747-55.
81. Hunter, D.J., et al., *A genome-wide association study identifies alleles in FGFR2 associated with risk of sporadic postmenopausal breast cancer*. Nat Genet, 2007. **39**(7): p. 870-4.
82. Easton, D.F., et al., *Genome-wide association study identifies novel breast cancer susceptibility loci*. Nature, 2007. **447**(7148): p. 1087-93.
83. Jackson, C.C., L.J. Medeiros, and R.N. Miranda, *8p11 myeloproliferative syndrome: a review*. Hum Pathol, 2010. **41**(4): p. 461-76.

## References

84. Gelsi-Boyer, V., et al., *Comprehensive profiling of 8p11-12 amplification in breast cancer*. Mol Cancer Res, 2005. **3**(12): p. 655-67.
85. Chin, K., et al., *Genomic and transcriptional aberrations linked to breast cancer pathophysiologies*. Cancer Cell, 2006. **10**(6): p. 529-41.
86. Letessier, A., et al., *Frequency, prognostic impact, and subtype association of 8p12, 8q24, 11q13, 12p13, 17q12, and 20q13 amplifications in breast cancers*. BMC Cancer, 2006. **6**: p. 245.
87. Mosesson, Y., G.B. Mills, and Y. Yarden, *Derailed endocytosis: an emerging feature of cancer*. Nat Rev Cancer, 2008. **8**(11): p. 835-50.
88. Fritzsche, S., et al., *Concomitant down-regulation of SPRY1 and SPRY2 in prostate carcinoma*. Endocr Relat Cancer, 2006. **13**(3): p. 839-49.
89. Darby, S., et al., *Similar expression to FGF (Sef) inhibits fibroblast growth factor-induced tumourigenic behaviour in prostate cancer cells and is downregulated in aggressive clinical disease*. Br J Cancer, 2009. **101**(11): p. 1891-9.
90. Shawver, L.K., D. Slamon, and A. Ullrich, *Smart drugs: tyrosine kinase inhibitors in cancer therapy*. Cancer Cell, 2002. **1**(2): p. 117-23.
91. Reichert, J.M. and V.E. Valge-Archer, *Development trends for monoclonal antibody cancer therapeutics*. Nat Rev Drug Discov, 2007. **6**(5): p. 349-56.
92. Knights, V. and S.J. Cook, *De-regulated FGF receptors as therapeutic targets in cancer*. Pharmacol Ther, 2010. **125**(1): p. 105-17.
93. Chen, L. and C.X. Deng, *Roles of FGF signaling in skeletal development and human genetic diseases*. Front Biosci, 2005. **10**: p. 1961-76.
94. Katoh, M., *Comparative genomics on FGF8, FGF17, and FGF18 orthologs*. Int J Mol Med, 2005. **16**(3): p. 493-6.
95. Hu, M.C., et al., *FGF-18, a novel member of the fibroblast growth factor family, stimulates hepatic and intestinal proliferation*. Mol Cell Biol, 1998. **18**(10): p. 6063-74.
96. Ohbayashi, N., et al., *Structure and expression of the mRNA encoding a novel fibroblast growth factor, FGF-18*. J Biol Chem, 1998. **273**(29): p. 18161-4.
97. Whitmore, T.E., et al., *Assignment of fibroblast growth factor 18 (FGF18) to human chromosome 5q34 by use of radiation hybrid mapping and fluorescence in situ hybridization*. Cytogenet Cell Genet, 2000. **90**(3-4): p. 231-3.
98. Cormier, S., et al., *Expression of fibroblast growth factors 18 and 23 during human embryonic and fetal development*. Gene Expr Patterns, 2005. **5**(4): p. 569-73.
99. Ohbayashi, N., et al., *FGF18 is required for normal cell proliferation and differentiation during osteogenesis and chondrogenesis*. Genes Dev, 2002. **16**(7): p. 870-9.
100. Ellsworth, J.L., et al., *Fibroblast growth factor-18 is a trophic factor for mature chondrocytes and their progenitors*. Osteoarthritis Cartilage, 2002. **10**(4): p. 308-20.
101. Ellsworth, J.L., et al., *Fibroblast growth factor-18 reduced infarct volumes and behavioral deficits after transient occlusion of the middle cerebral artery in rats*. Stroke, 2003. **34**(6): p. 1507-12.
102. Xu, J., Z. Liu, and D.M. Ornitz, *Temporal and spatial gradients of Fgf8 and Fgf17 regulate proliferation and differentiation of midline cerebellar structures*. Development, 2000. **127**(9): p. 1833-43.
103. Zhang, X., et al., *Receptor specificity of the fibroblast growth factor family. The complete mammalian FGF family*. The Journal of biological chemistry, 2006. **281**(23): p. 15694-700.
104. Ornitz, D.M., *FGF signaling in the developing endochondral skeleton*. Cytokine Growth Factor Rev, 2005. **16**(2): p. 205-13.

## References

105. Shimoaka, T., et al., *Regulation of osteoblast, chondrocyte, and osteoclast functions by fibroblast growth factor (FGF)-18 in comparison with FGF-2 and FGF-10*. J Biol Chem, 2002. **277**(9): p. 7493-500.
106. Maruoka, Y., et al., *Comparison of the expression of three highly related genes, Fgf8, Fgf17 and Fgf18, in the mouse embryo*. Mech Dev, 1998. **74**(1-2): p. 175-7.
107. Ohuchi, H., et al., *Involvement of fibroblast growth factor (FGF)18-FGF8 signaling in specification of left-right asymmetry and brain and limb development of the chick embryo*. Mech Dev, 2000. **95**(1-2): p. 55-66.
108. Sato, T., A.L. Joyner, and H. Nakamura, *How does Fgf signaling from the isthmic organizer induce midbrain and cerebellum development?* Dev Growth Differ, 2004. **46**(6): p. 487-94.
109. Usui, H., et al., *Fgf18 is required for embryonic lung alveolar development*. Biochem Biophys Res Commun, 2004. **322**(3): p. 887-92.
110. Dichmann, D.S., et al., *Expression and misexpression of members of the FGF and TGFbeta families of growth factors in the developing mouse pancreas*. Dev Dyn, 2003. **226**(4): p. 663-74.
111. Ohuchi, H., *[Roles for FGF-FGFR signaling during vertebrate development]*. Hum Cell, 2000. **13**(4): p. 169-75.
112. Hasegawa, H., et al., *Laminar patterning in the developing neocortex by temporally coordinated fibroblast growth factor signaling*. J Neurosci, 2004. **24**(40): p. 8711-9.
113. Kawano, M., et al., *Comprehensive analysis of FGF and FGFR expression in skin: FGF18 is highly expressed in hair follicles and capable of inducing anagen from telogen stage hair follicles*. J Invest Dermatol, 2005. **124**(5): p. 877-85.
114. Herzog, W., et al., *Fgf3 signaling from the ventral diencephalon is required for early specification and subsequent survival of the zebrafish adenohypophysis*. Development, 2004. **131**(15): p. 3681-92.
115. Hurley, A.A., *Principles of quality control*. Curr Protoc Cytom, 2001. **Chapter 3**: p. Unit 3 1.
116. Marie, P.J., *Fibroblast growth factor signaling controlling osteoblast differentiation*. Gene, 2003. **316**: p. 23-32.
117. Eswarakumar, V.P., et al., *The IIIc alternative of Fgfr2 is a positive regulator of bone formation*. Development, 2002. **129**(16): p. 3783-93.
118. Moore, E.E., et al., *Fibroblast growth factor-18 stimulates chondrogenesis and cartilage repair in a rat model of injury-induced osteoarthritis*. Osteoarthritis Cartilage, 2005. **13**(7): p. 623-31.
119. Liu, Z., et al., *Coordination of chondrogenesis and osteogenesis by fibroblast growth factor 18*. Genes Dev, 2002. **16**(7): p. 859-69.
120. Ozasa, A., et al., *Complementary antagonistic actions between C-type natriuretic peptide and the MAPK pathway through FGFR-3 in ATDC5 cells*. Bone, 2005. **36**(6): p. 1056-64.
121. Davidson, D., et al., *Fibroblast growth factor (FGF) 18 signals through FGF receptor 3 to promote chondrogenesis*. J Biol Chem, 2005. **280**(21): p. 20509-15.
122. Montero, A., et al., *Disruption of the fibroblast growth factor-2 gene results in decreased bone mass and bone formation*. J Clin Invest, 2000. **105**(8): p. 1085-93.
123. Kapadia, R.M., et al., *Glycogen synthase kinase 3 controls endochondral bone development: contribution of fibroblast growth factor 18*. Dev Biol, 2005. **285**(2): p. 496-507.

## References

124. Shimokawa, T., et al., *Involvement of the FGF18 gene in colorectal carcinogenesis, as a novel downstream target of the beta-catenin/T-cell factor complex*. *Cancer Res*, 2003. **63**(19): p. 6116-20.
125. Whitsett, J.A., et al., *Fibroblast growth factor 18 influences proximal programming during lung morphogenesis*. *J Biol Chem*, 2002. **277**(25): p. 22743-9.
126. Hoshikawa, M., et al., *FGF-18 is a neuron-derived glial cell growth factor expressed in the rat brain during early postnatal development*. *Brain Res Mol Brain Res*, 2002. **105**(1-2): p. 60-6.
127. Ornitz, D.M. and P.J. Marie, *FGF signaling pathways in endochondral and intramembranous bone development and human genetic disease*. *Genes Dev*, 2002. **16**(12): p. 1446-65.
128. Sonvilla, G., et al., *FGF18 in colorectal tumour cells: autocrine and paracrine effects*. *Carcinogenesis*, 2008. **29**(1): p. 15-24.
129. Gauglhofer, C., et al., *Up-regulation of the fibroblast growth factor 8 subfamily in human hepatocellular carcinoma for cell survival and neoangiogenesis*. *Hepatology*, 2011. **53**(3): p. 854-64.
130. Cummins, D.L., et al., *Cutaneous malignant melanoma*. *Mayo Clin Proc*, 2006. **81**(4): p. 500-7.
131. Clark, W.H., Jr., et al., *A study of tumor progression: the precursor lesions of superficial spreading and nodular melanoma*. *Hum Pathol*, 1984. **15**(12): p. 1147-65.
132. Hsu, M.Y., et al., *E-cadherin expression in melanoma cells restores keratinocyte-mediated growth control and down-regulates expression of invasion-related adhesion receptors*. *Am J Pathol*, 2000. **156**(5): p. 1515-25.
133. Jimbow, K., et al., *Some aspects of melanin biology: 1950-1975*. *J Invest Dermatol*, 1976. **67**(1): p. 72-89.
134. Haass, N.K., K.S. Smalley, and M. Herlyn, *The role of altered cell-cell communication in melanoma progression*. *J Mol Histol*, 2004. **35**(3): p. 309-18.
135. Haass, N.K., et al., *Adhesion, migration and communication in melanocytes and melanoma*. *Pigment Cell Res*, 2005. **18**(3): p. 150-9.
136. Boissy, R.E. and J.J. Nordlund, *Molecular basis of congenital hypopigmentary disorders in humans: a review*. *Pigment Cell Res*, 1997. **10**(1-2): p. 12-24.
137. Tang, A., et al., *E-cadherin is the major mediator of human melanocyte adhesion to keratinocytes in vitro*. *J Cell Sci*, 1994. **107 ( Pt 4)**: p. 983-92.
138. Hsu, M.Y., et al., *Shifts in cadherin profiles between human normal melanocytes and melanomas*. *J Invest Dermatol Symp Proc*, 1996. **1**(2): p. 188-94.
139. Haass, N.K., et al., *Differential induction of connexins 26 and 30 in skin tumors and their adjacent epidermis*. *J Histochem Cytochem*, 2006. **54**(2): p. 171-82.
140. Cano, A., et al., *The transcription factor snail controls epithelial-mesenchymal transitions by repressing E-cadherin expression*. *Nat Cell Biol*, 2000. **2**(2): p. 76-83.
141. Poser, I., et al., *Loss of E-cadherin expression in melanoma cells involves up-regulation of the transcriptional repressor Snail*. *J Biol Chem*, 2001. **276**(27): p. 24661-6.
142. Hoek, K., et al., *Expression profiling reveals novel pathways in the transformation of melanocytes to melanomas*. *Cancer Res*, 2004. **64**(15): p. 5270-82.
143. Smalley, K.S., et al., *Up-regulated expression of zonula occludens protein-1 in human melanoma associates with N-cadherin and contributes to invasion and adhesion*. *Am J Pathol*, 2005. **166**(5): p. 1541-54.

## References

144. Satyamoorthy, K., et al., *Mel-CAM-specific genetic suppressor elements inhibit melanoma growth and invasion through loss of gap junctional communication*. *Oncogene*, 2001. **20**(34): p. 4676-84.
145. Degen, W.G., et al., *MEMD, a new cell adhesion molecule in metastasizing human melanoma cell lines, is identical to ALCAM (activated leukocyte cell adhesion molecule)*. *Am J Pathol*, 1998. **152**(3): p. 805-13.
146. Holzmann, B., U. Gossler, and M. Bittner, *alpha 4 integrins and tumor metastasis*. *Curr Top Microbiol Immunol*, 1998. **231**: p. 125-41.
147. van Kempen, L.C., et al., *Activated leukocyte cell adhesion molecule/CD166, a marker of tumor progression in primary malignant melanoma of the skin*. *Am J Pathol*, 2000. **156**(3): p. 769-74.
148. Haass, N.K. and M. Herlyn, *Normal human melanocyte homeostasis as a paradigm for understanding melanoma*. *J Invest Dermatol Symp Proc*, 2005. **10**(2): p. 153-63.
149. Gray-Schopfer, V., C. Wellbrock, and R. Marais, *Melanoma biology and new targeted therapy*. *Nature*, 2007. **445**(7130): p. 851-7.
150. Miller, A.J. and M.C. Mihm, Jr., *Melanoma*. *N Engl J Med*, 2006. **355**(1): p. 51-65.
151. Wellbrock, C., M. Karasarides, and R. Marais, *The RAF proteins take centre stage*. *Nat Rev Mol Cell Biol*, 2004. **5**(11): p. 875-85.
152. Wellbrock, C., et al., *Activation of p59(Fyn) leads to melanocyte dedifferentiation by influencing MKP-1-regulated mitogen-activated protein kinase signaling*. *J Biol Chem*, 2002. **277**(8): p. 6443-54.
153. Bohm, M., et al., *Identification of p90RSK as the probable CREB-Ser133 kinase in human melanocytes*. *Cell Growth Differ*, 1995. **6**(3): p. 291-302.
154. Cohen, C., et al., *Mitogen-activated protein kinase activation is an early event in melanoma progression*. *Clin Cancer Res*, 2002. **8**(12): p. 3728-33.
155. Willmore-Payne, C., et al., *Human malignant melanoma: detection of BRAF- and c-kit-activating mutations by high-resolution amplicon melting analysis*. *Hum Pathol*, 2005. **36**(5): p. 486-93.
156. Milagre, C., et al., *A mouse model of melanoma driven by oncogenic KRAS*. *Cancer research*, 2010. **70**(13): p. 5549-57.
157. Davies, H., et al., *Mutations of the BRAF gene in human cancer*. *Nature*, 2002. **417**(6892): p. 949-54.
158. Garnett, M.J. and R. Marais, *Guilty as charged: B-RAF is a human oncogene*. *Cancer Cell*, 2004. **6**(4): p. 313-9.
159. Wan, P.T., et al., *Mechanism of activation of the RAF-ERK signaling pathway by oncogenic mutations of B-RAF*. *Cell*, 2004. **116**(6): p. 855-67.
160. Gray-Schopfer, V.C., S. da Rocha Dias, and R. Marais, *The role of B-RAF in melanoma*. *Cancer Metastasis Rev*, 2005. **24**(1): p. 165-83.
161. Sharma, A., et al., *Mutant V599EB-Raf regulates growth and vascular development of malignant melanoma tumors*. *Cancer Res*, 2005. **65**(6): p. 2412-21.
162. Shaw, R.J. and L.C. Cantley, *Ras, PI(3)K and mTOR signalling controls tumour cell growth*. *Nature*, 2006. **441**(7092): p. 424-30.
163. Omholt, K., et al., *Mutations of PIK3CA are rare in cutaneous melanoma*. *Melanoma Res*, 2006. **16**(2): p. 197-200.
164. Stahl, J.M., et al., *Deregulated Akt3 activity promotes development of malignant melanoma*. *Cancer Res*, 2004. **64**(19): p. 7002-10.
165. Wu, H., V. Goel, and F.G. Haluska, *PTEN signaling pathways in melanoma*. *Oncogene*, 2003. **22**(20): p. 3113-22.

## References

166. Smalley, K.S., et al., *Multiple signaling pathways must be targeted to overcome drug resistance in cell lines derived from melanoma metastases*. Molecular cancer therapeutics, 2006. **5**(5): p. 1136-44.
167. Levy, C., M. Khaled, and D.E. Fisher, *MITF: master regulator of melanocyte development and melanoma oncogene*. Trends in molecular medicine, 2006. **12**(9): p. 406-14.
168. Selzer, E., et al., *The melanocyte-specific isoform of the microphthalmia transcription factor affects the phenotype of human melanoma*. Cancer research, 2002. **62**(7): p. 2098-103.
169. Garraway, L.A., et al., *Integrative genomic analyses identify MITF as a lineage survival oncogene amplified in malignant melanoma*. Nature, 2005. **436**(7047): p. 117-22.
170. Takeda, K., et al., *Induction of melanocyte-specific microphthalmia-associated transcription factor by Wnt-3a*. The Journal of biological chemistry, 2000. **275**(19): p. 14013-6.
171. Omholt, K., et al., *Cytoplasmic and nuclear accumulation of beta-catenin is rarely caused by CTNNB1 exon 3 mutations in cutaneous malignant melanoma*. International journal of cancer. Journal international du cancer, 2001. **92**(6): p. 839-42.
172. Rimm, D.L., et al., *Frequent nuclear/cytoplasmic localization of beta-catenin without exon 3 mutations in malignant melanoma*. The American journal of pathology, 1999. **154**(2): p. 325-9.
173. Chen, D., et al., *SKI activates Wnt/beta-catenin signaling in human melanoma*. Cancer research, 2003. **63**(20): p. 6626-34.
174. Worm, J., et al., *Genetic and epigenetic alterations of the APC gene in malignant melanoma*. Oncogene, 2004. **23**(30): p. 5215-26.
175. Ben-Porath, I. and R.A. Weinberg, *The signals and pathways activating cellular senescence*. The international journal of biochemistry & cell biology, 2005. **37**(5): p. 961-76.
176. Mooi, W.J. and D.S. Peeper, *Oncogene-induced cell senescence--halting on the road to cancer*. The New England journal of medicine, 2006. **355**(10): p. 1037-46.
177. Wynford-Thomas, D., *Cellular senescence and cancer*. The Journal of pathology, 1999. **187**(1): p. 100-11.
178. Kim, W.Y. and N.E. Sharpless, *The regulation of INK4/ARF in cancer and aging*. Cell, 2006. **127**(2): p. 265-75.
179. Krimpenfort, P., et al., *p15Ink4b is a critical tumour suppressor in the absence of p16Ink4a*. Nature, 2007. **448**(7156): p. 943-6.
180. Sviderskaya, E.V., et al., *p16(Ink4a) in melanocyte senescence and differentiation*. Journal of the National Cancer Institute, 2002. **94**(6): p. 446-54.
181. Tyner, S.D., et al., *p53 mutant mice that display early ageing-associated phenotypes*. Nature, 2002. **415**(6867): p. 45-53.
182. Bennett, D.C., *How to make a melanoma: what do we know of the primary clonal events?* Pigment cell & melanoma research, 2008. **21**(1): p. 27-38.
183. Freedberg, D.E., et al., *Frequent p16-independent inactivation of p14ARF in human melanoma*. Journal of the National Cancer Institute, 2008. **100**(11): p. 784-95.
184. Chin, L., L.A. Garraway, and D.E. Fisher, *Malignant melanoma: genetics and therapeutics in the genomic era*. Genes & development, 2006. **20**(16): p. 2149-82.
185. Halaban, R., *Rb/E2F: a two-edged sword in the melanocytic system*. Cancer metastasis reviews, 2005. **24**(2): p. 339-56.



## References

186. Wilhelm, S.M., et al., *BAY 43-9006 exhibits broad spectrum oral antitumor activity and targets the RAF/MEK/ERK pathway and receptor tyrosine kinases involved in tumor progression and angiogenesis*. Cancer research, 2004. **64**(19): p. 7099-109.
187. Hauschild, A., et al., *Results of a phase III, randomized, placebo-controlled study of sorafenib in combination with carboplatin and paclitaxel as second-line treatment in patients with unresectable stage III or stage IV melanoma*. Journal of clinical oncology : official journal of the American Society of Clinical Oncology, 2009. **27**(17): p. 2823-30.
188. Eisen, T., et al., *Sorafenib in advanced melanoma: a Phase II randomised discontinuation trial analysis*. British journal of cancer, 2006. **95**(5): p. 581-6.
189. King, A.J., et al., *Demonstration of a genetic therapeutic index for tumors expressing oncogenic BRAF by the kinase inhibitor SB-590885*. Cancer research, 2006. **66**(23): p. 11100-5.
190. Tsai, J., et al., *Discovery of a selective inhibitor of oncogenic B-Raf kinase with potent antimelanoma activity*. Proceedings of the National Academy of Sciences of the United States of America, 2008. **105**(8): p. 3041-6.
191. Sondergaard, J.N., et al., *Differential sensitivity of melanoma cell lines with BRAFV600E mutation to the specific Raf inhibitor PLX4032*. Journal of translational medicine, 2010. **8**: p. 39.
192. Schwartz, G.K., et al., *A phase I study of XL281, a selective oral RAF kinase inhibitor, in patients (Pts) with advanced solid tumors*. Journal of Clinical Oncology, 2009. **27**(15).
193. Yang, H., et al., *RG7204 (PLX4032), a selective BRAFV600E inhibitor, displays potent antitumor activity in preclinical melanoma models*. Cancer research, 2010. **70**(13): p. 5518-27.
194. Bollag, G., et al., *Clinical efficacy of a RAF inhibitor needs broad target blockade in BRAF-mutant melanoma*. Nature, 2010. **467**(7315): p. 596-9.
195. Chapman, P.B., et al., *Improved Survival with Vemurafenib in Melanoma with BRAF V600E Mutation*. New England Journal of Medicine, 2011. **364**(26): p. 2507-2516.
196. Tap, W.D., et al., *Pharmacodynamic characterization of the efficacy signals due to selective BRAF inhibition with PLX4032 in malignant melanoma*. Neoplasia, 2010. **12**(8): p. 637-49.
197. Smalley, K.S. and G.A. McArthur, *The current state of targeted therapy in melanoma: this time it's personal*. Seminars in oncology, 2012. **39**(2): p. 204-14.
198. Anforth, R.M., et al., *Cutaneous Manifestations of Dabrafenib (GSK2118436): A Selective Inhibitor of Mutant BRAF in patients with Metastatic Melanoma*. The British journal of dermatology, 2012.
199. Arnault, J.P., et al., *Paradoxical cutaneous squamous cell proliferations in patients treated with sorafenib*. Journal of Clinical Oncology, 2009. **27**(15).
200. Konstantinopoulos, P.A., M.V. Karamouzis, and A.G. Papavassiliou, *Post-translational modifications and regulation of the RAS superfamily of GTPases as anticancer targets*. Nature reviews. Drug discovery, 2007. **6**(7): p. 541-55.
201. Gilmartin, A.G., et al., *GSK1120212 (JTP-74057) Is an Inhibitor of MEK Activity and Activation with Favorable Pharmacokinetic Properties for Sustained In Vivo Pathway Inhibition*. Clinical Cancer Research, 2011. **17**(5): p. 989-1000.
202. Handolias, D., et al., *Clinical responses observed with imatinib or sorafenib in melanoma patients expressing mutations in KIT*. British journal of cancer, 2010. **102**(8): p. 1219-23.

## References

203. Woodman, S.E. and M.A. Davies, *Targeting KIT in melanoma: a paradigm of molecular medicine and targeted therapeutics*. Biochemical pharmacology, 2010. **80**(5): p. 568-74.
204. Fedorenko, I.V., K.H. Paraiso, and K.S. Smalley, *Acquired and intrinsic BRAF inhibitor resistance in BRAF V600E mutant melanoma*. Biochemical pharmacology, 2011. **82**(3): p. 201-9.
205. Villanueva, J., et al., *Acquired resistance to BRAF inhibitors mediated by a RAF kinase switch in melanoma can be overcome by cotargeting MEK and IGF-1R/PI3K*. Cancer cell, 2010. **18**(6): p. 683-95.
206. Johannessen, C.M., et al., *COT drives resistance to RAF inhibition through MAP kinase pathway reactivation*. Nature, 2010. **468**(7326): p. 968-72.
207. Carnahan, J., et al., *Selective and potent Raf inhibitors paradoxically stimulate normal cell proliferation and tumor growth*. Molecular cancer therapeutics, 2010. **9**(8): p. 2399-410.
208. Hatzivassiliou, G., et al., *RAF inhibitors prime wild-type RAF to activate the MAPK pathway and enhance growth*. Nature, 2010. **464**(7287): p. 431-5.
209. Halaban, R., et al., *PLX4032, a selective BRAF(V600E) kinase inhibitor, activates the ERK pathway and enhances cell migration and proliferation of BRAF melanoma cells*. Pigment Cell Melanoma Res, 2010. **23**(2): p. 190-200.
210. Kaplan, F.M., et al., *Hyperactivation of MEK-ERK1/2 signaling and resistance to apoptosis induced by the oncogenic B-RAF inhibitor, PLX4720, in mutant N-RAS melanoma cells*. Oncogene, 2011. **30**(3): p. 366-71.
211. Mathieu, V., et al., *Aggressiveness of human melanoma xenograft models is promoted by aneuploidy-driven gene expression deregulation*. Oncotarget, 2012. **3**(4): p. 399-413.
212. Metzner, T., et al., *Fibroblast growth factor receptors as therapeutic targets in human melanoma: synergism with BRAF inhibition*. J Invest Dermatol, 2011. **131**(10): p. 2087-95.
213. Chien, A.J., et al., *Activated Wnt/beta-catenin signaling in melanoma is associated with decreased proliferation in patient tumors and a murine melanoma model*. Proc Natl Acad Sci U S A, 2009. **106**(4): p. 1193-8.
214. Bachmann, I.M., et al., *Importance of P-cadherin, beta-catenin, and Wnt5a/frizzled for progression of melanocytic tumors and prognosis in cutaneous melanoma*. Clin Cancer Res, 2005. **11**(24 Pt 1): p. 8606-14.
215. Kageshita, T., et al., *Loss of beta-catenin expression associated with disease progression in malignant melanoma*. Br J Dermatol, 2001. **145**(2): p. 210-6.
216. Kielhorn, E., et al., *Tissue microarray-based analysis shows phospho-beta-catenin expression in malignant melanoma is associated with poor outcome*. Int J Cancer, 2003. **103**(5): p. 652-6.
217. Shimokawa, T., et al., *Involvement of the FGF18 gene in colorectal carcinogenesis, as a novel downstream target of the beta-catenin/T-cell factor complex*. Cancer research, 2003. **63**(19): p. 6116-20.
218. Metzner, T., et al., *Fibroblast growth factor receptors as therapeutic targets in human melanoma: synergism with BRAF inhibition*. The Journal of investigative dermatology, 2011. **131**(10): p. 2087-95.
219. Cross, M.J. and L. Claesson-Welsh, *FGF and VEGF function in angiogenesis: signalling pathways, biological responses and therapeutic inhibition*. Trends Pharmacol Sci, 2001. **22**(4): p. 201-7.

## References

220. Kandel, J., et al., *Neovascularization is associated with a switch to the export of bFGF in the multistep development of fibrosarcoma*. Cell, 1991. **66**(6): p. 1095-104.
221. Wang, Y. and D. Becker, *Antisense targeting of basic fibroblast growth factor and fibroblast growth factor receptor-1 in human melanomas blocks intratumoral angiogenesis and tumor growth*. Nat Med, 1997. **3**(8): p. 887-93.
222. Liu, Z., et al., *FGF18 is required for early chondrocyte proliferation, hypertrophy and vascular invasion of the growth plate*. Dev Biol, 2007. **302**(1): p. 80-91.
223. Sviatoha, V., et al., *Immunohistochemical analysis of the S100A1, S100B, CD44 and Bcl-2 antigens and the rate of cell proliferation assessed by Ki-67 antibody in benign and malignant melanocytic tumours*. Melanoma research, 2010. **20**(2): p. 118-25.
224. Veeman, M.T., et al., *Zebrafish prickles, a modulator of noncanonical Wnt/Fz signaling, regulates gastrulation movements*. Current biology : CB, 2003. **13**(8): p. 680-5.
225. Fire, A.Z., *Gene silencing by double-stranded RNA*. Cell Death Differ, 2007. **14**(12): p. 1998-2012.
226. Lee, Y., et al., *The nuclear RNase III Drosha initiates microRNA processing*. Nature, 2003. **425**(6956): p. 415-9.
227. Silva, J.M., et al., *Second-generation shRNA libraries covering the mouse and human genomes*. Nature Genetics, 2005. **37**(11): p. 1281-1288.
228. Nicholson, D.W. and N.A. Thornberry, *Caspases: killer proteases*. Trends in biochemical sciences, 1997. **22**(8): p. 299-306.
229. Orford, K., et al., *Serine phosphorylation-regulated ubiquitination and degradation of beta-catenin*. J Biol Chem, 1997. **272**(40): p. 24735-8.
230. Aberle, H., et al., *beta-catenin is a target for the ubiquitin-proteasome pathway*. EMBO J, 1997. **16**(13): p. 3797-804.
231. Kinzler, K.W., et al., *Identification of FAP locus genes from chromosome 5q21*. Science, 1991. **253**(5020): p. 661-5.
232. Nishisho, I., et al., *Mutations of chromosome 5q21 genes in FAP and colorectal cancer patients*. Science, 1991. **253**(5020): p. 665-9.
233. Kinzler, K.W. and B. Vogelstein, *Lessons from hereditary colorectal cancer*. Cell, 1996. **87**(2): p. 159-70.
234. Reya, T. and H. Clevers, *Wnt signalling in stem cells and cancer*. Nature, 2005. **434**(7035): p. 843-50.
235. Jamieson, C.H., et al., *Granulocyte-macrophage progenitors as candidate leukemic stem cells in blast-crisis CML*. N Engl J Med, 2004. **351**(7): p. 657-67.
236. Lo Celso, C., D.M. Prowse, and F.M. Watt, *Transient activation of beta-catenin signalling in adult mouse epidermis is sufficient to induce new hair follicles but continuous activation is required to maintain hair follicle tumours*. Development, 2004. **131**(8): p. 1787-99.
237. Chan, E.F., et al., *A common human skin tumour is caused by activating mutations in beta-catenin*. Nat Genet, 1999. **21**(4): p. 410-3.

## References

## References

### IX. Curriculum Vitae

**Name:** Katharina Vejdovszky  
**Adress:** Lerchenfelderstrasse 70-72/3/38  
1080 Wien, Österreich  
**Telephone:** 0650-4705663  
**e-mail:** [katharina\\_vejdovszky@gmx.at](mailto:katharina_vejdovszky@gmx.at)  
a0502627@univie.ac.at  
**Date and Place of Birth:** 27<sup>th</sup> of August, 1986  
**Nationality:** Austrian

### Education

8.2011 – 8.2012 practical part in the course of the Diploma Thesis at the  
Institute of Cancer Research  
Development of Experimental Cancer Therapies  
in the team of Ass.Prof.Dr. Michael Grusch  
since 10.2005 University of Vienna, Austria  
Studies in Biology  
Disciplines of Specialisation: Microbiology und Genetics  
9.1996 – 6.2004 Academic Secondary School  
AHS Bundesrealgymnasium Klosterneuburg, Austria

### Languages

- German, native Language
- English, fluently
- French, basic

### Work Experience

10.2004 – 4.2005 Work and Travel in Australia  
Activity: WWOOFing (Willing Workers on Organic Farms)

Vienna, 30<sup>th</sup> of December, 2012